Stable Bilateral Teleoperation with Time-Varying Delays

by

Yuan Yang
B.Eng., Harbin Institute of Technology, 2015

A Thesis Submitted in Partial Fulfillment of the

Requirements for the Degree of

MASTER OF APPLIED SCIENCE

in the Department of Mechanical Engineering

Stable Bilateral Teleoperation with Time-Varying Delays

by

Yuan Yang
B.Eng., Harbin Institute of Technology, 2015

Supervisory Committee

Dr. Daniela Constantinescu, Co-Supervisor
(Department of Mechanical Engineering)

Dr. Yang Shi, Co-Supervisor
(Department of Mechanical Engineering)

ABSTRACT

A teleoperation system is a master-slave robotic system in which the master and slave robots are at different geographical locations and synchronize their motions through the communication channel, with the goal of enabling the human operator to interact with a remote environment. The two primary objectives of bilateral teleoperation systems, position tracking and force feedback, are necessary for providing the user with high fidelity telepresence. However, time delays in communication channels impede the realization of the two objectives and even destabilize the system. To guarantee stability and improve performance, several damping injection-based controllers have been developed in this thesis for two channel and four channel teleoperation systems. For two channel teleoperation, an adaptive bounded state feedback controller has firstly been proposed to address teleoperation with time-varying delays, model uncertainties and bounded actuations. Next, a simplified and augmented globally exponentially convergent velocity observer has been designed and incorporated in the conventional P+d control to obtain stable bilateral teleoperation without using velocity measurements. Then, the more challenging bounded output feedback control problem has been solved by combining the bounded state feedback control and output feedback control two techniques with more conservative control gains. In four channel teleoperation, a hybrid damping and stiffness adjustment strategy has been introduced to tightly constrain the master and slave robots and achieve robust stability. Further, the nonsingular version is developed to conquer the singularity problem in the hybrid strategy, which has been proved to avoid unexpected torque spikes due to the singularity problem at zero velocities. Besides, this thesis has also provided a reduced-order controller to guarantee position coordination for arbitrarily large position errors and maintain the tight coupling between the master and slave sites. After concluding all the research results, future study directions are pointed out at the end of this thesis.

Contents

List of Figures

Acronyms

TDPA Time Domain Passivity Algorithm

PD Proportional-Derivative

PD+d Proportional-Derivative plus damping

P+d Proportional plus damping

LMI linear-matrix-inequality

SP-SD Saturated Proportional-Saturated Derivative

PID Proportional-Integral-Derivative

I&I Immersion and Invariance

PDE partial differential equation

ISS input-to-state stable

DOF degree of freedom

Chapter 1

Introduction

In this chapter, a brief introduction of bilateral teleoperation systems is firstly presented. Then existing methodologies and available research results within damping injection-based control are reviewed. Open control problems for bilateral teleoperation systems are pointed out and the research objectives of this research project are proposed.

1.1 Bilateral Teleoperation Systems

The word teleoperation with the prefix tele meaning at a distance indicates remote operation. Therefore, a teleoperator naturally refers to a master-slave robotic system that permits an operator to interact with a remote environment and finish from a distance manipulation tasks that are inaccessible or hazardous. Generally, a teleoperation system consists of at least two robots: the master robot directly operated by the user, and the slave robot interacting with the unknown remote environment. The teleoperation system configuration is shown in Figure. 1.1.

From the point of view of the existing and potential applications of teleoperation systems, the two main objectives of teleoperation systems are position tracking and force feedback, i.e. teleoperation systems should be bilateral to provide telepresence [1–3]. For position tracking, the master and slave robot should follow each

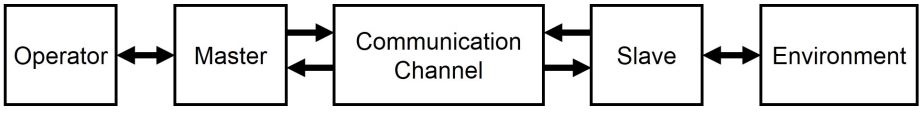

Figure 1.1: Teleoperation system configuration.

other's motion through control, that is, their motion should be synchronized through the communication channel [4, 5]. Then the user can control the movement of the remote slave robot by manipulating the master robot. Particularly, in cases like robot-assisted surgery, high-precision position control is a fundamental requirement for the system [6]. If large position errors happened between the master and slave sides, then the slave might move into unexpected areas and cause tissue damage, so the position tracking performance is crucial for the effectiveness and safety of this application [7]. Existing surgical robotic systems, such as the da Vinci surgical system, have already obtained satisfactory position control, but cannot provide surgeons with accurate force feedback during the surgical manipulation [8–11]. Because different tactile and kinesthetic experiences are elicited when touching different textures and when manipulating tissues with different stiffness, the teleoperation system should provide high-fidelity force feedback to help the surgeon distinguish different types of tissues through palpation and avoid unintended tissue damage due to large interaction forces [12–14]. Further, the mental load of the human operator can be reduced and their performance in assembly tasks in terms of task success rate and economy of exerted forces increases when the teleoperator provides force feedback in response to the user's motion [15].

Force feedback, also called haptic feedback, is demanded by surgeons during robotic surgery because it can improve the task performance significantly and thus, advance the development of the next-generation robotic surgery systems [11]. However, time delays existing in the forward and backward communication channels between the master and slave robots would damage the bilateral teleoperation system. As observed in [4], even small constant communication delays between the two sides would degrade the system performance and possibly destabilize the system because, at any moment in time, the forces applied to the operator are physically related to the operator's prior rather than current motion. The instability is more severe when the delays are time-varying since variable delays foil prediction. When the teleoperation system becomes unstable, the operator looses control of the slave robot and the system might be damaged as a result of violent vibrations. In terms of task completion, like the tele-surgery, the safety of the patient is also endangered since the physician cannot stop the slave upon contact. Keeping a bilateral teleoperation system stable and achieving the two main objectives, position tracking and force feedback, is a trade-off for bilateral teleoperation control [1, 16]. Therefore, an effective and practical control strategy is still needed for advancing the use of bilateral teleoperation

systems.

1.2 Damping Injection-Based Control

A large amount of work has been done to achieve stable bilateral teleoperation in the presence of communication delays, in which nonlinear control techniques, especially the passivity-based control strategy, play an important role. As an input-output property of dynamical systems, passivity characterizes the exchange of energy among interconnected systems. Specifically, a system is passive if and only if it can generate only limited energy. From the perspective of passivity-based control, the source of instability is active energy accumulation in the system. Therefore, the essence of passivity-based control is: 1) finding the redundant active energy accumulated in systems; 2) using passivity controller to dissipate the redundant energy. Generally, the redundant energy can be computed through measuring the system input-output pairs or through Lyapunov-krasovskii energy analysis. Correspondingly, the passivity controller consuming redundant energy by injecting varying or constant damping in the system because damping is an elementarily dissipative component in all mechanical systems.

Variable damping has been typically injected in bilateral teleoperation systems based on the Time Domain Passivity Algorithm (TDPA) that uses a time domain passivity observer to keep track of the energy generated in the communications and a time domain passivity controller to inject the damping required to deplete it [17]. An energy-bounding algorithm has achieved robust stability by restricting the energy generated by the sample-and-hold and communication time delays within the energy dissipated by the master and slave in [18]. Based on the TDPA, a two-layer approach has been proposed in [19] where the lower layer thwarts the generation of energy and thus keeps the system stable. Limited control output has been considered in [20] within the TDPA control scheme. A sufficient passivity condition has been derived based on TDPA in [21] by rendering the communication channels passive. Encoding position and velocity information to construct a composite signal, a feedback passivity scheme in [22] has mitigated the position drift problem in [17]. Time domain passivity has also been combined with scattering-based control in a nonlinear four-channel controller for position and force tracking in [23].

Constant damping injection is primarily based on Lyapunov-Krasovskii energy analysis. Using the simple Proportional-Derivative (PD) control in a passivity con-

text, the Lyapunov-Krasovskii technique has firstly been proposed in [24] to achieve stable teleoperation in the presence of constant time delays. However, the stability proof in [24] relies on the unverifiable assumption that the human and environment are defined $\mathcal{L}_\infty$-stable maps from velocity to force. Replacing this assumption with a passive external terminators assumption, [25, 26] have verified the effectiveness of the Proportional-Derivative plus damping (PD+d) control and have proposed a simpler Proportional plus damping (P+d) controller for position tracking in bilateral teleoperation with constant time delays. In [27–29], a new stability condition of the P+d control scheme for bilateral teleoperation systems with time-varying delays has been derived. Considering joint flexibility and gravity compensation of manipulators, the P+d controller was then extended by changing coordinates in [30]. A compensation component has been added to the PD+d controller in [31] to improve the interaction experience of the operator, but the additional control terms cause wave reflections similar to scattering-based control. Starting from the Lyapunov-Krasovskii energy analysis, stability conditions for bilateral teleoperation with time-varying and asymmetric delays have been derived by a delay-dependent linear-matrix-inequality(LMI) in [32]. Based on the delay-dependent LMI stability conditions, the P+d controller has further been applied to teleoperation with no gravity compensation in [33]. To achieve force feedback, a position-force strategy with P+d control at the slave and with force transmission to the master has been adopted in [32–34]. However, the force reflected to the master is the slave control force rather than the environment force and the round-delayed master position signals would induce wave reflections and decrease performance.

1.3 Open Problems

1.3.1 Bounded Damping Injection

Due to nonlinearities in the dynamics and torque output of robotic systems, the control of robot manipulators with actuator saturation is a challenging topic with a long history. When an actuator saturates, a controller designed without regard for torque limits is executed only partially, i.e. it loses the control of the robotic system. Thus, actuator saturation is a safety threat and needs to be considered in the controller design.

For robotic systems with actuator saturation, global position regulation has been

achieved via Saturated Proportional-Saturated Derivative (SP-SD) control with state feedback in [35–37], and with output feedback in [38,39]. Adaptive versions of the SP-SD controller have been proposed in [40, 41] to compensate gravity uncertainties, and in [42] to compensate both kinematic and dynamic uncertainties. Less conservative strategies, employing a single saturating function and extending the PD control have been reported in [43–45]. A saturated Proportional-Integral-Derivative (PID) strategy for semi-globally asymptotic position regulation has been introduced in [46, 47] using singular perturbation tools. Linear [48–50] and nonlinear [51] saturated PID controllers have also been developed to achieve globally asymptotic stability. Anti-windup has been applied in [52, 53] to improve the speed of recovery from saturation. Semi-globally asymptotic trajectory tracking has been achieved without velocity measurements and with model uncertainties in [54] and [55], respectively. Global tracking has also been obtained using PD plus dynamics compensation control in [56,57], adaptive control in [58] and robust integral of the sign of the error control in [59, 60].

In bilateral teleoperation, work considering actuator saturation has been largely based on the classical P+d control strategy [25, 29, 32], and has limited the proportional term [61, 62], the proportional and damping terms independently [63], the sum of the proportional and damping terms together [64], and has injected dynamic compensation [65]. Wave variable-based control and formation control with actuator saturation have also been discussed in [66] and [67]. Unlike in single robot control, where it needs to dissipate only kinetic energy, in teleoperation damping also needs to consume the energy created by the time-varying delays in order to guarantee bounded velocities of, and bounded position error between, the master and slave robots. When an actuator saturates, a P+d strategy that disregards torque limits cannot inject sufficient damping to guarantee safe teleoperation.

1.3.2 Output Feedback Damping Injection

Damping injection requires velocity information. Because most robots, including those used in teleoperation systems, lack velocity sensors, practical teleoperators need damping injection schemes that do not rely on velocity measurements. Velocity estimation through carefully designed observers has offered one approach to passivity-based control with only position measurements. Namely, a PD strategy augmented with a first-order estimator [68] has been developed for delay-free teleoperation. A fast terminal sliding-mode observer and a high-gain observer have been employed for

output feedback P+d control of delayed teleoperation in [62] and [69], respectively. A first-order velocity estimator has also been introduced for teleoperators with time-varying delays and actuator saturation [63].

In teleoperation systems, the user and environment are part of the control loop. Thus, the master and slave velocities are determined not only by the control inputs but also by the user and environment forces. Even if assumed passive, the user and environment may exert unexpectedly large forces during a short period of time. Such large forces can lead to large master and slave velocities despite injecting only limited energy in the teleoperation system. Therefore, one challenge facing the design of velocity observers for nonlinear bilateral teleoperation systems is the need to guarantee the convergence of velocity estimates without assuming bounded master and slave velocities. Recently, the Immersion and Invariance (I&I) velocity observer [70, 71] has been proven globally exponentially convergent and has been used for trajectory tracking in Euler-Lagrange systems [72, 73]. A constructive version of it [74], with simpler dynamics and computed based on the exact solution of a partial differential equation (PDE), has also been employed for output feedback tracking control of Euler-Lagrange dynamics [75]. Another challenge when using observers in teleoperation systems is that the estimation errors inject deleterious energy in the closed-loop system. Practically, damping injection based on velocity estimates dissipates the delay-induced energy but generates energy through estimation errors. For stability, the observers should converge fast enough to guarantee that the energy they create through estimation errors remains in a range that they can consume.

1.3.3 Four Channel Teleoperation

Stability ensures bilateral teleoperation safety, and transparency improves the user's telepresence. However, the two are generally in conflict with each other, especially in the presence of time-varying delays. Keeping a delayed bilateral teleoperation system stable and achieving precise position tracking and high-fidelity force feedback simultaneously remains a challenging research topic. From the perspective of stability, control of two channel teleoperstion in the presence of time-varying delays using only system states, positions and velocities, is simpler than that of four channel teleoperation, due to the fact that exchanging interacting forces in the two augmented channels are not system states. However, in terms of transparency, interacting forces can assist not only position synchronization but also human-environment interaction

telepresence.

Transparent teleoperation with time-varying delays has been sought through four-channel time domain passivity controllers in [76–78]. To the best of our knowledge, four channel teleoperation with static control has rarely been explored due to the difficulty of guaranteeing passive force transmission. Yet, four channel control is best suited to tightly constrain the master to the slave, and implicitly to the remote environment, during slave-environment contact. Sending the external user and environment forces to, and directly applying them on, the slave and master robots, respectively, is not the best method to exploit them. In general, the external forces include desired components that assist the controller to coordinate the two robots both in free motion and in contact, and undesirable components that damage the coupling between the robots and can even lead to finite time escaping velocities. Distinguishing the desirable from the harmful components and rejecting the latter without knowing their bounds is not trivial. In P+d control, fixed local damping injection is effective because the disturbances in the proportional term are related to the robot velocity at the other side. Considering the harmful components of the external forces as bounded disturbances is not helpful because it is impossible to determine a fixed damping sufficient to reject them without knowing their bounds.

1.4 Research Contributions

1.4.1 Bounded Damping Injection

A bounded P+d control with projection-based adaptive gravity compensation strategy has been developed to ensure the safety of bilateral teleoperation systems with model uncertainties, time-varying delays and bounded actuations. It employs two standard saturation functions: an inner saturation of the proportional term, and an outer saturation of the sum of the damping and saturated proportional terms. The outer saturation reserves sufficient actuator capability for gravity compensation, which keeps the two robots at rest at any point in their workspaces. The inner saturation limits the delay-induced disturbances to a range that leaves enough motor torque to suppress those disturbances through damping injection. The projection-based adaptive gravity compensation guarantees that the estimated gravity compensations always staying within the reasonable range without destabilizing the system.

1.4.2 Output Feedback Control

Globally stable output feedback synchronization has been achieved for bilateral teleoperation systems with time-varying delays by incorporating the simplified and augmented I&I velocity observer in the conventional P+d control. Compared to the I&I observers with $3n+1$ states in [70,71,79] and with $2n+2$ states in [74], our simplified I&I observer guarantees globally exponential convergence of the velocity estimates with only $n+2$ states, where n is the number of degrees of freedom of the robots. Compared to [70, 71, 79], the observer design procedure for Euler-Lagrange systems in this thesis is constructive and, thus, does not require an approximate solution of a PDE. Compared to [70, 71, 74, 79], the dynamics of the velocity estimates depend on dynamic scaling factors in this thesis. This augmentation of the observer dynamics increases the convergence speed of the velocity estimation and, thus, limits the energy injected by the estimation errors within a range that the observers themselves can dissipate. The integration of the new observer into conventional P+d control [29] permits the development of a rigorous proof of the global stability of the output feedback synchronization of teleoperation systems with time-varying delays.

1.4.3 Four Channel Teleoperation

To the best of our knowledge, four channel teleoperation with static control has rarely been explored due to the difficulty of guaranteeing passive force transmission. Yet, four channel control is best suited to tightly constrain the master to the slave, and implicitly to the remote environment, during slave-environment contact. Besides sharing this advantage of the four channel architecture, by introducing nonlinear position error-velocity coupling terms, our strategies render the closed-loop teleoperation system provably input-to-state stable (ISS), with the hand and environment forces as input and velocities and position error as state, without assuming passive operator or environment. The nonlinear coupling terms have a two-pronged effect: (i) it modulates the stiffness of the coordination between the master and slave to maintain the system ISS in the presence of non-passive input forces; and (ii) it injects additional damping to dissipate the energy generated by perturbing non-passive forces. In other words, the new strategies increase the robustness of teleoperation to the destabilizing components of the user and environment forces and their transmissions instead of assuming or rendering them passive.

Chapter 2

Two Channel Teleoperation

In this chapter, we first introduce the dynamics of bilateral teleoperation systems with some properties, assumptions and lemmas. Accounting bounded actuations, a bounded damping injection with adaptive gravity compensation control strategy has been developed to achieve globally asymptotically stable bilateral teleoperation. Then, a globally convergent velocity observer has been proposed and integrated into the conventional P+d control to rigorously stabilize teleoperation systems with time-varying delays. Further, the augmented I&I observer has also been integrated in the control with bounded actuations to achieve stable bilateral teleoperation with time-varying delays.

2.1 Preliminaries

Considering the master and slave robots to be n-degrees-of-freedom (DOF) serial manipulators with only revolute joints, their joint space dynamics are:

$$\begin{aligned} \mathbf{M}_m(\mathbf{q}_m)\ddot{\mathbf{q}}_m + \mathbf{C}_m(\mathbf{q}_m, \dot{\mathbf{q}}_m)\dot{\mathbf{q}}_m + \mathbf{g}_m(\mathbf{q}_m) =& \boldsymbol{\tau}_m + \boldsymbol{\tau}_h \\ \mathbf{M}_s(\mathbf{q}_s)\ddot{\mathbf{q}}_s + \mathbf{C}_s(\mathbf{q}_s, \dot{\mathbf{q}}_s)\dot{\mathbf{q}}_s + \mathbf{g}_s(\mathbf{q}_s) =& \boldsymbol{\tau}_s + \boldsymbol{\tau}_e \end{aligned}, \tag{2.1}$$

where the index $i = m, s$ indicates master and slave quantities, respectively, and for robot i: $\ddot{\mathbf{q}}_i$, $\dot{\mathbf{q}}_i$ and $\mathbf{q}_i$ are the joint acceleration, velocity and position; $\mathbf{M}_i(\mathbf{q}_i)$ and $\mathbf{C}_i(\mathbf{q}_i, \dot{\mathbf{q}}_i)$ are the matrices of inertia and of Coriolis and centrifugal effects; $\mathbf{g}_i(\mathbf{q}_i)$ are torques due to gravity; $\boldsymbol{\tau}_i$ are control torques; and $\boldsymbol{\tau}_h$ and $\boldsymbol{\tau}_e$ are the user and environment torques.

The properties of the dynamics of robot i in Equation (2.1), $i = m, s$, that facilitate

the stability analysis in the following sections are listed below.

P.1 The inertia matrices $\mathbf{M}_i$ are symmetric, positive definite and uniformly bounded by $\mathbf{0} \prec \lambda_{i1}\mathbf{I} \preceq \mathbf{M}_i \preceq \lambda_{i2}\mathbf{I} \prec \infty$, with $\lambda_{i1} > 0, \lambda_{i2} > 0$.

P.2 The matrix $\dot{\mathbf{M}}_i(\mathbf{q}_i) - 2\mathbf{C}_i(\mathbf{q}_i, \dot{\mathbf{q}}_i)$ is skew-symmetric.

P.3 There exists $c_i > 0$ such that $\|\mathbf{C}_i(\mathbf{q}_i, \mathbf{x})\mathbf{y}\| \leq c_i\|\mathbf{x}\| \cdot \|\mathbf{y}\|, \forall \mathbf{q}_i, \mathbf{x}, \mathbf{y}$.

P.4 The gravity torques $\mathbf{g}_i$ can be linearly parameterized by $\mathbf{g}_i = \mathbf{Z}(\mathbf{q}_i)\boldsymbol{\theta}_i$, for $i = m, s$, where $\mathbf{Z}(\mathbf{q}_i)$ is the regressor matrices of measurable system states and $\boldsymbol{\theta}_i$ are unknown but constant vectors of system parameters.

The following assumptions on communication delays and external terminators are assumed to be true:

A.1 The time delays from robot i to robot j, d_i, are non-negative and bounded, $0 \leq d_i \leq \overline{d}_i$, for $i, j = m, s$ and $i \neq j$.

A.2 The derivatives of the communication delays are bounded, $|\dot{d}_i| \leq \overline{\dot{d}}_i$, $i = m, s$.

A.3 The joint torques due to the hand and environment forces are bounded:

$$|\tau_{hk}| \leq \overline{\tau}_h, \quad |\tau_{ek}| \leq \overline{\tau}_e, \quad \forall k = 1, \cdots, n.$$

A.4 The human operator and environment are passive:

$$E_h - \int_0^t \dot{\mathbf{q}}_m^{\mathsf{T}} \boldsymbol{\tau}_h d\xi \geq 0, \quad E_e - \int_0^t \dot{\mathbf{q}}_s^{\mathsf{T}} \boldsymbol{\tau}_e d\xi \geq 0,$$

with E_h and E_e are positive constants.

A.5 The gravity joint torques are bounded by $\boldsymbol{\gamma}_i$ that are component-wise strictly smaller than the maximum actuator torques $\overline{\boldsymbol{\tau}}_i$:

$$|g_{ik}| \leq \gamma_{ik} < \overline{\tau}_{ik}, \quad i = m, s, \quad k = 1, \cdots, n,$$

i.e., the actuators can keep the master and slave at rest at any point in their workspaces.

In the following sections and chapters, the stability analysis relies on the following three lemmas.

L.1 For any vector signals $\mathbf{x}$, $\mathbf{y}$, any variable time delay $0 \leq d(t) \leq \overline{d} < \infty$ and any constant $\alpha > 0$, the following inequality holds [29]:

$$2\int_0^t \mathbf{x}^\mathsf{T}(\sigma)\int_0^{d(\sigma)} \mathbf{y}(\sigma-\theta)d\theta d\sigma \leq \alpha\int_0^t \|\mathbf{x}(\sigma)\|^2 d\sigma + \frac{\overline{d}^2}{\alpha}\int_0^t \|\mathbf{y}(\sigma)\|^2 d\sigma.$$

L.2 For a positive definite matrix $\boldsymbol{\Upsilon}$, the following inequality holds [32]:

$$\pm 2\mathbf{a}^\mathsf{T}(t)\int_{t-d(t)}^t \mathbf{b}(\xi)d\xi - \int_{t-d(t)}^t \mathbf{b}^\mathsf{T}(\xi)\boldsymbol{\Upsilon}\mathbf{b}(\xi)d\xi \leq \overline{d}\mathbf{a}^\mathsf{T}(t)\boldsymbol{\Upsilon}^{-1}\mathbf{a}(t)$$

for all $\mathbf{a}(t)$, $\mathbf{b}(t)$ and $0 \leq d(t) \leq \overline{d}$.

L.3 For a convex set $\Pi = \{\hat{\boldsymbol{\theta}} \in \mathbb{R}^n | \mathcal{P}(\hat{\boldsymbol{\theta}}) \leq 0)\}$ with interior $\mathring{\Pi}$, let us consider an other convex set $\Pi_\epsilon = \{\hat{\boldsymbol{\theta}} \in \mathbb{R}^n | \mathcal{P}(\hat{\boldsymbol{\theta}}) \leq \epsilon\}$ with boundary layer $O(\epsilon)$ around Π where $\mathcal{P}(\cdot)$ is a smooth convex function, let $\boldsymbol{\Gamma}(t)$, $\boldsymbol{\tau}(t)$ be continuously differentiable and $\dot{\hat{\boldsymbol{\theta}}} = \text{Proj}\{\boldsymbol{\tau}\}$, $\hat{\boldsymbol{\theta}}(0) \in \Pi_\epsilon$ where

$$\text{Proj}\{\boldsymbol{\tau}\} = \begin{cases} \boldsymbol{\tau}, & \hat{\boldsymbol{\theta}} \in \mathring{\Pi} \text{ or } \nabla_{\hat{\theta}}\mathcal{P}^\mathsf{T}\boldsymbol{\tau} \leq 0 \\ \left(\mathbf{I} - c(\hat{\boldsymbol{\theta}})\boldsymbol{\Gamma}\frac{\nabla_{\hat{\theta}}\mathcal{P}\nabla_{\hat{\theta}}\mathcal{P}^\mathsf{T}}{\nabla_{\hat{\theta}}\mathcal{P}^\mathsf{T}\boldsymbol{\Gamma}\nabla_{\hat{\theta}}\mathcal{P}}\right)\boldsymbol{\tau}, & \hat{\boldsymbol{\theta}} \in \Pi_\epsilon \backslash \mathring{\Pi} \text{ and } \nabla_{\hat{\theta}}\mathcal{P}^\mathsf{T}\boldsymbol{\tau} > 0 \end{cases}$$

with $c(\hat{\boldsymbol{\theta}}) = \min\left\{1, \frac{\mathcal{P}(\hat{\boldsymbol{\theta}})}{\epsilon}\right\}$ and $\nabla_{\hat{\theta}}\mathcal{P}$ the gradient of $\mathcal{P}(\hat{\boldsymbol{\theta}})$. Then, on its domain of definition, the solution $\hat{\boldsymbol{\theta}}(t)$ remains in Π_ϵ and $-\tilde{\boldsymbol{\theta}}^\mathsf{T}\boldsymbol{\Gamma}^{-1}\text{Proj}\{\boldsymbol{\tau}\} \leq -\tilde{\boldsymbol{\theta}}^\mathsf{T}\boldsymbol{\Gamma}^{-1}\boldsymbol{\tau}$, where $\tilde{\boldsymbol{\theta}} = \boldsymbol{\theta} - \hat{\boldsymbol{\theta}}$, $\forall \hat{\boldsymbol{\theta}} \in \Pi_\epsilon, \boldsymbol{\theta} \in \Pi$ [80].

In teleoperation control, lemma L.1 and the time integration of lemma L.2 from 0 to t both suggest the fact that scaled redundant energy generated by the delay-induced disturbances (left-hand side) can be upper-bounded by the energy consumed by injected damping on master and slave sides (right-hand side). For lemma L.3, the role of projection operator is to render the estimation $\hat{\boldsymbol{\theta}}$ in the feasible set Π_ϵ and protect estimation convergence.

2.2 Adaptive Bounded State Feedback Control

In the classical P+d control strategy, sufficient damping injection can suppress the disturbances introduced in the proportional control term by the time-varying delays. However, the conventional strategy does not account for the torque limitations of

practical actuators and, therefore, is potentially dangerous. This section proposes a bounded damping extension of the P+d control that suitably limits the proportional term to reserve sufficient actuator torque for damping injection. Moreover, a projection-based adaptive law has also been developed to dynamically compensate uncertain gravities of the system.

For ease of understanding, the conventional P+d control with gravity compensation [25, 32] is reviewed first before introducing the bounded state feedback control. In the conventional P+d control strategy, the master and slave control torques $\boldsymbol{\tau}_m$ and $\boldsymbol{\tau}_s$ are computed as

$$\begin{aligned} \boldsymbol{\tau}_m &= -\mathbf{P}(\mathbf{q}_m - \mathbf{q}_{sd}) - \mathbf{K}_m\dot{\mathbf{q}}_m + \mathbf{g}_m \\ \boldsymbol{\tau}_s &= -\mathbf{P}(\mathbf{q}_s - \mathbf{q}_{md}) - \mathbf{K}_s\dot{\mathbf{q}}_s + \mathbf{g}_s \end{aligned}, \tag{2.2}$$

where $\mathbf{q}_{sd} = \mathbf{q}_s(t - d_s(t))$ and $\mathbf{q}_{md} = \mathbf{q}_m(t - d_m(t))$ are the delayed slave position at the master site and the delayed master position at the slave site, respectively; and the gains $\mathbf{P}$, $\mathbf{K}_m$ and $\mathbf{K}_s$ are constant positive definite diagonal matrices. The framework of the bilateral teleoperation systems under the P+d control is shown in Figure. 2.1.

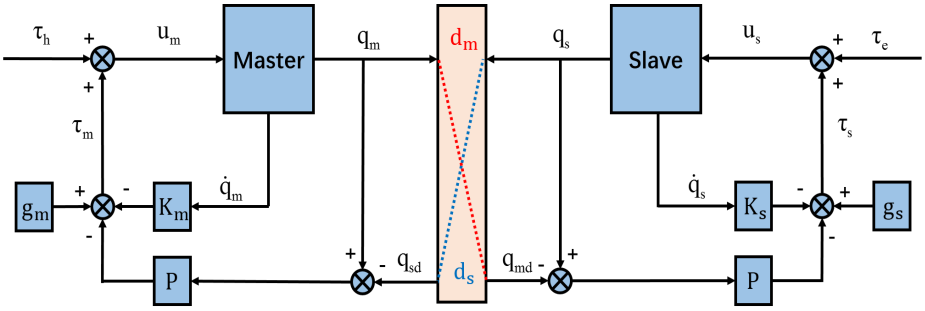

Figure 2.1: Teleoperation system with the P+d controller in Equation (2.2).

The velocities of, and the position error between, the master and slave robots are analyzed by using the following Lyapunov-Krasovskii functional [25]:

$$\begin{aligned} V_u =& \frac{1}{2}\dot{\mathbf{q}}_m^\mathsf{T}\mathbf{M}_m\dot{\mathbf{q}}_m + \frac{1}{2}\dot{\mathbf{q}}_s^\mathsf{T}\mathbf{M}_s\dot{\mathbf{q}}_s + \frac{1}{2}(\mathbf{q}_m - \mathbf{q}_s)^\mathsf{T}\mathbf{P}(\mathbf{q}_m - \mathbf{q}_s) \\ &- \int_0^t \dot{\mathbf{q}}_m^\mathsf{T}\boldsymbol{\tau}_h d\xi + E_h - \int_0^t \dot{\mathbf{q}}_s^\mathsf{T}\boldsymbol{\tau}_e d\xi + E_e. \end{aligned} \tag{2.3}$$

In Equation (2.3): the first three quadratic terms are the kinetic energy of the master and slave robots and the potential energy stored in the proportional control term; the two integral terms are the energies input by the operator and the environment.

Therefore, from assumption A.4, V_u is positive if the velocities of, and the position error between the two robots are not zero. Further, V_u is bounded if the velocities of, and the position error between the two robots are bounded, and vice versa.

After substituting Equation (2.2) in Equation (2.1) and using lemma L.1, the derivative of V_u becomes

$$\begin{aligned}
\dot{V}_u =& \frac{1}{2}\dot{\mathbf{q}}_m^\mathsf{T}\dot{\mathbf{M}}_m\dot{\mathbf{q}}_m + \dot{\mathbf{q}}_m^\mathsf{T}\mathbf{M}_m\ddot{\mathbf{q}}_m + \dot{\mathbf{q}}_m^\mathsf{T}\mathbf{P}(\mathbf{q}_m - \mathbf{q}_s) - \dot{\mathbf{q}}_m^\mathsf{T}\boldsymbol{\tau}_h \\
&+ \frac{1}{2}\dot{\mathbf{q}}_s^\mathsf{T}\dot{\mathbf{M}}_s\dot{\mathbf{q}}_s + \dot{\mathbf{q}}_s^\mathsf{T}\mathbf{M}_s\ddot{\mathbf{q}}_s + \dot{\mathbf{q}}_s^\mathsf{T}\mathbf{P}_s(\mathbf{q}_s - \mathbf{q}_m) - \dot{\mathbf{q}}_s^\mathsf{T}\boldsymbol{\tau}_e \\
=& \frac{1}{2}\dot{\mathbf{q}}_m^\mathsf{T}\mathbf{M}_m\dot{\mathbf{q}}_m - \dot{\mathbf{q}}_m^\mathsf{T}\mathbf{C}_m\dot{\mathbf{q}}_m - \dot{\mathbf{q}}_m^\mathsf{T}\mathbf{g}_m - \dot{\mathbf{q}}_m^\mathsf{T}\mathbf{P}(\mathbf{q}_m - \mathbf{q}_s) - \dot{\mathbf{q}}_m^\mathsf{T}\mathbf{P}(\mathbf{q}_s - \mathbf{q}_{sd}) \\
&- \dot{\mathbf{q}}_m^\mathsf{T}\mathbf{K}_m\dot{\mathbf{q}}_m + \dot{\mathbf{q}}_m^\mathsf{T}\mathbf{g}_m + \dot{\mathbf{q}}_m^\mathsf{T}\boldsymbol{\tau}_h + \dot{\mathbf{q}}_m^\mathsf{T}\mathbf{P}(\mathbf{q}_m - \mathbf{q}_s) - \dot{\mathbf{q}}_m^\mathsf{T}\boldsymbol{\tau}_h \\
&+ \frac{1}{2}\dot{\mathbf{q}}_s^\mathsf{T}\mathbf{M}_s\dot{\mathbf{q}}_s - \dot{\mathbf{q}}_s^\mathsf{T}\mathbf{C}_s\dot{\mathbf{q}}_s - \dot{\mathbf{q}}_s^\mathsf{T}\mathbf{g}_s - \dot{\mathbf{q}}_s^\mathsf{T}\mathbf{P}(\mathbf{q}_s - \mathbf{q}_m) - \dot{\mathbf{q}}_s^\mathsf{T}\mathbf{P}(\mathbf{q}_m - \mathbf{q}_{sd}) \\
&- \dot{\mathbf{q}}_s^\mathsf{T}\mathbf{K}_s\dot{\mathbf{q}}_s + \dot{\mathbf{q}}_s^\mathsf{T}\mathbf{g}_s + \dot{\mathbf{q}}_s^\mathsf{T}\boldsymbol{\tau}_e + \dot{\mathbf{q}}_s^\mathsf{T}\mathbf{P}(\mathbf{q}_s - \mathbf{q}_m) - \dot{\mathbf{q}}_s^\mathsf{T}\boldsymbol{\tau}_e \\
=& - \dot{\mathbf{q}}_m^\mathsf{T}\mathbf{P}(\mathbf{q}_s - \mathbf{q}_{sd}) - \dot{\mathbf{q}}_m^\mathsf{T}\mathbf{K}_m\dot{\mathbf{q}}_m - \dot{\mathbf{q}}_s^\mathsf{T}\mathbf{P}(\mathbf{q}_m - \mathbf{q}_{md}) - \dot{\mathbf{q}}_s^\mathsf{T}\mathbf{K}_s\dot{\mathbf{q}}_s.
\end{aligned} \tag{2.4}$$

Equation (2.4) shows that the disturbances $-\mathbf{P}(\mathbf{q}_s - \mathbf{q}_{sd})$ and $-\mathbf{P}(\mathbf{q}_m - \mathbf{q}_{md})$ introduced by the time-varying delays in the proportional control terms of the master and slave robots threaten the safety of the bilateral teleoperation system. Since only the upper bound of the delays are known, the worst scenario needs to be considered, in which the time-varying delays continuously inject energy in the system, i.e., $-\dot{\mathbf{q}}_m^\mathsf{T}\mathbf{P}(\mathbf{q}_s - \mathbf{q}_{sd}) > 0$ and $-\dot{\mathbf{q}}_s^\mathsf{T}\mathbf{P}(\mathbf{q}_m - \mathbf{q}_{md}) > 0$, $\forall t > 0$. Therefore, if the energy generated by delays can not be dissipated through damping, then $\dot{V}_u > 0$ and $V_u \to \infty$ as $t \to \infty$, i.e., the system is unstable.

Integration of both sides of Equation (2.4) together with lemma L.1 leads to:

$$\begin{aligned}
& V_u(t) - V_u(0) \\
=& - \int_0^t \dot{\mathbf{q}}_m^\mathsf{T}\mathbf{P}\int_{\sigma-d_s}^{\sigma} \dot{\mathbf{q}}_s d\theta d\sigma - \int_0^t \dot{\mathbf{q}}_m^\mathsf{T}\mathbf{K}_m\dot{\mathbf{q}}_m d\sigma \\
& - \int_0^t \dot{\mathbf{q}}_s^\mathsf{T}\mathbf{P}\int_{\sigma-d_m}^{\sigma} \dot{\mathbf{q}}_m d\theta d\sigma - \int_0^t \dot{\mathbf{q}}_s^\mathsf{T}\mathbf{K}_s\dot{\mathbf{q}}_s d\sigma \\
\leq& \frac{\overline{p}}{2}\left(\alpha\|\dot{\mathbf{q}}_m\|_2^2 + \frac{\overline{d}_s^2}{\alpha}\|\dot{\mathbf{q}}_s\|_2^2\right) - \underline{k}_m\|\dot{\mathbf{q}}_m\|_2^2 + \frac{\overline{p}}{2}\left(\beta\|\dot{\mathbf{q}}_s\|_2^2 + \frac{\overline{d}_m^2}{\beta}\|\dot{\mathbf{q}}_m\|_2^2\right) - \underline{k}_s\|\dot{\mathbf{q}}_s\|_2^2 \\
=& - \left[\underline{k}_m - \frac{\overline{p}}{2}\left(\alpha + \frac{\overline{d}_m^2}{\beta}\right)\right]\|\dot{\mathbf{q}}_m\|_2^2 - \left[\underline{k}_s - \frac{\overline{p}}{2}\left(\beta + \frac{\overline{d}_s^2}{\alpha}\right)\right]\|\dot{\mathbf{q}}_s\|_2^2,
\end{aligned} \tag{2.5}$$

where: $\overline{p}$ is the largest eigenvalue of $\mathbf{P}$; $\underline{k}_m$ and $\underline{k}_s$ are the smallest eigenvalues of $\mathbf{K}_m$ and $\mathbf{K}_s$; and α and β are positive constants. Selecting the damping gains $\mathbf{K}_m$ and $\mathbf{K}_s$ sufficiently large with respect to the proportional gain $\mathbf{P}$ makes the last two terms strictly negative and guarantees that V_u is bounded. In turn, a bounded V_u guarantees that the velocities of, and the position error between, the master and slave are bounded.

The P+d control strategy (2.5) illustrates the fact: injecting sufficiently large local damping in the system can suppress the instability induced by time-varying delays. One of the most significant advantages of the P+d control over other approaches is its simple structure and design criterion as shown above. The proportional control is used for synchronizing the positions of the master and slave robots, which behaves like a virtual spring connecting the two robots. As the proportional gain increasing, the stiffness of the spring becomes larger and larger. In other word, the coupling relationship of the two sites is kept through proportional control. It should be known that, due to the special scheme of the system, the master and slave robots have no other knowledge about the model parameters and motion information of each other, except the the delayed position information. Therefore, the proportional terms can only adopt the delayed position of the other sides, which contain the disturbances induced by time-varying delays. Because the disturbances are related to the velocities of the other side and the magnitude of time delays, the local damping terms can be used to suppress instability caused by the disturbances.

To guarantee that teleoperation systems with actuator saturation can fully execute the control action, this section proposes the following bounded P+d controller:

$$\begin{aligned} \boldsymbol{\tau}_m =& \mathrm{Sat}_m\Big(-\mathrm{Sat}_p\Big[\mathbf{P}(\mathbf{q}_m - \mathbf{q}_{sd})\Big] - \mathbf{K}_m\dot{\mathbf{q}}_m\Big) + \hat{\mathbf{g}}_m \\ \boldsymbol{\tau}_s =& \mathrm{Sat}_s\Big(-\mathrm{Sat}_p\Big[\mathbf{P}(\mathbf{q}_s - \mathbf{q}_{md})\Big] - \mathbf{K}_s\dot{\mathbf{q}}_s\Big) + \hat{\mathbf{g}}_s \end{aligned}, \tag{2.6}$$

where:

$$\mathrm{Sat}_i(\mathbf{u}) = \Big[\mathrm{sat}_{i1}(u_1), \cdots, \mathrm{sat}_{in}(u_n)\Big]^{\mathsf{T}},$$

$$\mathrm{sat}_{ik}(u_k) = \begin{cases} u_k & |u_k| \le s_{ik} \\ \mathrm{sgn}(u_k)s_{ik} & |u_k| > s_{ik} \end{cases}$$

and: $\mathrm{Sat}_p(\cdot)$ is the inner saturation of the P term on the master and slave sides; $\mathrm{Sat}_m(\cdot)$ and $\mathrm{Sat}_s(\cdot)$ are the outer saturations of the P+d term on the master and

slave sides, respectively; $\hat{\mathbf{g}}_m$ and $\hat{\mathbf{g}}_s$ are gravity estimates; $k = 1, \cdots, n$ is the joint index; $\text{sgn}(\cdot)$ is the sign function. s_{ik} are positive constants to be determined through stability analysis and with ranges constrained by

$$\begin{cases} s_{pk} \leq s_{ik} \\ s_{ik} + \gamma_{ik} \leq \overline{\tau}_{ik} \end{cases} \tag{2.7}$$

with $i = m, s$ and $k = 1, \cdots, n$ to guarantee that control torques remain within the actuator bounds at all times. The closed-loop bilateral teleoperation system with dynamics Equation (2.1) under the control of bounded damping injection strategy with adaptive gravity compensation Equation (2.6) is shown in Figure. 2.2.

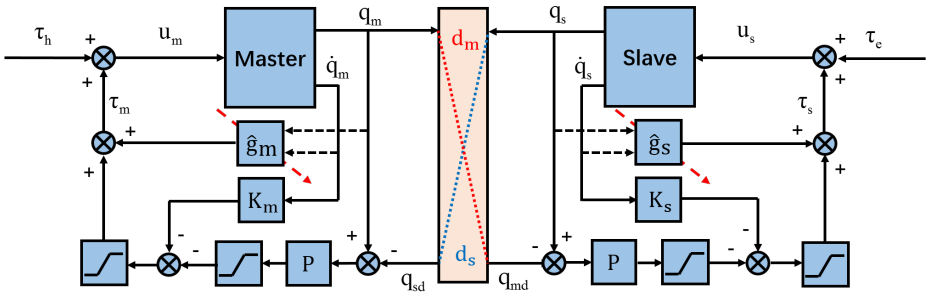

Figure 2.2: Teleoperation system under the bounded P+d control with adaptive gravity compensation in Equation (2.6).

From property P.4 and assumption A.5, gravities are bounded and can be further linearly parameterized as $\mathbf{g}_i = \mathbf{Z}(\mathbf{q}_i)\boldsymbol{\theta}_i$, with $\mathbf{Z}(\mathbf{q}_i)$ are known regressor matrices depending on position and $\boldsymbol{\theta}_i$ are unknown but constant vectors depending on robots' physical parameters, masses and lengths of links, and $\underline{\boldsymbol{\theta}}_i \leq \boldsymbol{\theta}_i \leq \overline{\boldsymbol{\theta}}_i$. Therefore, the estimated gravity is designed by

$$\hat{\mathbf{g}}_i = \mathbf{Z}(\mathbf{q}_i)\hat{\boldsymbol{\theta}}_i \tag{2.8}$$

with parameter update law $\dot{\hat{\boldsymbol{\theta}}}_i = \text{Proj}_{\hat{\theta}_i}(\boldsymbol{\omega}_i)$ and $\boldsymbol{\omega}_i = -\mathbf{Z}(\mathbf{q}_i)^{\mathsf{T}}\dot{\mathbf{q}}_i$, $i = m, s$. Since $\dot{\hat{\boldsymbol{\theta}}}_i$ are vectors, the projection is element-wise. Define ϵ a small positive constant used for making the projection smooth and

$$c_{lb}(\hat{\theta}_{ik}) = \min\left\{1, \frac{\underline{\theta}_{ik} + \epsilon - \hat{\theta}_{ik}}{\epsilon}\right\}, \quad c_{ub}(\hat{\theta}_{ik}) = \min\left\{1, \frac{\hat{\theta}_{ik} - \overline{\theta}_{ik} + \epsilon}{\epsilon}\right\},$$

then we design the following smooth projection operator:

$$\dot{\hat{\theta}}_{ik} = \mathrm{Proj}_{\hat{\theta}_{ik}}(\omega_{ik}) = \begin{cases} \left(1 - c_{lb}(\hat{\theta}_{ik})\right)\omega_{ik} & \underline{\theta}_{ik} \le \hat{\theta}_{ik} \le \underline{\theta}_{ik} + \epsilon \ \&\ \omega_{ik} < 0 \\ \omega_{ik} & \underline{\theta}_{ik} + \epsilon < \hat{\theta}_{ik} < \overline{\theta}_{ik} - \epsilon \\ & \text{or } \underline{\theta}_{ik} \le \hat{\theta}_{ik} \le \underline{\theta}_{ik} + \epsilon \ \&\ \omega_{ik} \ge 0 \\ & \text{or } \overline{\theta}_{ik} - \epsilon \le \hat{\theta}_{ik} \le \overline{\theta}_{ik} \ \&\ \omega_{ik} \le 0 \\ \left(1 - c_{ub}(\hat{\theta}_{ik})\right)\omega_{ik} & \overline{\theta}_{ik} - \epsilon \le \hat{\theta}_{ik} \le \overline{\theta}_{ik} \ \&\ \omega_{ik} > 0 \end{cases}. \quad (2.9)$$

The performance analysis is based on the following Lyapunov-Krasovskii function:

$$\begin{aligned} V =& \frac{1}{2}\dot{\mathbf{q}}_m^\mathsf{T}\mathbf{M}_m\dot{\mathbf{q}}_m + \frac{1}{2}\dot{\mathbf{q}}_s^\mathsf{T}\mathbf{M}_s\dot{\mathbf{q}}_s + \sum_{k=1}^{n}\int_0^{q_{mk}-q_{sk}} \mathrm{sat}_{pk}(p_k\sigma)d\sigma \\ & - \int_0^t \dot{\mathbf{q}}_m^\mathsf{T}\boldsymbol{\tau}_h d\xi + E_h - \int_0^t \dot{\mathbf{q}}_s^\mathsf{T}\boldsymbol{\tau}_e d\xi + E_e + \frac{1}{2}\tilde{\boldsymbol{\theta}}_m^\mathsf{T}\tilde{\boldsymbol{\theta}}_m + \frac{1}{2}\tilde{\boldsymbol{\theta}}_s^\mathsf{T}\tilde{\boldsymbol{\theta}}_s, \end{aligned} \quad (2.10)$$

where p_k is the k-th diagonal element of $\mathbf{P}$ and $\tilde{\boldsymbol{\theta}}_i = \boldsymbol{\theta}_i - \hat{\boldsymbol{\theta}}_i$, $i = m, s$, are parameter estimation errors. Note that the function in Equation (2.10) uses the quasi-natural potential function [35], $\sum_{k=1}^{n}\int_0^{q_{mk}-q_{sk}} \mathrm{sat}_{pk}(p_k\sigma)d\sigma$, in place of the potential energy $\frac{1}{2}(\mathbf{q}_m - \mathbf{q}_s)^\mathsf{T}\mathbf{P}(\mathbf{q}_m - \mathbf{q}_s)$ used in Equation (2.3). Because the saturation function is odd, the quasi-natural potential function is positive definite and radially unbounded in terms of the position error $q_{mk} - q_{sk}$. Consequently, bounded V is equivalent to bounded velocities of, and bounded position error between, the master and slave robots.

After substituting from Equation (2.6) into (2.1), the derivative of V becomes:

$$\begin{aligned} \dot{V} =& \frac{1}{2}\dot{\mathbf{q}}_m^\mathsf{T}\dot{\mathbf{M}}_m\dot{\mathbf{q}}_m + \dot{\mathbf{q}}_m^\mathsf{T}\mathbf{M}_m\ddot{\mathbf{q}}_m + \frac{1}{2}\dot{\mathbf{q}}_s^\mathsf{T}\dot{\mathbf{M}}_s\dot{\mathbf{q}}_s + \dot{\mathbf{q}}_s^\mathsf{T}\mathbf{M}_s\ddot{\mathbf{q}}_s - \dot{\mathbf{q}}_m^\mathsf{T}\boldsymbol{\tau}_h - \dot{\mathbf{q}}_s^\mathsf{T}\boldsymbol{\tau}_e \\ & + \sum_{k=1}^{n}(\dot{q}_{mk} - \dot{q}_{sk})\mathrm{sat}_{pk}[p_k(q_{mk} - q_{sk})] + \tilde{\boldsymbol{\theta}}_m^\mathsf{T}\dot{\tilde{\boldsymbol{\theta}}}_m + \tilde{\boldsymbol{\theta}}_s^\mathsf{T}\dot{\tilde{\boldsymbol{\theta}}}_s \\ =& \frac{1}{2}\dot{\mathbf{q}}_m^\mathsf{T}\left(\dot{\mathbf{M}}_m - 2\mathbf{C}_m\right)\dot{\mathbf{q}}_m - \dot{\mathbf{q}}_m^\mathsf{T}\mathbf{g}_m - \tilde{\boldsymbol{\theta}}_m^\mathsf{T}\dot{\hat{\boldsymbol{\theta}}}_m + \frac{1}{2}\dot{\mathbf{q}}_s^\mathsf{T}\left(\dot{\mathbf{M}}_s - \mathbf{C}_s\right)\dot{\mathbf{q}}_s - \dot{\mathbf{q}}_s^\mathsf{T}\hat{\mathbf{g}}_s - \tilde{\boldsymbol{\theta}}_s^\mathsf{T}\dot{\hat{\boldsymbol{\theta}}}_s \\ & + \sum_{k=1}^{n}\left\{\dot{q}_{mk}\mathrm{sat}_{pk}\left[p_k(q_{mk} - q_{sk})\right]\right\} + \sum_{k=1}^{n}\left\{\dot{q}_{sk}\mathrm{sat}_{pk}\left[p_k(q_{sk} - q_{mk})\right]\right\} \\ =& -\dot{\mathbf{q}}_m^\mathsf{T}\mathbf{g}_m + \dot{\mathbf{q}}_m^\mathsf{T}\mathrm{Sat}_m\left(-\mathrm{Sat}_p\left[\mathbf{P}(\mathbf{q}_m - \mathbf{q}_{sd})\right] - \mathbf{K}_m\dot{\mathbf{q}}_m\right) + \dot{\mathbf{q}}_m^\mathsf{T}\hat{\mathbf{g}}_m - \tilde{\boldsymbol{\theta}}_m^\mathsf{T}\dot{\hat{\boldsymbol{\theta}}}_m \\ & - \dot{\mathbf{q}}_s^\mathsf{T}\mathbf{g}_s + \dot{\mathbf{q}}_s^\mathsf{T}\mathrm{Sat}_s\left(-\mathrm{Sat}_p\left[\mathbf{P}(\mathbf{q}_s - \mathbf{q}_{md})\right] - \mathbf{K}_s\dot{\mathbf{q}}_s\right) + \dot{\mathbf{q}}_s^\mathsf{T}\hat{\mathbf{g}}_s - \tilde{\boldsymbol{\theta}}_s^\mathsf{T}\dot{\hat{\boldsymbol{\theta}}}_s \end{aligned}$$

$$+ \dot{\mathbf{q}}_m^\mathsf{T}\mathrm{Sat}_p\left[\mathbf{P}(\mathbf{q}_m - \mathbf{q}_s)\right] + \dot{\mathbf{q}}_s^\mathsf{T}\mathrm{Sat}_p\left[\mathbf{P}(\mathbf{q}_s - \mathbf{q}_m)\right].$$

Using lemma L.3,

$$\begin{aligned}
&- \dot{\mathbf{q}}_i^\mathsf{T}\mathbf{g}_i + \dot{\mathbf{q}}_i^\mathsf{T}\hat{\mathbf{g}}_i - \tilde{\boldsymbol{\theta}}_i^\mathsf{T}\dot{\hat{\boldsymbol{\theta}}}_i = -\dot{\mathbf{q}}_i^\mathsf{T}\mathbf{Z}(\mathbf{q}_i)\boldsymbol{\theta}_i + \dot{\mathbf{q}}_i^\mathsf{T}\mathbf{Z}(\mathbf{q}_i)\hat{\boldsymbol{\theta}}_i - \tilde{\boldsymbol{\theta}}_i^\mathsf{T}\dot{\hat{\boldsymbol{\theta}}}_i \\
=& - \dot{\mathbf{q}}_i^\mathsf{T}\mathbf{Z}(\mathbf{q}_i)\tilde{\boldsymbol{\theta}}_i - \tilde{\boldsymbol{\theta}}_i^\mathsf{T}\mathrm{Proj}_{\hat{\theta}_i}\left(-\mathbf{Z}(\mathbf{q}_i)^\mathsf{T}\dot{\mathbf{q}}_i\right) = \tilde{\boldsymbol{\theta}}_i^\mathsf{T}\left[-\mathbf{Z}(\mathbf{q}_i)^\mathsf{T}\dot{\mathbf{q}}_i - \mathrm{Proj}_{\hat{\theta}_i}\left(-\mathbf{Z}(\mathbf{q}_i)^\mathsf{T}\dot{\mathbf{q}}_i\right)\right] \leq 0,
\end{aligned}$$

then the derivative of V can be upper bounded by

$$\begin{aligned}
\dot{V} \leq& \dot{\mathbf{q}}_m^\mathsf{T}\mathrm{Sat}_m\Big(- \mathrm{Sat}_p\Big[\mathbf{P}(\mathbf{q}_m - \mathbf{q}_{sd})\Big] - \mathbf{K}_m\dot{\mathbf{q}}_m\Big) + \dot{\mathbf{q}}_m^\mathsf{T}\mathrm{Sat}_p\left[\mathbf{P}(\mathbf{q}_m - \mathbf{q}_s)\right] \\
&+ \dot{\mathbf{q}}_s^\mathsf{T}\mathrm{Sat}_s\Big(- \mathrm{Sat}_p\Big[\mathbf{P}(\mathbf{q}_s - \mathbf{q}_{md})\Big] - \mathbf{K}_s\dot{\mathbf{q}}_s\Big) + \dot{\mathbf{q}}_s^\mathsf{T}\mathrm{Sat}_p\left[\mathbf{P}(\mathbf{q}_s - \mathbf{q}_m)\right].
\end{aligned} \tag{2.11}$$

In general, each motor has different capability, i.e. $\overline{\tau}_{ik}$ are different for $i = m, s$ and $k = 1, \cdots, n$ and its saturation state is uncertain and time-varying. Nevertheless, for each pair of corresponding master and slave joints, there are only four different scenarios: 1) $\mathrm{sat}_{mk}(\cdot)$ and $\mathrm{sat}_{sk}(\cdot)$ are both unsaturated; 2) $\mathrm{sat}_{mk}(\cdot)$ and $\mathrm{sat}_{sk}(\cdot)$ are both saturated; 3) $\mathrm{sat}_{mk}(\cdot)$ is unsaturated while $\mathrm{sat}_{sk}(\cdot)$ is saturated; 4) $\mathrm{sat}_{mk}(\cdot)$ is saturated while $\mathrm{sat}_{sk}(\cdot)$ is unsaturated. Correspondingly, the derivative of V can be divided into four parts:

$$\dot{V} = \dot{V}_{uu} + \dot{V}_{ss} + \dot{V}_{us} + \dot{V}_{su}, \tag{2.12}$$

with subscripts uu, ss, us and su representing the cases 1)-4) above, respectively; and $k \in k_j,\ j = uu, ss, us, su$ indexing the joint pairs whose control torques belong in the four groups.

In $\dot{V}$, $\dot{V}_{uu}$ collects all terms that correspond to joint pairs with unsaturated P+d torques at both the master and slave sides, i.e., P+d torque pairs $-\mathrm{sat}_{pk}[p_k(q_{mk} - q_{sdk})] - k_{mk}\dot{q}_{mk}$ and $-\mathrm{sat}_{pk}[p_k(q_{sk} - q_{mdk})] - k_{sk}\dot{q}_{sk}$ for all $k \in k_{uu}$. Therefore, $\dot{V}_{uu}$ can be upper bounded by:

$$\begin{aligned}
\dot{V}_{uu} =& \sum_{k\in k_{uu}} \Big\{ - \dot{q}_{mk}\mathrm{sat}_{pk}[p_k(q_{mk} - q_{sdk})] - k_{mk}\dot{q}_{mk}^2 + \dot{q}_{mk}\mathrm{sat}_{pk}[p_k(q_{mk} - q_{sk})] \\
&\qquad - \dot{q}_{sk}\mathrm{sat}_{pk}[p_k(q_{sk} - q_{mdk})] - k_{sk}\dot{q}_{sk}^2 + \dot{q}_{sk}\mathrm{sat}_{pk}[p_k(q_{sk} - q_{mk})]\Big\} \\
\leq& \sum_{k\in k_{uu}} \Big\{|\dot{q}_{mk}|p_k\int_{t-d_s}^{t}|\dot{q}_{sk}|d\xi - k_{mk}\dot{q}_{mk}^2 + |\dot{q}_{sk}|p_k\int_{t-d_m}^{t}|\dot{q}_{mk}|d\xi - k_{sk}\dot{q}_{sk}^2\Big\}.
\end{aligned} \tag{2.13}$$

Note that, because $s_{pk} \leq s_{mk}$ and $s_{pk} \leq s_{sk}$ by Equation (2.7), only the injected

damping $-k_{mk}\dot{q}_{mk}$ and $-k_{sk}\dot{q}_{sk}$ can saturate the P+d component of a joint control torque and, therefore, $\text{sgn}\left(\text{sat}_{ik}(\cdot)\right) = \text{sgn}(-\dot{q}_{ik})$ for any such joint.

In $\dot{V}$, $\dot{V}_{ss}$ collects all terms that correspond to joint pairs with P+d torques saturated both on the master and slave sides, i.e., P+d torque pairs $\text{sat}_{mk}(\cdot)$ and $\text{sat}_{sk}(\cdot)$ for all $k \in k_{ss}$. Therefore, $\dot{V}_{ss}$ can be bounded by:

$$\begin{aligned}\dot{V}_{ss} &= \sum_{k\in k_{ss}} \Big\{ \dot{q}_{mk}\text{sat}_{pk}[p_k(q_{mk}-q_{sk})] + \dot{q}_{sk}\text{sat}_{pk}[p_k(q_{sk}-q_{mk})] - |\dot{q}_{mk}|s_{mk} - |\dot{q}_{sk}|s_{sk} \Big\} \\ &\leq \sum_{k\in k_{ss}} \Big\{ -|\dot{q}_{mk}|s_{mk} + |\dot{q}_{mk}|s_{pk} - |\dot{q}_{sk}|s_{sk} + |\dot{q}_{sk}|s_{pk} \Big\} \leq 0.\end{aligned} \tag{2.14}$$

Collecting in $\dot{V}_{us}$ all terms that correspond to joint pairs with P+d torques unsaturated on the master side and saturated on the slave side, i.e., $-\text{sat}_{pk}[p_k(q_{mk} - q_{sdk})] - k_{mk}\dot{q}_{mk}$ and $\text{sat}_{sk}(\cdot)$ for all $k \in k_{us}$, $\dot{V}_{us}$ can be bounded by:

$$\begin{aligned}\dot{V}_{us} &= \sum_{k\in k_{us}} \Big\{ -\dot{q}_{mk}\text{sat}_{pk}\Big[p_k(q_{mk}-q_{sdk})\Big] + \dot{q}_{mk}\text{sat}_{pk}\Big[p_k(q_{mk}-q_{sk})\Big] \\ &\qquad\qquad - k_{mk}\dot{q}_{mk}^2 - |\dot{q}_{sk}|s_{sk} + \dot{q}_{sk}\text{sat}_{pk}\Big[p_k(q_{sk}-q_{mk})\Big]\Big\} \\ &\leq \sum_{k\in k_{us}} \Big\{ |\dot{q}_{mk}|s_{pk} - k_{mk}\dot{q}_{mk}^2 + |\dot{q}_{mk}|s_{pk} - |\dot{q}_{sk}|s_{sk} + |\dot{q}_{sk}|s_{pk} \Big\} \\ &\leq \sum_{k\in k_{us}} \Big\{ k_{mk}^{-1}s_{pk}^2 - |\dot{q}_{sk}|(s_{sk}-s_{pk}) \Big\}.\end{aligned} \tag{2.15}$$

Because $|\text{sat}_{sk}(\cdot)| = s_{sk}$ and $s_{sk} \geq s_{pk}$, the slave joint velocity $\dot{q}_{sk}$ must satisfy:

$$s_{pk} + k_{sk}|\dot{q}_{sk}| \geq s_{sk} \Leftrightarrow |\dot{q}_{sk}| \geq k_{sk}^{-1}(s_{sk} - s_{pk}).$$

Then, selecting

$$s_{pk} \leq \frac{\sqrt{k_{mk}}}{\sqrt{k_{mk}} + \sqrt{k_{sk}}} s_{sk}, \tag{2.16}$$

guarantees that

$$\dot{V}_{us} \leq \sum_{k\in k_{us}} \Big\{ k_{mk}^{-1}s_{pk}^2 - k_{sk}^{-1}(s_{sk}-s_{pk})^2 \Big\} \leq 0. \tag{2.17}$$

Similarly, collecting in $\dot{V}_{su}$ all terms that correspond to joint pairs with P+d torques saturated on the master side and unsaturated on the slave side, i.e., $\text{sat}_{mk}(\cdot)$

and $-\text{sat}_{pk}[p_k(q_{sk} - q_{mdk})] - k_{sk}\dot{q}_{sk}$ for all $k \in k_{su}$, and selecting

$$s_{pk} \leq \frac{\sqrt{k_{sk}}}{\sqrt{k_{mk}} + \sqrt{k_{sk}}} s_{mk}, \tag{2.18}$$

guarantees that

$$\dot{V}_{su} \leq \sum_{k \in k_{su}} \Big\{ -k_{mk}^{-1}(s_{mk} - s_{pk})^2 + k_{sk}^{-1} s_{pk}^2 \Big\} \leq 0. \tag{2.19}$$

Equations (2.13), (2.14), (2.17) and (2.19) upper bound $\dot{V}$ by

$$\dot{V} \leq \sum_{k \in k_{uu}} \Big\{ |\dot{q}_{mk}| p_k \int_{t-d_s}^{t} |\dot{q}_{sk}| d\xi - k_{mk}\dot{q}_{mk}^2 + |\dot{q}_{sk}| p_k \int_{t-d_m}^{t} |\dot{q}_{mk}| d\xi - k_{sk}\dot{q}_{sk}^2 \Big\}. \tag{2.20}$$

Integration from 0 to t of Equation (2.20) together with lemma L.1 yields

$$\begin{aligned} V(t) \leq & \sum_{k \in k_{uu}} \Big\{ \frac{p_k}{2} \Big(\alpha \|\dot{q}_{mk}\|_2^2 + \frac{\overline{d}_s^2}{\alpha} \|\dot{q}_{sk}\|_2^2 \Big) - k_{mk} \|\dot{q}_{mk}\|_2^2 \\ & + \frac{p_k}{2} \Big(\beta \|\dot{q}_{sk}\|_2^2 + \frac{\overline{d}_m^2}{\beta} \|\dot{q}_{mk}\|_2^2 \Big) - k_{sk} \|\dot{q}_{sk}\|_2^2 \Big\} + V(0) \\ = & V(0) - \sum_{k \in k_{uu}} \Big\{ \Big[k_{mk} - \frac{p_k}{2} \Big(\alpha + \frac{\overline{d}_m^2}{\beta} \Big) \Big] \|\dot{q}_{mk}\|_2^2 + \Big[k_{sk} - \frac{p_k}{2} \Big(\beta + \frac{\overline{d}_s^2}{\alpha} \Big) \Big] \|\dot{q}_{sk}\|_2^2 \Big\}, \end{aligned} \tag{2.21}$$

which implies that $V(t)$ is bounded and the system is stable if

$$\begin{cases} k_{mk} \geq & \frac{p_k}{2} \Big(\alpha + \frac{\overline{d}_m^2}{\beta} \Big) \\ k_{sk} \geq & \frac{p_k}{2} \Big(\beta + \frac{\overline{d}_s^2}{\alpha} \Big) \end{cases}. \tag{2.22}$$

Theorem 1. *For the teleoperation system in Equation (2.1) with bounded actuation, system uncertainties and time-varying delays under the bounded P+d control Equation (2.6), if the proportional and local damping gains are selected to obey conditions (2.7), (2.16), (2.18) and (2.22) and the daptive gravity compensations update follows Equations (2.8)-(2.9), then:*

1 *The velocities and position error are bounded, i.e.,* $\{\dot{\mathbf{q}}_m, \dot{\mathbf{q}}_s, \mathbf{q}_m - \mathbf{q}_s\} \in \mathcal{L}_\infty$, *moreover,* $\{\dot{\mathbf{q}}_m, \dot{\mathbf{q}}_s\} \in \mathcal{L}_2$.

2 *The velocities and position error globally asymptotically converge to zero when*

the hand and environment forces vanish, i.e., $\{\dot{\mathbf{q}}_m, \dot{\mathbf{q}}_s, \mathbf{q}_m - \mathbf{q}_s\} \to \mathbf{0}$ *as* $t \to \infty$.

Proof. The proof is similar to that in [29], so it is omitted here. □

The performance of the proposed bounded P+d with adaptive gravity compensation controller is verified through simulations on a planar 2-DOF teleoperation system as shown in Figure. 2.3. The master and slave masses and link lengths are $m_{ik} = 0.1$ kg, $l_{ik} = 0.5$ m, $i = m, s$ and $k = 1, 2$. The upper and lower bounds of the unknown parameter vectors $\boldsymbol{\theta}_i$ are $\overline{\boldsymbol{\theta}}_i = (0.6 \quad 1.1)^\mathsf{T}$ and $\underline{\boldsymbol{\theta}}_i = (0.4 \quad 0.9)^\mathsf{T}$, $i = m, s$, respectively. Then, their gravity torques are upper-bounded by $\boldsymbol{\gamma}_i = (1.7 \quad 0.6)^\mathsf{T}$ Nm. The maximum torques of actuators of the first and second robot joints are $\overline{\tau}_{i1} = 2.5$ Nm and $\overline{\tau}_{i2} = 1$ Nm. The asymmetric time-varying delays d_m and d_s are upper bounded by $\overline{d}_m = 0.2$ s and $\overline{d}_s = 0.1$ s. The simulated environment is a wall with stiffness $k_e = 1000$ N/m, located at $y_e = 0.2$ m. In the simulations, the robots move in the vertical plane, starting at rest at the configuration $\left(\mathbf{q}_{m0}^\mathsf{T} \quad \dot{\mathbf{q}}_{m0}^\mathsf{T}\right)^\mathsf{T} = \left(\mathbf{q}_{s0}^\mathsf{T} \quad \dot{\mathbf{q}}_{s0}^\mathsf{T}\right)^\mathsf{T} = \left(\mathbf{0}^\mathsf{T} \quad \mathbf{0}^\mathsf{T}\right)^\mathsf{T}$ with initial estimated parameter vectors $\hat{\boldsymbol{\theta}}_m = \hat{\boldsymbol{\theta}}_s = (0.5 \quad 1)^\mathsf{T}$, and under the user-applied vertical (along the y-axis) sinusoidal force $F_{hy} = 0.5\sin(0.2\pi t) + 0.2$ N.

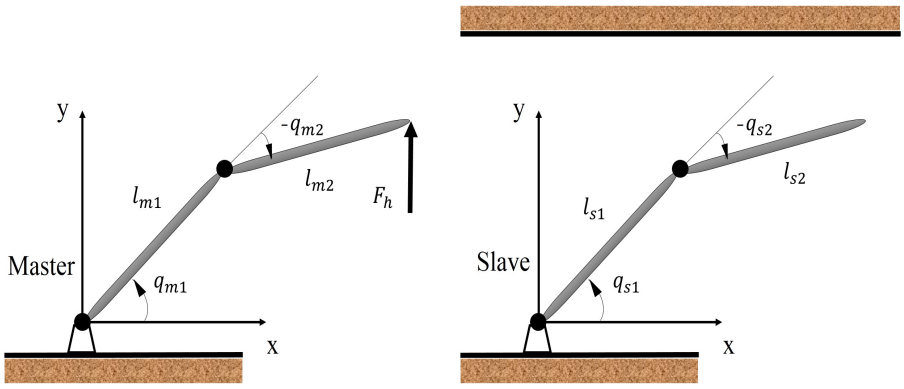

Figure 2.3: Teleoperation system based on 2-DOF arm robots.

After choosing $\alpha = \beta = 0.2$ and $\mathbf{P}_m = \mathbf{P}_s = 10\mathbf{I}$, condition (2.22) can be fulfilled by selecting $\mathbf{K}_m = \mathbf{K}_s = 2\mathbf{I}$. Further, conditions (2.7), (2.16) and (2.18) are met by selecting the inner saturation of the proportional terms $s_{p1} = 0.4$ Nm and $s_{p2} = 0.2$ Nm and the outer saturation of the damping plus saturated proportional terms $s_{i1} = 0.8$ Nm and $s_{i2} = 0.4$ Nm for all joints of both robots.

To save space, only position, control torque and gravity compensation information of the master and slave first joints are presented here. The master and slave positions

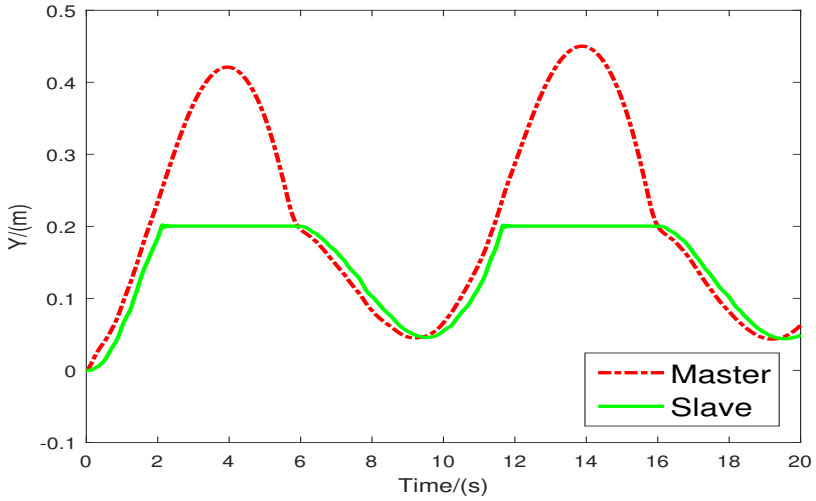

Figure 2.4: Simulated position tracking along y-axis, under sinusoidal user force, during interaction with a passive wall with stiffness $k_e = 1000$ N/m.

along the vertical y-axis are presented in Figure. 2.4. This figure shows that, in free motion ($y < 0.2$ m), the slave follows the master, with small fluctuations caused by the time-varying communication delays. During slave-environment contact ($y \geq 0.2$ m), the master continues to move forward and, similarly to the classical P+d control, the position error between the master and slave increases.

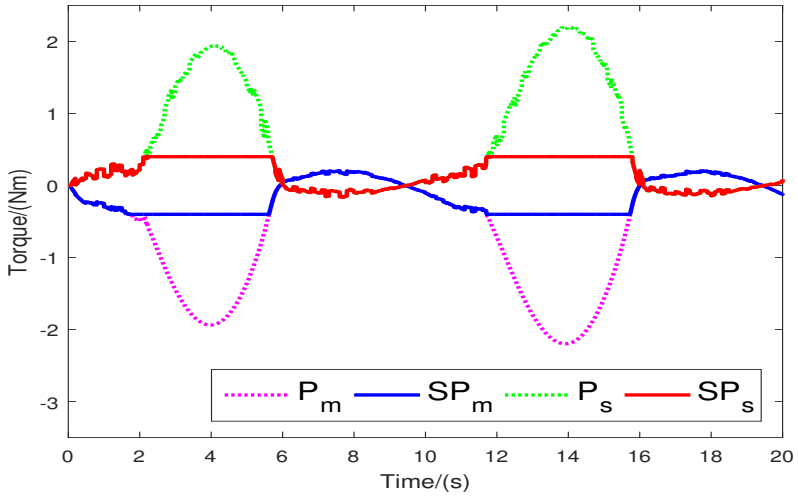

Figure 2.5: Unsaturated and saturated proportional terms on master: P_m, SP_m and on slave: P_s and SP_s.

Figure. 2.5 depicts the saturated proportional control terms on the master $SP_m =$

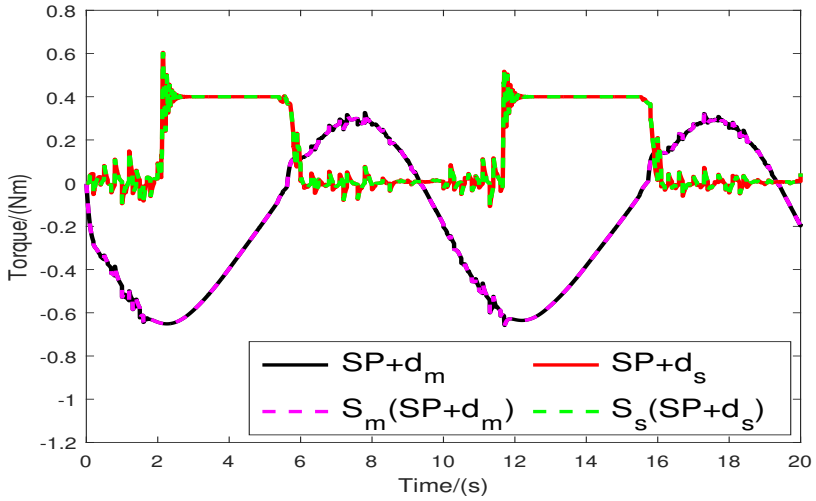

Figure 2.6: Unsaturated and saturated SP+d terms on master: $\mathrm{SP{+}d_m}$, $\mathrm{S_m(SP{+}d_m)}$ and on slave: $\mathrm{SP{+}d_s}$ and $\mathrm{S_s(SP{+}d_s)}$.

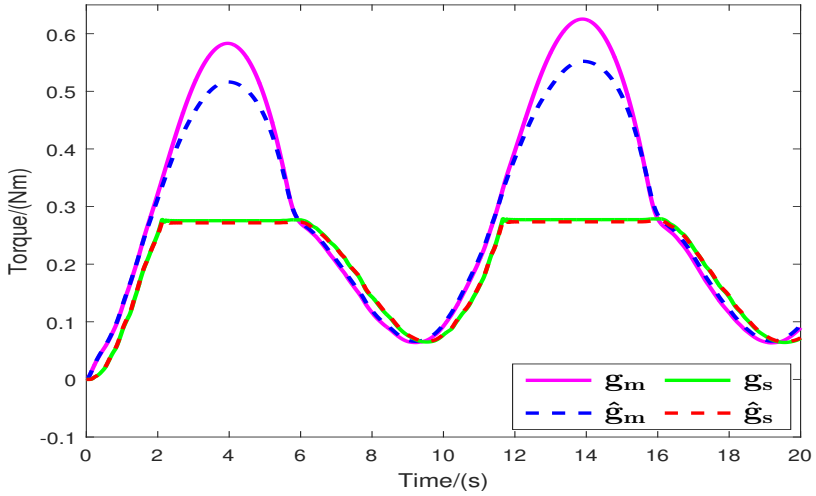

Figure 2.7: Actual and estimated gravity torques g_{m1}, $\hat{g}_{m1}$, g_{s1}, $\hat{g}_{s1}$ in master and slave controllers.

$\mathrm{Sat}_p\Big(-\mathbf{P}(\mathbf{q}_m-\mathbf{q}_{sd})\Big)$ and slave $\mathrm{SP_s}=\mathrm{Sat}_p\Big(-\mathbf{P}(\mathbf{q}_s-\mathbf{q}_{md})\Big)$ sides together with their unsaturated versions $\mathrm{P_m}=-\mathbf{P}(\mathbf{q}_m-\mathbf{q}_{sd})$ and $\mathrm{P_s}=-\mathbf{P}(\mathbf{q}_s-\mathbf{q}_{md})$. It illustrates that the inner saturation functions $\mathrm{Sat}_p(\cdot)$ limit the proportional control terms, especially during slave contact with the environment. Figure. 2.6 shows the saturated proportional plus damping control terms of the two robots $\mathrm{SP{+}d_m}=\mathrm{Sat}_p\Big(-\mathbf{P}(\mathbf{q}_m-\mathbf{q}_{sd})\Big)-\mathbf{K}_m\dot{\mathbf{q}}_m$ and $\mathrm{SP{+}d_s}=\mathrm{Sat}_p\Big(-\mathbf{P}(\mathbf{q}_s-\mathbf{q}_{md})\Big)-\mathbf{K}_s\dot{\mathbf{q}}_s$ together

with their saturated versions $\mathrm{S_m(SP{+}d_m)} = \mathrm{Sat}_m\Big(\mathrm{Sat}_p\Big[-\mathbf{P}(\mathbf{q}_m - \mathbf{q}_{sd})\Big] - \mathbf{K}_m\dot{\mathbf{q}}_m\Big)$ and $\mathrm{S_s(SP{+}d_s)} = \mathrm{Sat}_s\Big(\mathrm{Sat}_p\Big[-\mathbf{P}(\mathbf{q}_s - \mathbf{q}_{md})\Big] - \mathbf{K}_s\dot{\mathbf{q}}_s\Big)$. It illustrates that the outer saturations $\mathrm{Sat}_m(\cdot)$ and $\mathrm{Sat}_s(\cdot)$ have not been breached, which implies that the bounded P+d strategy is conservative in the sense that it does not exploit actuator capabilities fully.

The estimated gravity torques through the designed update laws in master and slave controllers are compared with the real master and slave gravity torques in Figure. 2.7. It shows that the estimated gravity torques used in the controllers are close to the system's gravity torques with only observable estimation errors in $\hat{g}_{m1}$ at about 4 s and 14 s.

2.3 Output Feedback Control

Stable bilateral teleoperation with time-varying delays under the conventional P+d control relies on master and slave velocity measurements. To stabilize the system without using velocity measurements, a simplified and augmented I&I globally convergent velocity observer is introduced in this section, which can be integrated in the conventional P+d control to stabilize the system with exponential velocity estimation convergence.

Rewrite the dynamics of the master and slave robots (2.1) in state space:

$$\begin{aligned}\dot{\mathbf{y}}_i =& \mathbf{x}_i \\ \dot{\mathbf{x}}_i =& \mathbf{M}_i^{-1}(\mathbf{y}_i)\left[-\mathbf{C}_i(\mathbf{y}_i,\mathbf{x}_i)\mathbf{x}_i - \mathbf{g}_i(\mathbf{y}_i) + \mathbf{u}_i\right]\end{aligned} \tag{2.23}$$

where: $\mathbf{y}_i = \mathbf{q}_i$, $\mathbf{x}_i = \dot{\mathbf{q}}_i$, $\mathbf{u}_m = \boldsymbol{\tau}_m + \boldsymbol{\tau}_h$ and $\mathbf{u}_s = \boldsymbol{\tau}_s + \boldsymbol{\tau}_e$ with $i = m, s$. Then the simplified and augmented I&I observers on the master and slave sides can be designed as:

$$\begin{aligned}\hat{\mathbf{x}}_i =& \boldsymbol{\xi}_i + k_{xi}(r_i,\hat{\sigma}_i)\mathbf{y}_i \\ \dot{\boldsymbol{\xi}}_i =& \mathbf{f}_i - k_{xi}(r_i,\hat{\sigma}_i)\hat{\mathbf{x}}_i - \frac{\partial k_{xi}(r_i,\hat{\sigma}_i)}{\partial r_i}\dot{r}_i\mathbf{y}_i - \frac{\partial k_{xi}(r_i,\hat{\sigma}_i)}{\partial \hat{\sigma}_i}\dot{\hat{\sigma}}_i\mathbf{y}_i \\ \dot{r}_i =& -\frac{k_r}{2}(r_i - c_{ri}) + \frac{1}{\lambda_{i1}}\bar{\Delta}_{\sigma i}(\sigma_i,\hat{\sigma}_i)|\tilde{\sigma}_i|r_i \\ \dot{\hat{\sigma}}_i =& \mathrm{Proj}_{\hat{\sigma}_i}\left(2\left[\hat{\mathbf{x}}_i^{\mathsf{T}}\mathbf{f}_i + k_{\sigma i}(\hat{\mathbf{x}}_i,r_i,\hat{\sigma}_i)\tilde{\sigma}_i\right]\right)\end{aligned} \tag{2.24}$$

where $i = m, s$ and:

$$\begin{aligned}
\mathbf{f}_i =& \mathbf{M}_i^{-1}(\mathbf{y}_i)\left[-\mathbf{C}_i(\mathbf{y}_i, \hat{\mathbf{x}}_i)\hat{\mathbf{x}}_i - \mathbf{g}_i(\mathbf{y}_i) + \mathbf{u}_i\right] \\
\Delta_{\sigma i}(\sigma_i, \hat{\sigma}_i) =& c_i \left|\sqrt{1+\sigma_i} - \sqrt{1+\hat{\sigma}_i}\right| \\
\bar{\Delta}_{\sigma i}(\sigma_i, \hat{\sigma}_i) =& \begin{cases} \frac{\Delta_{\sigma i}(\sigma_i, \hat{\sigma}_i)}{|\tilde{\sigma}_i|} & \Delta_{\sigma i}(\sigma_i, \hat{\sigma}_i) > \epsilon_{\sigma i} \\ \frac{\Delta_{\sigma i}(\sigma_i, \hat{\sigma}_i)}{|\Delta_{\sigma i} - \epsilon_{\sigma i}| + |\tilde{\sigma}_i|} & \text{else} \end{cases} \\
\text{Proj}_{\hat{\sigma}_i}(\tau) =& \begin{cases} \tau & \hat{\sigma}_i > 0 \text{ or } \tau \geq 0 \\ (1 - c_{\sigma i}(\hat{\sigma}_i))\tau & -\epsilon_i \leq \hat{\sigma}_i \leq 0, \tau < 0 \end{cases} \\
k_{xi}(r_i, \hat{\sigma}_i) =& \frac{1}{\lambda_{i1}}\left[c_i\sqrt{1+\hat{\sigma}_i} + \frac{k_r}{4}(2\lambda_{i1} + \lambda_{i2} + 1) + \epsilon_{\sigma i} + \frac{\alpha_i}{2}\overline{k}_i r_i^2\right] \\
k_{\sigma i}(\hat{\mathbf{x}}_i, r_i, \hat{\sigma}_i) =& k_r + \frac{r_i^2}{k_r}\left(\frac{\bar{\Delta}_{\sigma i}^2(\sigma_i, \hat{\sigma}_i)}{\lambda_{i1}^2} + k_{xi}^2(r_i, \hat{\sigma}_i)\|\hat{\mathbf{x}}_i\|^2\right)
\end{aligned}$$

with c_{ri}, k_r and $\epsilon_{\sigma i}$ positive constants and $c_{\sigma i}(\hat{\sigma}_i) = \min\{1, \frac{-\hat{\sigma}_i}{\epsilon_i}\}$ for $0 < \epsilon_i < 1$. The observer output $\hat{\mathbf{x}}_i$ and the observer state $\hat{\sigma}_i$ are estimates of $\mathbf{x}_i$ and $\sigma_i = \|\hat{\mathbf{x}}_i\|^2$, respectively, with corresponding estimation errors $\tilde{\mathbf{x}}_i = \mathbf{x}_i - \hat{\mathbf{x}}_i$ and $\tilde{\sigma}_i = \sigma_i - \hat{\sigma}_i$.

The main challenge in the design of observers for Euler-Lagrange systems is posed by the Coriolis and centrifugal forces that appear as square nonlinearities in the system dynamics. To dominate the nonlinear Coriolis and centrifugal effects, we employ the dynamic scaling factor r_i and the projection-based adaptive law $\dot{\hat{\sigma}}$. By design, $[c_{ri}, +\infty)$ is an invariant set of r_i, i.e., if $r_i(0) \geq c_{ri} > 0$, then $r_i(t) \geq c_{ri} > 0$, $\forall t \geq 0$.

Compared with [70, 71, 74, 79], the estimates of $\mathbf{y}_i$ are removed in our observer, so the dimensions of the new observers are reduced from $2n + 2$ in [74] to $n + 2$, which simplifies the observer design procedure. It is important that, to dissipate the redundant energy generated by time delays and velocity estimation errors, the gains $k_{xi}(r_i, \hat{\sigma}_i)$ adapt with dynamic scaling factors r_i, indicating that faster velocity estimation convergence is required for guaranteed stability of bilateral teleoperation systems with time-varying delays. Further, the new constructive observers avoid using approximation techniques to solve the PDE of the estimates dynamics [70, 71, 79].

Given the velocity observers in Equation (2.24), correspondingly, the conventional P+d teleoperation control can be implemented using the velocity estimates $\dot{\hat{\mathbf{q}}}_i = \hat{\mathbf{x}}_i$

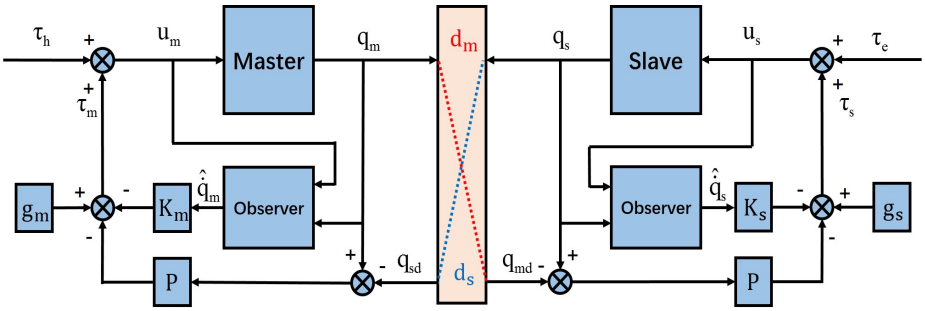

Figure 2.8: Teleoperation system under the augmented I&I observer-based P+d control in Equation (2.25).

instead of the velocity measurements, as shown in Figure. 2.8:

$$\begin{aligned} \boldsymbol{\tau}_m &= -\mathbf{P}(\mathbf{q}_m - \mathbf{q}_{sd}) - \mathbf{K}_m \dot{\hat{\mathbf{q}}}_m + \mathbf{g}_m \\ \boldsymbol{\tau}_s &= -\mathbf{P}(\mathbf{q}_s - \mathbf{q}_{md}) - \mathbf{K}_s \dot{\hat{\mathbf{q}}}_s + \mathbf{g}_s \end{aligned} . \tag{2.25}$$

Compared to Equation (2.2), since the damping injection in Equation (2.25) is based on estimated velocities, the estimation errors can also inject energy in the closed-loop system and potentially lead to instability. The design methodology is then to use the augmented I&I observers to consume the energy generated by the estimation errors. To this end, the master and slave observers have more general dynamics than in [74], with gains $k_{xi}(r_i, \hat{\sigma}_i)$ that depend not only on $\hat{\sigma}_i$ but also on the scaling factors r_i. The more general dynamics require additional care to be taken in the observer design to reduce the partial derivative of $k_{xi}(r_i, \hat{\sigma}_i)$ with respect to r_i in $\dot{\xi}_i$.

To prove the system stability and velocity estimation convergence, consider the following Lyapunov-Krasovskii functional:

$$V = V_p + V_\eta + V_r + V_\sigma \tag{2.26}$$

with

$$\begin{aligned} V_p =& \frac{1}{2}\dot{\mathbf{q}}_m^\mathsf{T}\mathbf{M}_m\dot{\mathbf{q}}_m + \frac{1}{2}\dot{\mathbf{q}}_s^\mathsf{T}\mathbf{M}_s\dot{\mathbf{q}}_s + \frac{1}{2}(\mathbf{q}_m - \mathbf{q}_s)^\mathsf{T}\mathbf{P}(\mathbf{q}_m - \mathbf{q}_s) - \int_0^t \dot{\mathbf{q}}_m^\mathsf{T}\boldsymbol{\tau}_h d\xi + E_h \\ & - \int_0^t \dot{\mathbf{q}}_s^\mathsf{T}\boldsymbol{\tau}_e d\xi + E_e + \int_{-\bar{d}_m}^0 \int_{t+\theta}^t \dot{\mathbf{q}}_m^\mathsf{T}\mathbf{Q}_m\dot{\mathbf{q}}_m d\xi d\theta + \int_{-\bar{d}_s}^0 \int_{t+\theta}^t \dot{\mathbf{q}}_s^\mathsf{T}\mathbf{Q}_s\dot{\mathbf{q}}_s d\xi d\theta \\ V_\eta =& \frac{1}{2}\boldsymbol{\eta}_m^\mathsf{T}\mathbf{M}_m\boldsymbol{\eta}_m + \frac{1}{2}\boldsymbol{\eta}_s^\mathsf{T}\mathbf{M}_s\boldsymbol{\eta}_s, \\ V_r =& \frac{1}{2}(r_m - c_{rm})^2 + \frac{1}{2}(r_s - c_{rs})^2, \end{aligned}$$

$$V_\sigma = \frac{1}{4}\tilde{\sigma}_m^2 + \frac{1}{4}\tilde{\sigma}_s^2.$$

In Equation (2.26): V_p has already been defined in Section 2.2; V_η, V_r and V_σ are quadratic terms related to the observer states, with $\boldsymbol{\eta}_i = \frac{\tilde{\mathbf{x}}_i}{r_i}$ being scaled versions of the velocity estimation errors, i.e., of the off-the-manifold coordinates according to the I&I observer design methodology. The V_η, V_r and V_σ will be used to prove both global convergence of the velocity estimates and that the observers themselves dissipate the harmful energy generated by the estimation errors.

From Equation (2.4) and lemma L.2, the derivative of V_p is upper bounded by

$$\begin{aligned}
\dot{V}_p \leq & -\dot{\mathbf{q}}_m^\mathsf{T}\mathbf{K}_m\dot{\tilde{\mathbf{q}}}_m + \overline{d}_m\dot{\mathbf{q}}_m^\mathsf{T}\mathbf{Q}_m\dot{\mathbf{q}}_m + \frac{1}{4}\overline{d}_s\dot{\mathbf{q}}_m^\mathsf{T}\mathbf{P}\mathbf{Q}_s^{-1}\mathbf{P}^\mathsf{T}\dot{\mathbf{q}}_m \\
& -\dot{\mathbf{q}}_s^\mathsf{T}\mathbf{K}_s\dot{\tilde{\mathbf{q}}}_s + \overline{d}_s\dot{\mathbf{q}}_s^\mathsf{T}\mathbf{Q}_s\dot{\mathbf{q}}_s + \frac{1}{4}\overline{d}_m\dot{\mathbf{q}}_s^\mathsf{T}\mathbf{P}\mathbf{Q}_m^{-1}\mathbf{P}^\mathsf{T}\dot{\mathbf{q}}_s \\
\leq & -\dot{\mathbf{q}}_m^\mathsf{T}\left(\mathbf{K}_m - \frac{1}{\alpha_m}\mathbf{K}_m - \overline{d}_m\mathbf{Q}_m - \frac{1}{4}\overline{d}_s\mathbf{P}\mathbf{Q}_s^{-1}\mathbf{P}^\mathsf{T}\right)\dot{\mathbf{q}}_m + \frac{1}{4}\alpha_m\dot{\tilde{\mathbf{q}}}_m^\mathsf{T}\mathbf{K}_m\dot{\tilde{\mathbf{q}}}_m \\
& -\dot{\mathbf{q}}_s^\mathsf{T}\left(\mathbf{K}_s - \frac{1}{\alpha_s}\mathbf{K}_s - \overline{d}_s\mathbf{Q}_s - \frac{1}{4}\overline{d}_m\mathbf{P}\mathbf{Q}_m^{-1}\mathbf{P}^\mathsf{T}\right)\dot{\mathbf{q}}_s + \frac{1}{4}\alpha_s\dot{\tilde{\mathbf{q}}}_s^\mathsf{T}\mathbf{K}_s\dot{\tilde{\mathbf{q}}}_s.
\end{aligned} \tag{2.27}$$

And in Equation (2.24), the derivatives of $\hat{\mathbf{x}}_i$ are

$$\begin{aligned}
\dot{\hat{\mathbf{x}}}_i =& \dot{\boldsymbol{\xi}}_i + k_{xi}(r_i,\hat{\sigma}_i)\dot{\mathbf{y}}_i + \frac{\partial k_{xi}(r_i,\hat{\sigma}_i)}{\partial r_i}\dot{r}_i\mathbf{y}_i + \frac{\partial k_{xi}(r_i,\hat{\sigma}_i)}{\partial \hat{\sigma}_i}\dot{\hat{\sigma}}_i\mathbf{y}_i \\
=& \mathbf{f}_i - k_{xi}(r_i,\hat{\sigma}_i)\hat{\mathbf{x}}_i + k_{xi}(r_i,\hat{\sigma}_i)\dot{\mathbf{y}}_i = \mathbf{f}_i + k_{xi}(r_i,\hat{\sigma}_i)\tilde{\mathbf{x}}_i.
\end{aligned} \tag{2.28}$$

Therefore, subtracting Equation (2.28) from Equation (2.23) and using property P.2 leads to

$$\begin{aligned}
\dot{\tilde{\mathbf{x}}}_i =& \mathbf{M}_i^{-1}(\mathbf{y}_i)\left[-\mathbf{C}_i(\mathbf{y}_i,\mathbf{x}_i)\mathbf{x}_i - \mathbf{g}_i(\mathbf{y}_i) + \mathbf{u}_i\right] - \mathbf{f}_i - k_{xi}(r_i,\hat{\sigma}_i)\tilde{\mathbf{x}}_i \\
=& \mathbf{M}_i^{-1}(\mathbf{y}_i)\left[\mathbf{u}_i - \mathbf{C}_i(\mathbf{y}_i,\mathbf{x}_i)\mathbf{x}_i - \mathbf{g}_i(\mathbf{y}_i) + \mathbf{C}_i(\mathbf{y}_i,\hat{\mathbf{x}}_i)\hat{\mathbf{x}}_i + \mathbf{g}_i(\mathbf{y}_i) - \mathbf{u}_i\right] - k_{xi}(r_i,\hat{\sigma}_i)\tilde{\mathbf{x}}_i \\
=& \mathbf{M}_i^{-1}(\mathbf{y}_i)\left[\mathbf{C}_i(\mathbf{y}_i,\mathbf{x}_i)\hat{\mathbf{x}}_i - \mathbf{C}_i(\mathbf{y}_i,\mathbf{x}_i)\mathbf{x}_i + \mathbf{C}_i(\mathbf{y}_i,\hat{\mathbf{x}}_i)\hat{\mathbf{x}}_i - \mathbf{C}_i(\mathbf{y}_i,\mathbf{x}_i)\hat{\mathbf{x}}_i\right] - k_{xi}(r_i,\hat{\sigma}_i)\tilde{\mathbf{x}}_i \\
=& -\mathbf{M}_i^{-1}(\mathbf{y}_i)\left[\mathbf{C}_i(\mathbf{y}_i,\mathbf{x}_i)\tilde{\mathbf{x}}_i + \mathbf{C}_i(\mathbf{y}_i,\tilde{\mathbf{x}}_i)\hat{\mathbf{x}}_i\right] - k_{xi}(r_i,\hat{\sigma}_i)\tilde{\mathbf{x}}_i,
\end{aligned} \tag{2.29}$$

where

$$\begin{aligned}
\|\mathbf{C}_i(\mathbf{y}_i,\tilde{\mathbf{x}}_i)\hat{\mathbf{x}}_i\| \leq & c_i\|\tilde{\mathbf{x}}_i\|\|\hat{\mathbf{x}}_i\| < c_i\|\tilde{\mathbf{x}}_i\|\sqrt{1+\sigma_i} \\
\leq & c_i\|\tilde{\mathbf{x}}_i\|\sqrt{1+\hat{\sigma}_i} + c_i\|\tilde{\mathbf{x}}_i\|\left|\sqrt{1+\sigma_i} - \sqrt{1+\hat{\sigma}_i}\right| \\
\leq & c_i\|\tilde{\mathbf{x}}_i\|\sqrt{1+\hat{\sigma}_i} + \bar{\Delta}_{\sigma i}(\sigma_i,\hat{\sigma}_i)|\tilde{\sigma}_i|\|\tilde{\mathbf{x}}_i\| + \epsilon_{\sigma i}\|\tilde{\mathbf{x}}_i\|,
\end{aligned} \tag{2.30}$$

because $\Delta_{\sigma i}(\sigma_i, \hat{\sigma}_i) \leq \bar{\Delta}_{\sigma i}(\sigma_i, \hat{\sigma}_i)|\tilde{\sigma}_i| + \epsilon_{\sigma i}$. Further, given the derivative of $\boldsymbol{\eta}_i$,

$$\begin{aligned}\dot{\boldsymbol{\eta}}_i =& \frac{1}{r_i}\dot{\tilde{\mathbf{x}}}_i - \frac{\dot{r}_i}{r_i^2}\tilde{\mathbf{x}}_i \\ =& -\mathbf{M}_i^{-1}(\mathbf{y}_i)\mathbf{C}_i(\mathbf{y}_i, \mathbf{x}_i)\boldsymbol{\eta}_i - \frac{1}{r_i}\mathbf{M}_i^{-1}(\mathbf{y}_i)\mathbf{C}_i(\mathbf{y}_i, \tilde{\mathbf{x}}_i)\hat{\mathbf{x}}_i - k_{xi}(r_i, \hat{\sigma}_i)\boldsymbol{\eta}_i - \frac{\dot{r}_i}{r_i}\boldsymbol{\eta}_i,\end{aligned} \tag{2.31}$$

the derivative of V_η can be bounded by

$$\begin{aligned}\dot{V}_\eta =& \frac{1}{2}\boldsymbol{\eta}_m^\mathsf{T}\dot{\mathbf{M}}_m\boldsymbol{\eta}_m + \boldsymbol{\eta}_m^\mathsf{T}\mathbf{M}_m\dot{\boldsymbol{\eta}}_m + \frac{1}{2}\boldsymbol{\eta}_s^\mathsf{T}\dot{\mathbf{M}}_s\boldsymbol{\eta}_s + \boldsymbol{\eta}_s^\mathsf{T}\mathbf{M}_s\dot{\boldsymbol{\eta}}_s \\ =& -\frac{\dot{r}_i}{r_i}\boldsymbol{\eta}_m^\mathsf{T}\mathbf{M}_m\boldsymbol{\eta}_m - k_{xi}(r_i, \hat{\sigma}_i)\boldsymbol{\eta}_m^\mathsf{T}\mathbf{M}_m\boldsymbol{\eta}_m - \frac{1}{r_m}\boldsymbol{\eta}_m^\mathsf{T}\mathbf{C}_i(\mathbf{y}_i, \tilde{\mathbf{x}}_m)\hat{\mathbf{x}}_m \\ & - \frac{\dot{r}_s}{r_s}\boldsymbol{\eta}_s^\mathsf{T}\mathbf{M}_s\boldsymbol{\eta}_s - k_{xs}(r_s, \hat{\sigma}_s)\boldsymbol{\eta}_s^\mathsf{T}\mathbf{M}_s\boldsymbol{\eta}_s - \frac{1}{r_s}\boldsymbol{\eta}_s^\mathsf{T}\mathbf{C}_s(\mathbf{y}_s, \tilde{\mathbf{x}}_s)\hat{\mathbf{x}}_s \\ & + \frac{1}{2}\boldsymbol{\eta}_m^\mathsf{T}\left(\dot{\mathbf{M}}_m - 2\mathbf{C}_m(\mathbf{y}_m, \mathbf{x}_m)\right)\boldsymbol{\eta}_m + \frac{1}{2}\boldsymbol{\eta}_s^\mathsf{T}\left(\dot{\mathbf{M}}_s - 2\mathbf{C}_s(\mathbf{y}_s, \mathbf{x}_s)\right)\boldsymbol{\eta}_s \\ \leq& -\frac{\dot{r}_m}{r_m}\lambda_{m1}\boldsymbol{\eta}_m^\mathsf{T}\boldsymbol{\eta}_m - k_{xm}(r_m, \hat{\sigma}_m)\lambda_{m1}\boldsymbol{\eta}_m^\mathsf{T}\boldsymbol{\eta}_m - \frac{1}{r_m}\boldsymbol{\eta}_m^\mathsf{T}\mathbf{C}_m(\mathbf{y}_m, \tilde{\mathbf{x}}_m)\hat{\mathbf{x}}_m \\ & - \frac{\dot{r}_s}{r_s}\lambda_{s1}\boldsymbol{\eta}_s^\mathsf{T}\boldsymbol{\eta}_s - k_{xs}(r_s, \hat{\sigma}_s)\lambda_{s1}\boldsymbol{\eta}_s^\mathsf{T}\boldsymbol{\eta}_s - \frac{1}{r_s}\boldsymbol{\eta}_s^\mathsf{T}\mathbf{C}_s(\mathbf{y}_s, \tilde{\mathbf{x}}_s)\hat{\mathbf{x}}_s.\end{aligned}$$

It may appear that the nonlinear terms could be dominated by $\frac{1}{r_i}\|\boldsymbol{\eta}_i\|\|\mathbf{C}_i(\mathbf{y}_i, \tilde{\mathbf{x}}_i)\hat{\mathbf{x}}_i\| \leq c_i\|\boldsymbol{\eta}_i\|^2\|\hat{\mathbf{x}}_i\|$ for suitable gains k_{xi}. However, because k_{xi} are not independent of $\hat{\mathbf{x}}_i$, a term that depends on the partial derivative of k_{xi} with respect to $\hat{\mathbf{x}}_i$, $\frac{\partial k_{xi}}{\partial \hat{\mathbf{x}}_i}\dot{\hat{\mathbf{x}}}_i\mathbf{y}_i$, should be included in the dynamics of $\dot{\hat{\mathbf{x}}}_i$ in Equation (2.28) and also added in the dynamics of $\dot{\boldsymbol{\xi}}_i$ for cancellation. This term makes the dynamics of $\dot{\boldsymbol{\xi}}_i$ an analytically unsolvable PDE. The difficulty caused by the dependence of k_{xi} on $\hat{\mathbf{x}}_i$ can be avoided through the additional observer state $\hat{\sigma}_i$ estimating $\|\hat{\mathbf{x}}_i\|^2$:

$$\begin{aligned}\dot{V}_\eta \leq& c_m\sqrt{1+\hat{\sigma}_m}\|\boldsymbol{\eta}_m\|^2 + \epsilon_{\sigma m}\|\boldsymbol{\eta}_m\|^2 - \frac{\dot{r}_m}{r_m}\lambda_{m1}\|\boldsymbol{\eta}_m\|^2 - k_{xm}(r_m, \hat{\sigma}_m)\lambda_{m1}\|\boldsymbol{\eta}_m\|^2 \\ & + c_s\sqrt{1+\hat{\sigma}_s}\|\boldsymbol{\eta}_s\|^2 + \epsilon_{\sigma s}\|\boldsymbol{\eta}_s\|^2 - \frac{\dot{r}_s}{r_s}\lambda_{s1}\|\boldsymbol{\eta}_s\|^2 - k_{xs}(r_s, \hat{\sigma}_s)\lambda_{s1}\|\boldsymbol{\eta}_s\|^2 \\ & + \bar{\Delta}_{\sigma m}(\sigma_m, \hat{\sigma}_m)|\tilde{\sigma}_m|\|\boldsymbol{\eta}_m\|^2 + \bar{\Delta}_{\sigma s}(\sigma_s, \hat{\sigma}_s)|\tilde{\sigma}_s|\|\boldsymbol{\eta}_s\|^2.\end{aligned} \tag{2.32}$$

From the dynamics of r_i in Equation (2.24), it follows that

$$-\frac{\dot{r}_i}{r_i}\lambda_{i1}\|\boldsymbol{\eta}_i\|^2 \leq \frac{k_r}{2}\lambda_{i1}\|\boldsymbol{\eta}_i\|^2 - \bar{\Delta}_{\sigma i}(\sigma_i, \hat{\sigma}_i)|\tilde{\sigma}_i|\|\boldsymbol{\eta}_i\|^2,$$

$$\bar{\Delta}_{\sigma i}(\sigma_i,\hat{\sigma}_i)|\tilde{\sigma}_i|\|\boldsymbol{\eta}_i\|^2-\frac{\dot{r}_i}{r_i}\lambda_{i1}\|\boldsymbol{\eta}_i\|^2\leq\frac{k_r}{2}\lambda_{i1}\|\boldsymbol{\eta}_i\|^2.$$

Therefore, the derivative of V_η can be bounded by

$$\begin{aligned}\dot{V}_\eta\leq&c_m\sqrt{1+\hat{\sigma}_m}\|\boldsymbol{\eta}_m\|^2+\frac{k_r}{2}\lambda_{m1}\|\boldsymbol{\eta}_m\|^2+\epsilon_{\sigma m}\|\boldsymbol{\eta}_m\|^2-k_{xm}(r_m,\hat{\sigma}_m)\lambda_{m1}\|\boldsymbol{\eta}_m\|^2\\&+c_s\sqrt{1+\hat{\sigma}_s}\|\boldsymbol{\eta}_s\|^2+\frac{k_r}{2}\lambda_{s1}\|\boldsymbol{\eta}_s\|^2+\epsilon_{\sigma s}\|\boldsymbol{\eta}_s\|^2-k_{xs}(r_s,\hat{\sigma}_s)\lambda_{s1}\|\boldsymbol{\eta}_s\|^2.\end{aligned}\tag{2.33}$$

In Equation (2.32), the Coriolis and centrifugal forces of each robot lead to three nonlinear velocity terms, $c_i\sqrt{1+\hat{\sigma}_i}\|\boldsymbol{\eta}_i\|^2$, $\epsilon_{\sigma i}\|\boldsymbol{\eta}_i\|^2$ and $\bar{\Delta}_{\sigma i}(\sigma_i,\hat{\sigma}_i)|\tilde{\sigma}_i|\|\boldsymbol{\eta}_i\|^2$. The dynamic scaling factors r_i are used to dominate the third nonlinear velocity term at each robot side, $\bar{\Delta}_{\sigma i}(\sigma_i,\hat{\sigma}_i)|\tilde{\sigma}_i|\|\boldsymbol{\eta}_i\|^2$. Then, $-k_{xi}(r_i,\hat{\sigma}_i)\lambda_{i1}\|\boldsymbol{\eta}_i\|^2$ can be used to dominate the sum of $c_i\sqrt{1+\hat{\sigma}_i}\|\boldsymbol{\eta}_i\|^2$ and $\epsilon_{\sigma i}\|\boldsymbol{\eta}_i\|^2$ with $\frac{k_r}{2}\lambda_{i1}\|\boldsymbol{\eta}_i\|^2$ in Equation (2.33), because $\epsilon_{\sigma i}$ and $\frac{k_r}{2}\lambda_{i1}$ are constants and $k_{xi}(r_i,\hat{\sigma}_i)$ depend on $\hat{\sigma}_i$.

Although the dynamic scaling factors r_i dominate the nonlinear velocity terms $\bar{\Delta}_{\sigma i}(\sigma_i,\hat{\sigma}_i)|\tilde{\sigma}_i|\|\boldsymbol{\eta}_i\|^2$, they are potentially unbounded. Their boundedness can be analyzed by considering the derivative of V_r:

$$\begin{aligned}\dot{V}_r=&(r_m-c_{rm})\dot{r}_m+(r_s-c_{rs})\dot{r}_s\\=&\frac{r_m}{\lambda_{m1}}(r_m-c_{rm})\bar{\Delta}_{\sigma m}(\sigma_m,\hat{\sigma}_m)|\tilde{\sigma}_m|-\frac{k_r}{2}(r_m-c_{rm})^2\\&+\frac{r_s}{\lambda_{s1}}(r_s-c_{rs})\bar{\Delta}_{\sigma s}(\sigma_s,\hat{\sigma}_s)|\tilde{\sigma}_s|-\frac{k_r}{2}(r_s-c_{rs})^2.\end{aligned}\tag{2.34}$$

The sign-indefinite terms in Equation (2.34) can be bounded by

$$\frac{r_i}{\lambda_{i1}}(r_i-c_{ri})\bar{\Delta}_{\sigma i}(\sigma_i,\hat{\sigma}_i)|\tilde{\sigma}_i|\leq\frac{k_r}{4}(r_i-c_{ri})^2+\frac{r_i^2}{k_r\lambda_{i1}^2}\bar{\Delta}_{\sigma i}^2(\sigma_i,\hat{\sigma}_i)\tilde{\sigma}_i^2,\quad i=m,s.\tag{2.35}$$

Then, it follows that

$$\dot{V}_r=\frac{r_m^2}{k_r\lambda_{m1}^2}\bar{\Delta}_{\sigma m}^2(\sigma_m,\hat{\sigma}_m)\tilde{\sigma}_m^2+\frac{r_s^2}{k_r\lambda_{s1}^2}\bar{\Delta}_{\sigma s}^2(\sigma_s,\hat{\sigma}_s)\tilde{\sigma}_s^2-\frac{k_r}{4}\left[(r_m-c_{rm})^2+(r_s-c_{rs})^2\right].\tag{2.36}$$

The projection-based adaptive laws in $\dot{\hat{\sigma}}_i$ help dominate $\frac{r_i^2}{k_r\lambda_{i1}^2}\bar{\Delta}_{\sigma i}^2(\sigma_i,\hat{\sigma}_i)\tilde{\sigma}_i^2$ in Equation (2.36). Since $\sigma_i=\|\hat{\mathbf{x}}_i\|^2$, it follows that

$$\dot{\sigma}_i=2\hat{\mathbf{x}}_i^{\mathsf{T}}\dot{\hat{\mathbf{x}}}_i=2\hat{\mathbf{x}}_i^{\mathsf{T}}\mathbf{f}_i+2\hat{\mathbf{x}}_i^{\mathsf{T}}k_{xi}(r_i,\hat{\sigma}_i)\tilde{\mathbf{x}}_i\tag{2.37}$$

and, further, that

$$\begin{aligned}\dot{\tilde{\sigma}}_i =&\dot{\sigma}_i - \dot{\hat{\sigma}}_i = 2\hat{\mathbf{x}}_i^\mathsf{T}\mathbf{f}_i + 2k_{\sigma i}(\hat{\mathbf{x}}_i, r_i, \hat{\sigma}_i)\tilde{\sigma}_i - \mathrm{Proj}_{\hat{\sigma}_i}\left(2[\hat{\mathbf{x}}_i^\mathsf{T}\mathbf{f}_i + k_{\sigma i}(\hat{\mathbf{x}}_i, r_i, \hat{\sigma}_i)\tilde{\sigma}_i]\right)\\ &+ 2\hat{\mathbf{x}}_i^\mathsf{T}k_{xi}(r_i, \hat{\sigma}_i)\tilde{\mathbf{x}}_i - 2k_{\sigma i}(\hat{\mathbf{x}}_i, r_i, \hat{\sigma}_i)\tilde{\sigma}_i.\end{aligned} \tag{2.38}$$

From lemma L.3, the projection operator in Equation (2.24) guarantees that

$$[\tau - \mathrm{Proj}_{\hat{\sigma}}(\tau)]\,\tilde{\sigma} \leq 0, \quad \forall \sigma \geq 0,\, \hat{\sigma} \geq -\epsilon, \tag{2.39}$$

which leads to

$$\begin{aligned}\dot{V}_\sigma =&\frac{1}{2}\tilde{\sigma}_m\dot{\tilde{\sigma}}_m + \frac{1}{2}\tilde{\sigma}_s\dot{\tilde{\sigma}}_s\\ \leq&\tilde{\sigma}_m\hat{\mathbf{x}}_m^\mathsf{T}k_{xm}(r_m, \hat{\sigma}_m)\tilde{\mathbf{x}}_m - k_{\sigma m}(\hat{\mathbf{x}}_m, r_m, \hat{\sigma}_m)\tilde{\sigma}_m^2\\ &+ \tilde{\sigma}_s\hat{\mathbf{x}}_s^\mathsf{T}k_{xs}(r_s, \hat{\sigma}_s)\tilde{\mathbf{x}}_s - k_{\sigma s}(\hat{\mathbf{x}}_s, r_s, \hat{\sigma}_s)\tilde{\sigma}_s^2.\end{aligned} \tag{2.40}$$

Further, $\tilde{\sigma}_i\hat{\mathbf{x}}_i^\mathsf{T}k_{xi}(r_i, \hat{\sigma}_i)\tilde{\mathbf{x}}_i$ in Equation (2.40) can be upper bounded by

$$\tilde{\sigma}_i\hat{\mathbf{x}}_i^\mathsf{T}k_{xi}(r_i, \hat{\sigma}_i)\tilde{\mathbf{x}}_i \leq \frac{r_i^2k_{xi}^2(r_i, \hat{\sigma}_i)}{k_r}\|\hat{\mathbf{x}}_i\|^2\tilde{\sigma}_i^2 + \frac{k_r}{4}\|\boldsymbol{\eta}_i\|^2, \tag{2.41}$$

where $\frac{k_r}{4}\|\boldsymbol{\eta}_i\|^2$ and $\frac{r_i^2k_{xi}^2(r_i,\hat{\sigma}_i)}{k_r}\|\hat{\mathbf{x}}_i\|^2\tilde{\sigma}_i^2$ can be dominated by $-k_{xi}(r_i, \hat{\sigma}_i)\lambda_{i1}\|\boldsymbol{\eta}_i\|^2$ and $-k_{\sigma i}(\hat{\mathbf{x}}_i, r_i, \hat{\sigma}_i)\tilde{\sigma}_i^2$, respectively. It can then follows that

$$\begin{aligned}\dot{V}_\sigma \leq&\frac{r_m^2k_{xm}^2(r_m, \hat{\sigma}_m)}{k_r}\|\hat{\mathbf{x}}_m\|^2\tilde{\sigma}_m^2 - k_{\sigma m}(\hat{\mathbf{x}}_m, r_m, \hat{\sigma}_m)\tilde{\sigma}_m^2 + \frac{r_s^2k_{xs}^2(r_s, \hat{\sigma}_s)}{k_r}\|\hat{\mathbf{x}}_s\|^2\tilde{\sigma}_s^2\\ &- k_{\sigma s}(\hat{\mathbf{x}}_s, r_s, \hat{\sigma}_s)\tilde{\sigma}_s^2 + \frac{k_r}{4}\|\boldsymbol{\eta}_m\|^2 + \frac{k_r}{4}\|\boldsymbol{\eta}_s\|^2.\end{aligned} \tag{2.42}$$

Equations (2.28)-(2.42) show that the observer states r_i and $\hat{\sigma}_i$ are used to dominate the dynamic nonlinearities due to Coriolis and centrifugal effects. However, because the velocity estimation errors generate potentially destabilizing energy that cannot be dissipated by the P+d controllers through damping injection based on velocity estimates, the designed I&I observers need to be augmented to dissipate this energy themselves.

Considering that the terms dependent on the velocity estimation errors in Equation (2.27) are bounded by

$$\frac{\alpha_i}{4}\dot{\tilde{\mathbf{q}}}_i^\mathsf{T}\mathbf{K}_i\dot{\tilde{\mathbf{q}}}_i \leq \frac{\alpha_i}{4}\overline{k}_i r_i^2\|\boldsymbol{\eta}_i\|^2, \tag{2.43}$$

and adding Equation (2.33), (2.36), (2.42) and (2.43) leads to

$$\begin{aligned}&\frac{\alpha_m}{4}\dot{\tilde{\mathbf{q}}}_m^\mathsf{T}\mathbf{K}_m\dot{\tilde{\mathbf{q}}}_m+\frac{\alpha_s}{4}\dot{\tilde{\mathbf{q}}}_s^\mathsf{T}\mathbf{K}_s\dot{\tilde{\mathbf{q}}}_s+\dot{V}_\sigma+\dot{V}_\eta+\dot{V}_r\\ \leq&-\psi_{\eta m}\|\boldsymbol{\eta}_m\|^2-\psi_{\eta s}\|\boldsymbol{\eta}_s\|^2-\psi_{\sigma m}\tilde{\sigma}_m^2-\psi_{\sigma s}\tilde{\sigma}_s^2-\frac{k_r}{4}(r_m-c_{rm})^2-\frac{k_r}{4}(r_s-c_{rs})^2\end{aligned} \tag{2.44}$$

with

$$\begin{aligned}\psi_{\eta m}=&k_{xm}(r_m,\hat{\sigma}_m)\lambda_{m1}-c_m\sqrt{1+\hat{\sigma}_m}-\frac{k_r}{4}(2\lambda_{m1}+1)-\epsilon_{\sigma m}-\frac{\alpha_m}{4}\overline{k}_m r_m^2\\ \psi_{\eta s}=&k_{xs}(r_s,\hat{\sigma}_s)\lambda_{s1}-c_s\sqrt{1+\hat{\sigma}_s}-\frac{k_r}{4}(2\lambda_{s1}+1)-\epsilon_{\sigma s}-\frac{\alpha_s}{4}\overline{k}_s r_s^2\\ \psi_{\sigma m}=&k_{\sigma m}(\hat{\mathbf{x}}_m,r_m,\hat{\sigma}_m)-\frac{r_m^2}{k_r}\left(\frac{\bar{\Delta}_{\sigma m}^2(\sigma_m,\hat{\sigma}_m)}{\lambda_{m1}^2}+k_{xi}^2(r_m,\hat{\sigma}_m)\|\hat{\mathbf{x}}_m\|^2\right)\\ \psi_{\sigma s}=&k_{\sigma s}(\hat{\mathbf{x}}_s,r_s,\hat{\sigma}_s)-\frac{r_s^2}{k_r}\left(\frac{\bar{\Delta}_{\sigma s}^2(\sigma_s,\hat{\sigma}_s)}{\lambda_{s1}^2}+k_{xi}^2(r_s,\hat{\sigma}_s)\|\hat{\mathbf{x}}_s\|^2\right).\end{aligned}$$

For the observer dynamics with parameters properly selected as in Equation (2.24), then Equation (2.44) can be rewritten as

$$\frac{\alpha_m}{4}\dot{\tilde{\mathbf{q}}}_m^\mathsf{T}\mathbf{K}_m\dot{\tilde{\mathbf{q}}}_m+\frac{\alpha_s}{4}\dot{\tilde{\mathbf{q}}}_s^\mathsf{T}\mathbf{K}_s\dot{\tilde{\mathbf{q}}}_s+\dot{V}_\eta+\dot{V}_\sigma+\dot{V}_r\leq-\frac{k_r}{2}\left(V_\eta+V_\sigma+V_r\right). \tag{2.45}$$

Equation (2.45) indicates that the energy generated by the velocity estimation errors is dissipated by the velocity observers through the augmented dynamics in the observer, i.e., by adding $\frac{\alpha_i r_i^2\overline{k}_i}{2\lambda_{i1}}$ in $k_{xi}(r_i,\hat{\sigma}_i)$ and reducing $\frac{\partial k_{xi}(r_i,\hat{\sigma}_i)}{\partial r_i}\dot{r}_i\mathbf{y}_i$ in $\dot{\boldsymbol{\xi}}_i$. More specifically, the dynamics of $\hat{\mathbf{x}}_i$ in Equation (2.24) behave like filters, i.e., $\dot{\hat{\mathbf{x}}}_i=\mathbf{f}_i+k_{xi}(r_i,\hat{\sigma}_i)\tilde{\mathbf{x}}_i$. Correspondingly, the estimation error dynamics in Equation (2.29) suggest that the augmentations $\frac{\alpha_i r_i^2\overline{k}_i}{2\lambda_{i1}}$ in $k_{xi}(r_i,\hat{\sigma}_i)$ increase the speed of convergence of estimation errors. Hence, making the estimation convergence speed depend on the dynamic scaling factors limits the energy generated by the estimation errors within a range that the observers can consume.

After choosing the P+d control gains to obey

$$\begin{cases}\mathbf{K}_m\succeq&\overline{d}_m\mathbf{Q}_m+\frac{1}{4}\overline{d}_s\mathbf{P}\mathbf{Q}_s^{-1}\mathbf{P}^\mathsf{T}+\frac{1}{\alpha_m}\mathbf{K}_m\\ \mathbf{K}_s\succeq&\overline{d}_s\mathbf{Q}_s+\frac{1}{4}\overline{d}_m\mathbf{P}\mathbf{Q}_m^{-1}\mathbf{P}^\mathsf{T}+\frac{1}{\alpha_s}\mathbf{K}_s\end{cases} \tag{2.46}$$

and combining Equation (2.26) and (2.44), the time derivative of V is upper-bounded

by

$$\dot{V} = \dot{V}_p + \dot{V}_\eta + \dot{V}_r + \dot{V}_\sigma \leq -\frac{k_r}{2}\Big(V_\sigma + V_\eta + V_r\Big) \leq 0. \tag{2.47}$$

Theorem 2. *For the teleoperation system in Equation (2.1) with time-varying delays under the output feedback control Equation (2.25) with the I&I observer Equation (2.24), if the proportional and local damping gains are selected to obey condition (2.46), then:*

1 *The velocities and position error are bounded, i.e.,* $\{\dot{\mathbf{q}}_m, \dot{\mathbf{q}}_s, \mathbf{q}_m - \mathbf{q}_s\} \in \mathcal{L}_\infty$, *moreover,* $\{\dot{\mathbf{q}}_m, \dot{\mathbf{q}}_s\} \in \mathcal{L}_2$.

2 *The velocities and position error globally asymptotically converge to zero when the hand and environment forces vanish, i.e.,* $\{\dot{\mathbf{q}}_m, \dot{\mathbf{q}}_s, \mathbf{q}_m - \mathbf{q}_s\} \to \mathbf{0}$ *as* $t \to \infty$.

3 *The velocity estimations* $\dot{\hat{\mathbf{q}}}_i$ *globally exponentially converge to the robot velocities* $\dot{\mathbf{q}}_i$, $i = m, s$.

Proof. The proof of the first two items in Theorem 2 is the same as in Theorem 1, so it is omitted here. To prove velocity estimation globally exponential convergence, in Equation (2.45), $\frac{\alpha_m}{4}\dot{\tilde{\mathbf{q}}}_m^\mathsf{T}\mathbf{K}_m\dot{\tilde{\mathbf{q}}}_m \geq 0$ and $\frac{\alpha_s}{4}\dot{\tilde{\mathbf{q}}}_s^\mathsf{T}\mathbf{K}_s\dot{\tilde{\mathbf{q}}}_s \geq 0$, it follows that $\dot{V}_\sigma + \dot{V}_\eta + \dot{V}_r \leq -\frac{k_r}{2}\left(V_\sigma + V_\eta + V_r\right)$, and, further, that

$$V_\sigma(t) + V_\eta(t) + V_r(t) \leq e^{-\frac{k_r}{2}t}\left(V_\sigma(0) + V_\eta(0) + V_r(0)\right),$$

which implies that $V_\sigma + V_\eta + V_r$ globally exponentially converges to zero. Because r_i are bounded and $\tilde{\mathbf{x}}_i = r_i\boldsymbol{\eta}_i$, it follows that the velocity estimation errors $\tilde{\mathbf{x}}_i$ globally exponentially converge to zero themselves. The proof is complete. □

The performance of bilateral teleoperation systems under the observer-based output feedback P+d control is verified through simulations on the same 2-DOF planar teleoperation model as in Section 2.2. After choosing $\mathbf{Q}_i = 10\mathbf{I}$, $\alpha_i = 2$ and $\mathbf{P} = 10\mathbf{I}$, the damping gains are selected $\mathbf{K}_i = 3\mathbf{I}$ to satisfy Equation (2.46). The observers have parameters $c_r = c_i = 0.1$, $k_r = 50$, $\epsilon_\sigma = 0.01$, $\epsilon = 0.01$, and initial states $r_0 = 0.2$, $\hat{\mathbf{x}}_0 = (0.02\ 0.02)^\mathsf{T}$, $\hat{\sigma}_0 = \|\hat{\mathbf{x}}_0\|^2$ and $\boldsymbol{\xi}_0 = \hat{\mathbf{x}}_0$.

For space saving reasons, Figures. 2.9-2.11 show only the results for the first joints of the two simulated robots. In Figure. 2.9, the slave tracks the position of the master in free motion. During slave contact with the environment, when $q_{m1} > 0.06$ rad, the slave robot stops in contact with the wall and the master continues to

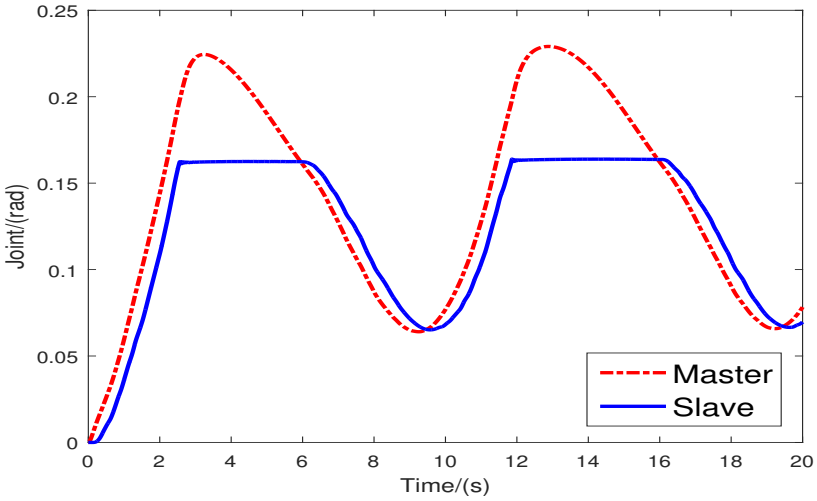

Figure 2.9: Master q_{m1} and slave q_{s1} positions of the first joint.

move forward, as it would under state feedback P+d control. In Figure. 2.10, the force feedback to the master reflects the environment torque during contact, and is noisy due to communication delays during free motion. In Figure. 2.11, the velocity estimate converges to the master velocity right away and the estimation error remains about zero even for relatively large initial velocity estimation error (0.02 rad/s). The simulations illustrate that the proposed output feedback synchronization strategy has similar performance as state feedback P+d control although it does not rely on velocity measurements.

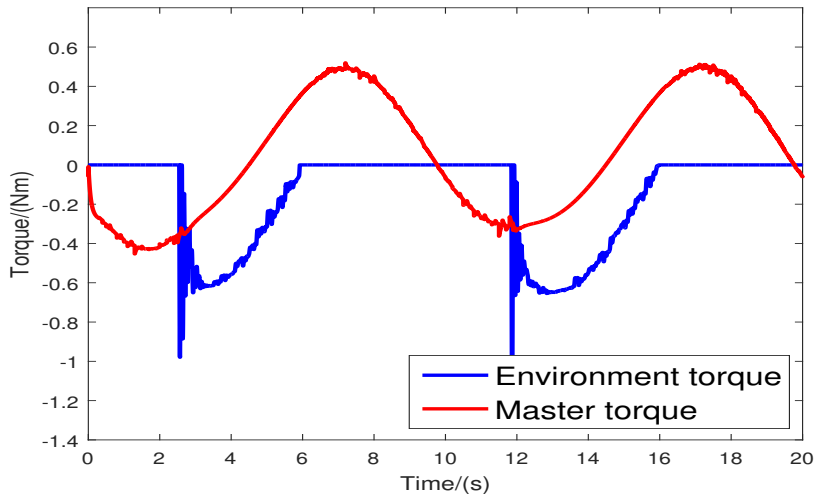

Figure 2.10: Environment τ_{e1} and master τ_{m1} torques at the first joint.

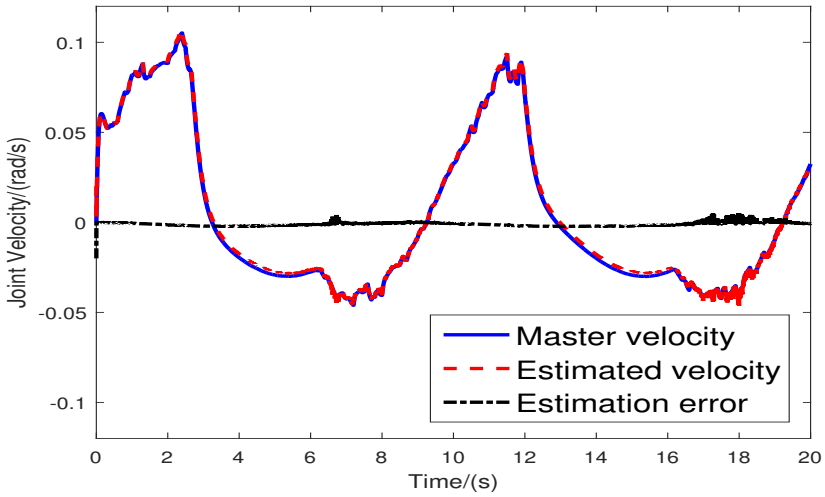

Figure 2.11: Velocity $\dot{q}_{m1}$, estimated velocity $\dot{\hat{q}}_{m1}$, and estimation error $\dot{q}_{m1} - \dot{\hat{q}}_{m1}$ for the first joint of the master robot.

Another advantage of the proposed strategy is the simple implementation of the new constructive I&I observers at the master and slave sides. The new observers require no state transformations of the robot dynamics and use only scalar gains, $k_{xi}(r_i, \hat{\sigma}_i)$, $k_{\sigma i}(\hat{\mathbf{x}}_i, r_i, \hat{\sigma}_i)$, $i = m, s$, in their dynamics. These gains and the partial derivatives of $k_{xi}(r_i, \hat{\sigma}_i)$ with respect to r_i and $\hat{\sigma}_i$ are independent of n, the number of master and slave DOFs. In contrast, the I&I observers for Euler-Lagrange systems in [70, 71, 79] and [74] require several matrices to be derived analytically, including $\mathbf{T}(\mathbf{q})$ and $\mathbf{L}(\mathbf{q})$, where $\mathbf{M}(\mathbf{q}) = \mathbf{T}^{\mathsf{T}}(\mathbf{q})\mathbf{T}(\mathbf{q})$ and $\mathbf{L}(\mathbf{q}) = \mathbf{T}^{-1}(\mathbf{q})$. They also require the analytical partial derivatives either of an n-dimensional vector $\boldsymbol{\beta}$ with respect to two n-dimensional vectors $\hat{\mathbf{q}}$ and $\hat{\mathbf{x}}$ in [70, 71, 79]), or of a $n \times n$-dimensional matrix $\mathbf{K}_x(\hat{\sigma}, \hat{\mathbf{y}})$ with respect to the n-dimensional vector $\hat{\mathbf{y}}$ and the scalar $\hat{\sigma}$ in [74]. These derivations can pose a significant practical challenge, especially for 6-DOF master and slave robots.

2.4 Bounded Output Feedback Control

This section considers a more challenging problem: output feedback control of bilateral teleoperation systems with time-varying delays and bounded actuations. The augmented I&I observer has been incorporated in the bounded P+d control to estimate velocities of the master and slave robots and to inject damping in the system.

The observer dynamics are the same as in Equation (2.24) with parameters to be determined through stability analysis, and the observer-based output feedback controller is designed as:

$$\begin{aligned}\boldsymbol{\tau}_m =& \mathrm{Sat}_m\Big(-\mathrm{Sat}_p\big[\mathbf{P}(\mathbf{q}_m - \mathbf{q}_{sd})\big] - \mathbf{K}_m\dot{\hat{\mathbf{q}}}_m\Big) + \mathbf{g}_m \\ \boldsymbol{\tau}_s =& \mathrm{Sat}_s\Big(-\mathrm{Sat}_p\big[\mathbf{P}(\mathbf{q}_s - \mathbf{q}_{md})\big] - \mathbf{K}_s\dot{\hat{\mathbf{q}}}_s\Big) + \mathbf{g}_s\end{aligned}, \tag{2.48}$$

where $\dot{\hat{\mathbf{q}}}_i$ with $i = m, s$ are estimated master and slave velocities by the designed I&I observer.

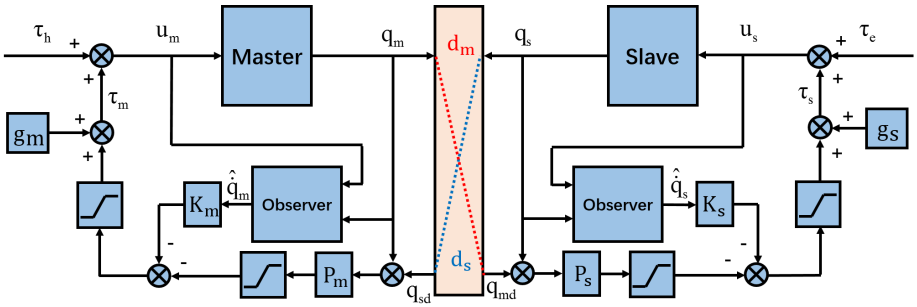

Figure 2.12: Teleoperation system under the observer-based bounded output feedback P+d control in Equation (2.48).

Figure. 2.12 displays the closed-loop bilateral teleoperation system Equation (2.1) under the observer-based bounded output feedback control Equation (2.48). The system stability is proved by the following Lyapunov-Krasovskii functional:

$$V = V_p + V_\eta + V_r + V_\sigma, \tag{2.49}$$

where: V_η, V_r and V_σ defined the same as in Equation (2.26) and

$$\begin{aligned}V_p =& \frac{1}{2}\dot{\mathbf{q}}_m^\top\mathbf{M}_m\dot{\mathbf{q}}_m + \frac{1}{2}\dot{\mathbf{q}}_s^\top\mathbf{M}_s\dot{\mathbf{q}}_s + \sum_{k=1}^{n}\int_0^{q_{mk}-q_{sk}}\mathrm{sat}_{pk}(p_k\sigma)d\sigma \\ &- \int_0^t \dot{\mathbf{q}}_m^\top\boldsymbol{\tau}_h d\xi - \int_0^t \dot{\mathbf{q}}_s^\top\boldsymbol{\tau}_e d\xi + E_h + E_e.\end{aligned}$$

The derivative of V_p along Equation (2.1) controlled by Equation (2.48) is

$$
\begin{aligned}
\dot{V}_p =& \frac{1}{2}\dot{\mathbf{q}}_m^{\mathsf{T}}\dot{\mathbf{M}}_m\dot{\mathbf{q}}_m + \dot{\mathbf{q}}_m^{\mathsf{T}}\mathbf{M}_m\ddot{\mathbf{q}}_m + \frac{1}{2}\dot{\mathbf{q}}_s^{\mathsf{T}}\dot{\mathbf{M}}_s\dot{\mathbf{q}}_s + \dot{\mathbf{q}}_s^{\mathsf{T}}\mathbf{M}_s\ddot{\mathbf{q}}_s - \dot{\mathbf{q}}_m^{\mathsf{T}}\boldsymbol{\tau}_h - \dot{\mathbf{q}}_s^{\mathsf{T}}\boldsymbol{\tau}_e \\
&+ \sum_{k=1}^{n}\Big\{(\dot{q}_{mk} - \dot{q}_{sk})\mathrm{sat}_{pk}\big[p_k(q_{mk} - q_{sk})\big]\Big\} \\
=& \frac{1}{2}\dot{\mathbf{q}}_m^{\mathsf{T}}\Big(\dot{\mathbf{M}}_m - 2\mathbf{C}_m\Big)\dot{\mathbf{q}}_m - \dot{\mathbf{q}}_m^{\mathsf{T}}\mathbf{g}_m + \dot{\mathbf{q}}_m^{\mathsf{T}}\boldsymbol{\tau}_m + \sum_{k}^{n}\dot{q}_{mk}\mathrm{sat}_{pk}\big[p_k(q_{mk} - q_{sk})\big] \\
&+ \frac{1}{2}\dot{\mathbf{q}}_s^{\mathsf{T}}\Big(\dot{\mathbf{M}}_s - 2\mathbf{C}_s\Big)\dot{\mathbf{q}}_s - \dot{\mathbf{q}}_s^{\mathsf{T}}\mathbf{g}_s + \dot{\mathbf{q}}_s^{\mathsf{T}}\boldsymbol{\tau}_s + \sum_{k=1}^{n}\dot{q}_{sk}\mathrm{sat}_{pk}\big[p_k(q_{sk} - q_{mk})\big] \\
=& \dot{\mathbf{q}}_m^{\mathsf{T}}\mathrm{Sat}_m\Big(-\mathrm{Sat}_p\big[\mathbf{P}(\mathbf{q}_m - \mathbf{q}_{sd})\big] - \mathbf{K}_m\dot{\hat{\mathbf{q}}}_m\Big) + \dot{\mathbf{q}}_m^{\mathsf{T}}\mathrm{Sat}_p\big[\mathbf{P}(\mathbf{q}_m - \mathbf{q}_s)\big] \\
&+ \dot{\mathbf{q}}_s^{\mathsf{T}}\mathrm{Sat}_s\Big(-\mathrm{Sat}_p\big[\mathbf{P}(\mathbf{q}_s - \mathbf{q}_{md})\big] - \mathbf{K}_s\dot{\hat{\mathbf{q}}}_s\Big) + \dot{\mathbf{q}}_s^{\mathsf{T}}\mathrm{Sat}_p\big[\mathbf{P}(\mathbf{q}_s - \mathbf{q}_m)\big].
\end{aligned}
\tag{2.50}
$$

Similar to the above section, in $\dot{V}_p$, $\dot{V}_{puu}$ collects all terms that correspond to joint pairs with unsaturated P+d torques at both master and slave side, i.e., P+d torque pairs $-\mathrm{sat}_{pk}[p_k(q_{mk}-q_{sdk})]-k_{mk}\dot{\hat{q}}_{mk}$ and $-\mathrm{sat}_{pk}[p_k(q_{sk}-q_{mdk})]-k_{sk}\dot{\hat{q}}_{sk}$ for all $k \in k_{uu}$. Therefore, $\dot{V}_{puu}$ can be upper bounded by:

$$
\begin{aligned}
\dot{V}_{puu} &= \sum_{k\in k_{uu}}\sum_{i=m,s}\Big\{\dot{q}_{ik}\mathrm{sat}_{pk}\big[p_k(q_{ik} - q_{jk})\big] - \dot{q}_{ik}\mathrm{sat}_{pk}\big[p_k(q_{ik} - q_{jdk})\big] - \dot{q}_{ik}k_{ik}\dot{\hat{q}}_{ik}\Big\} \\
&\le \sum_{k\in k_{uu}}\sum_{i=m,s}\Big\{|\dot{q}_{ik}|p_k\int_{t-d_j}^{t}|\dot{q}_{jk}|d\xi - k_{ik}\dot{q}_{ik}^2 + k_{ik}\dot{q}_{ik}\dot{\tilde{q}}_{ik}\Big\} \\
&\le \sum_{k\in k_{uu}}\sum_{i=m,s}\Big\{|\dot{q}_{ik}|p_k\int_{t-d_j}^{t}|\dot{q}_{jk}|d\xi - \left(1 - \frac{1}{\gamma_i}\right)k_{ik}\dot{q}_{ik}^2 + \frac{\gamma_i}{4}k_{ik}\dot{\tilde{q}}_{ik}^2\Big\},
\end{aligned}
\tag{2.51}
$$

where: subscript k index the k-th element of the correspond vector or the k-th diagonal element of the corresponding matrix; γ_m and γ_s are two positive constants.

Because of $s_{pk} \le \min(s_{mk}, s_{sk})$ by Equation (2.48), only the pseudo injected damping based on estimated velocities $-k_{mk}\dot{\hat{q}}_{mk}$ and $-k_{sk}\dot{\hat{q}}_{sk}$ can saturate the P+d component of a joint control torque and, therefore, $\mathrm{sgn}\left(\mathrm{sat}_{ik}(\cdot)\right) = \mathrm{sgn}(-\dot{\hat{q}}_{ik})$, $i = m, s$ for any such joint.

In $\dot{V}$, $\dot{V}_{pss}$ collects all terms that correspond to joint pairs with P+d torques saturated both on the master and slave sides, i.e., P+d torque pairs $\mathrm{sat}_{mk}(\cdot)$ and

$\text{sat}_{sk}(\cdot)$ for all $k \in k_{ss}$. Therefore, $\dot{V}_{pss}$ can be bounded by

$$\begin{aligned}
\dot{V}_{pss} &= \sum_{k\in k_{ss}} \sum_{i=m,s} \Big\{ -\dot{q}_{ik}\text{sgn}(\dot{\hat{q}}_{ik})s_{ik} + \dot{q}_{ik}\text{sat}_{pk}\big[p_k(q_{ik}-q_{jk})\big] \Big\} \\
&\le \sum_{k\in k_{ss}} \sum_{i=m,s} \Big\{ |\dot{q}_{ik}|s_{pk} - (\dot{\hat{q}}_{ik}+\dot{\tilde{q}}_{ik})\text{sgn}(\dot{\hat{q}}_{ik})s_{ik} \Big\} \\
&\le \sum_{k\in k_{ss}} \sum_{i=m,s} \Big\{ -|\dot{\hat{q}}_{ik}|s_{ik} + |\dot{\tilde{q}}_{ik}|s_{ik} + |\dot{q}_{ik}|s_{pk} \Big\} \\
&\le \sum_{k\in k_{ss}} \sum_{i=m,s} \Big\{ -|\dot{\hat{q}}_{ik}|s_{ik} + |\dot{\tilde{q}}_{ik}|(s_{ik}+s_{pk}) + |\dot{\hat{q}}_{ik}|s_{pk} \Big\} \\
&\le \sum_{k\in k_{ss}} \sum_{i=m,s} \Big\{ -|\dot{\hat{q}}_{ik}|(s_{ik}-s_{pk}) + \frac{\rho_i}{4}\dot{\tilde{q}}_{ik}^2 + \frac{1}{\rho_i}(s_{ik}+s_{pk})^2 \Big\}
\end{aligned} \tag{2.52}$$

where ρ_m and ρ_s are two positive constants.

Because $|\text{sat}_{ik}(\cdot)| = s_{ik}$ and $s_{ik} \ge s_{pk}$, $i = m, s$, the master and slave joint velocities $\dot{q}_{ik}$ must satisfy

$$s_{pk} + k_{ik}|\dot{\hat{q}}_{ik}| \ge s_{ik}, \quad \Longrightarrow \quad |\dot{\hat{q}}_{ik}| \ge k_{mk}^{-1}(s_{mk}-s_{pk}), \quad i = m, s. \tag{2.53}$$

Then, selecting

$$s_{pk} \le \frac{\sqrt{\rho_m}-\sqrt{k_{ik}}}{\sqrt{\rho_m}+\sqrt{k_{ik}}}s_{ik}, \quad i = m, s \tag{2.54}$$

guarantees that

$$\dot{V}_{pss} \le \sum_{k\in k_{ss}} \sum_{i=m,s} \Big\{ \left(\frac{1}{\rho_i} - \frac{1}{k_{ik}}\right)(s_{ik}+s_{pk})^2 + \frac{\rho_i}{4}\dot{\tilde{q}}_{ik}^2 \Big\} \le \sum_{k\in k_{ss}} \sum_{i=m,s} \frac{\rho_i}{4}\dot{\tilde{q}}_{ik}^2. \tag{2.55}$$

Collecting in $\dot{V}_{pus}$ all terms that correspond to joint pairs with P+d torques unsaturated on the master side and saturated on the slave side, i.e., $-\text{sat}_{pk}[p_k(q_{mk}-q_{sdk})] - k_{mk}\dot{\hat{q}}_{mk}$ and $\text{sat}_{sk}(\cdot)$ for all $k \in k_{us}$, $\dot{V}_{pus}$ can be bounded by

$$\begin{aligned}
\dot{V}_{pus} &= \sum_{k\in k_{us}} \Big\{ \dot{q}_{mk}\text{sat}_{pk}\big[p_k(q_{mk}-q_{sk}) - \dot{q}_{mk}\text{sat}_{pk}\big[p_k(q_{mk}-q_{sdk})\big] - \dot{q}_{mk}k_{mk}\dot{\hat{q}}_{mk}\big] \\
&\qquad - \dot{q}_{sk}\text{sgn}(\dot{\hat{q}}_{sk})s_{sk} + \dot{q}_{sk}\text{sat}_{pk}\big[p_k(q_{sk}-q_{mk})\big] \Big\} \\
&\le \sum_{k\in k_{us}} \Big\{ (2|\dot{q}_{mk}| + |\dot{q}_{sk}|)s_{pk} - \dot{q}_{mk}k_{mk}(\dot{q}_{mk} - \dot{\tilde{q}}_{mk}) - (\dot{\hat{q}}_{sk}+\dot{\tilde{q}}_{sk})\text{sgn}(\dot{\hat{q}}_{sk})s_{sk} \Big\}
\end{aligned}$$

$$
\begin{aligned}
&\leq \sum_{k\in k_{us}} \Big\{ 2|\dot{q}_{mk}|s_{pk} - k_{mk}\dot{q}_{mk}^2 + \frac{1}{\zeta_m}k_{mk}\dot{q}_{mk}^2 + \frac{\zeta_m}{4}k_{mk}\dot{\tilde{q}}_{mk}^2 \\
&\qquad - |\dot{\hat{q}}_{sk}|s_{sk} + |\dot{\tilde{q}}_{sk}|s_{sk} + |\dot{\hat{q}}_{sk} + \dot{\tilde{q}}_{sk}|s_{pk} \Big\} \\
&\leq \sum_{k\in k_{us}} \Big\{ \frac{\zeta_m s_{pk}^2}{(\zeta_m - 1)k_{mk}} + \frac{\zeta_m}{4}k_{mk}\dot{\tilde{q}}_{mk}^2 - |\dot{\hat{q}}_{sk}|(s_{sk} - s_{pk}) + \frac{1}{\mu_s}(s_{sk} + s_{pk})^2 + \frac{\mu_s}{4}\dot{\tilde{q}}_{sk}^2 \Big\}.
\end{aligned} \tag{2.56}
$$

Because $|\mathrm{sat}_{sk}(\cdot)| = s_{sk}$, the slave joint velocity must satisfy Equation (2.53), and

$$
\dot{V}_{pus} \leq \sum_{k\in k_{us}} \Big\{ \frac{\zeta_m s_{pk}^2}{(\zeta_m - 1)k_{mk}} + \frac{\zeta_m}{4}k_{mk}\dot{\tilde{q}}_{mk}^2 - \frac{(s_{sk} - s_{pk})^2}{k_{sk}} + \frac{(s_{sk} + s_{pk})^2}{\mu_s} + \frac{\mu_s}{4}\dot{\tilde{q}}_{sk}^2 \Big\}
$$

if

$$
-\frac{(s_{sk} - s_{pk})^2}{k_{sk}} + \frac{(s_{sk} + s_{pk})^2}{\mu_s} + \frac{\zeta_m s_{pk}^2}{(\zeta_m - 1)k_{mk}} \leq 0 \tag{2.57}
$$

then

$$
\dot{V}_{pus} \leq \sum_{k\in k_{us}} \Big\{ \frac{\zeta_m}{4}k_{mk}\dot{\tilde{q}}_{mk}^2 + \frac{\mu_s}{4}\dot{\tilde{q}}_{sk}^2 \Big\}. \tag{2.58}
$$

Similarly, collecting in $\dot{V}_{psu}$ all terms corresponding to joint pairs with P+d torques saturated on the master side and unsaturated on the slave side, i.e., $\mathrm{sat}_{mk}(\cdot)$ and $-\mathrm{sat}_{pk}[p_k(q_{sk} - q_{mdk})] - k_{sk}\dot{\hat{q}}_{sk}$ for all $k \in k_{su}$, and if

$$
-\frac{(s_{mk} - s_{pk})^2}{k_{mk}} + \frac{(s_{mk} + s_{pk})^2}{\mu_m} + \frac{\zeta_s s_{pk}^2}{(\zeta_s - 1)k_{sk}} \leq 0 \tag{2.59}
$$

then

$$
\dot{V}_{psu} \leq \sum_{k\in k_{su}} \Big\{ \frac{\zeta_s}{4}k_{sk}\dot{\tilde{q}}_{sk}^2 + \frac{\mu_m}{4}\dot{\tilde{q}}_{mk}^2 \Big\}. \tag{2.60}
$$

Adding Equations (2.51), (2.55), (2.58) and (2.60) together leads to

$$
\begin{aligned}
\dot{V}_p \leq &\sum_{k\in k_{uu}} \sum_{i=m,s} \Big\{ |\dot{q}_{ik}| p_k \int_{t-d_j}^{t} |\dot{q}_{jk}| d\xi - \left(1 - \frac{1}{\gamma_i}\right) k_{ik}\dot{q}_{ik}^2 \Big\} \\
&+ \sum_{i=m,s} \frac{1}{4}\left[\rho_i + \overline{k}_i\left(\zeta_i + \gamma_i\right) + \mu_i\right] \dot{\tilde{\mathbf{q}}}_i^{\mathsf{T}} \dot{\tilde{\mathbf{q}}}_i.
\end{aligned} \tag{2.61}
$$

The last term in Equation (2.61) represent the energy generated by velocity estimation errors, which is dissipated by the augmented I&I observer. Because $\dot{\tilde{\mathbf{q}}}_i = \dot{\tilde{\mathbf{x}}}_i = r_i\boldsymbol{\eta}_i$ for $i = m, s$, then $\dot{\tilde{\mathbf{q}}}_i^{\mathsf{T}}\dot{\tilde{\mathbf{q}}}_i \leq r_i^2\|\boldsymbol{\eta}_i\|^2$. Therefore, the sum of Equa-

tions (2.33), (2.36), (2.42) and the last term in Equation (2.61) becomes

$$\begin{aligned}&\sum_{i=m,s}\frac{1}{4}\left[\rho_i+\overline{k}_i\left(\zeta_i+\gamma_i\right)+\mu_i\right]\dot{\tilde{\mathbf{q}}}_i^{\mathsf{T}}\dot{\tilde{\mathbf{q}}}_i+\dot{V}_\eta+\dot{V}_r+\dot{V}_\sigma\\&\leq-\sum_{i=m,s}\left\{\psi_{\eta i}\|\boldsymbol{\eta}_i\|^2+\psi_{\sigma i}\tilde{\sigma}_i^2+\frac{k_r}{4}(r_i-c_{ri})^2\right\}\end{aligned}\tag{2.62}$$

with $i=m,s$ and

$$\begin{aligned}\psi_{\eta i}=&k_{xi}(r_i,\hat{\sigma}_i)\lambda_{i1}-c_i\sqrt{1+\hat{\sigma}_i}-\frac{k_r}{4}(2\lambda_{i1}+1)-\epsilon_{\sigma i}\\&-\frac{1}{4}\left[\rho_i+\overline{k}_i\left(\zeta_i+\gamma_i\right)+\mu_i\right]r_i^2,\\\psi_{\sigma i}=&k_{\sigma i}(\hat{\mathbf{x}}_i,r_i,\hat{\sigma}_i)-\frac{r_i^2}{k_r}\left(\frac{\bar{\Delta}_{\sigma i}^2(\sigma_i,\hat{\sigma}_i)}{\lambda_{i1}^2}+k_{xi}^2(r_i,\hat{\sigma}_i)\|\hat{\mathbf{x}}_i\|^2\right).\end{aligned}$$

Combining Equation (2.61) and Equation (2.62) and selecting all observer parameters the same as in Equation (2.24) except that

$$k_{xi}(r_i,\hat{\sigma}_i)=\frac{1}{\lambda_{i1}}\left[c_i\sqrt{1+\hat{\sigma}_i}+\frac{k_r}{4}(2\lambda_{i1}+\lambda_{i2}+1)+\epsilon_{\sigma i}+\frac{1}{4}\left[\rho_i+\overline{k}_i(\zeta_i+\gamma_i)+\mu_i\right]r_i^2\right]\tag{2.63}$$

guarantees that

$$\dot{V}\leq\sum_{k\in k_{uu}}\sum_{i=m,s}\left\{|\dot{q}_{ik}|p_k\int_{t-d_j}^{t}|\dot{q}_{jk}|d\xi-\left(1-\frac{1}{\gamma_i}\right)k_{ik}\dot{q}_{ik}^2\right\}.\tag{2.64}$$

Then, integration of Equation (2.64) from 0 to t using lemma L.1 shows

$$\begin{aligned}V(t)-V(0)\leq\sum_{k\in k_{uu}}\Bigg\{&\frac{p_k}{2}\left(\alpha\|\dot{q}_{mk}\|_2^2+\frac{\overline{d}_s^2}{\alpha}\|\dot{q}_{sk}\|_2^2\right)-\left(1-\frac{1}{\gamma_m}\right)k_{mk}\|\dot{q}_{mk}\|_2^2\\&+\frac{p_k}{2}\left(\beta\|\dot{q}_{sk}\|_2^2+\frac{\overline{d}_m^2}{\beta}\|\dot{q}_{mk}\|^2\right)-\left(1-\frac{1}{\gamma_s}\right)k_{sk}\|\dot{q}_{sk}\|_2^2\Bigg\},\end{aligned}\tag{2.65}$$

which implies that V is bounded and thus the system is stable if

$$\begin{cases}k_{mk}\geq&\frac{\gamma_m p_k}{2(\gamma_m-1)}\left(\alpha+\frac{\overline{d}_m^2}{\beta}\right)\\k_{sk}\geq&\frac{\gamma_s p_k}{2(\gamma_s-1)}\left(\beta+\frac{\overline{d}_s^2}{\alpha}\right)\end{cases}.\tag{2.66}$$

Theorem 3. *For the teleoperation system in Equation (2.1) with bounded actuation and time-varying delays under the bounded output feedback control Equation (2.48) with the I&I observer Equation (2.24), if the proportional and local damping gains are selected to obey conditions (2.7), (2.54), (2.57), (2.59) and (2.66), and the I&I observer gains $k_{xi}(r_i, \hat{\sigma}_i)$ satisfy (2.57), then the system meets three the same properties as in Theorem 2.*

Proof. The proof is similar to the proof of Theorem 2, so it is omitted here. □

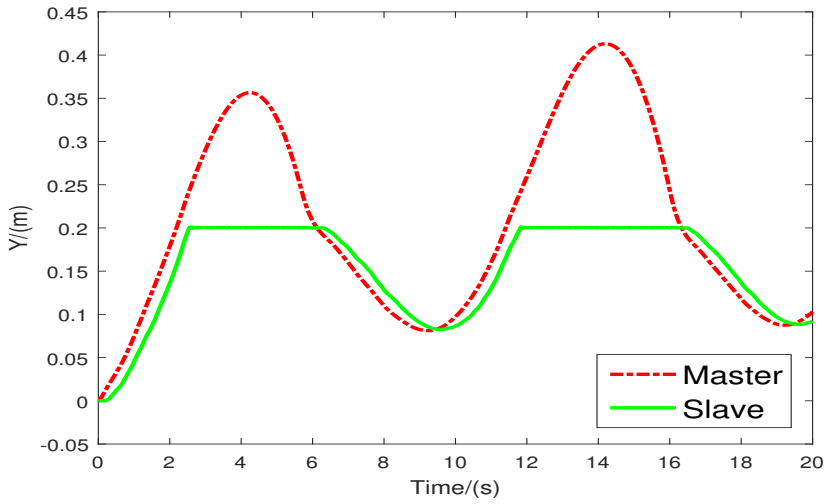

Figure 2.13: Simulated position tracking along y-axis, under sinusoidal user force, during interaction with a passive wall with stiffness $k_e = 1000$ N/m.

The stability and performance of the bilateral teleoperation systems with the bounded output feedback P+d control has been verified through simulations. The parameters of the simulated teleoperation system is the same as in Section 2.2. After selecting $\mathbf{P} = 10\mathbf{I}$, $\alpha = \beta = 0.2$ and $\gamma_i = 10$, $\mathbf{K}_i = 3\mathbf{I}$ can be chosen to satisfy condition (2.66). Then, $\rho_i = 100$ and $s_p = (0.4 \;\; 0.2)^\mathsf{T}$ can be selected from Equation (2.54). To satisfy conditions (2.57) and (2.59), we can choose sufficiently large $\mu_i = 40$ and $\zeta_i = 10$. For I&I observer design, all parameters are the same as in Section 2.3 except that $k_{xi}(r_i, \hat{\sigma}_i)$ are chosen to satisfy (2.63).

For saving space reason, only motion and control torque informations of the first joint are presented. Figure. 2.13 shows the position synchronization performance of the master and slave robots along y-axis. Compared with Figure. 2.3, Figure. 2.13 implies that the simulated bilateral teleoperation system behaves similarly under the

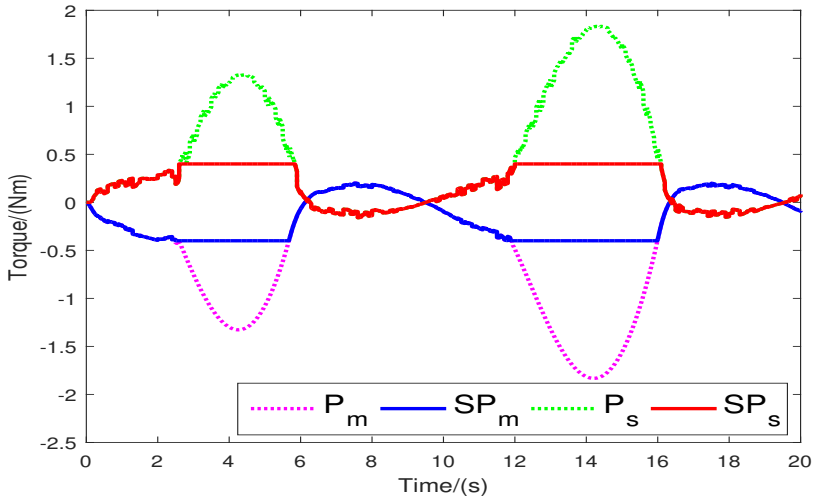

Figure 2.14: Unsaturated and saturated proportional terms on master: P_m, SP_m and on slave: P_s and SP_s.

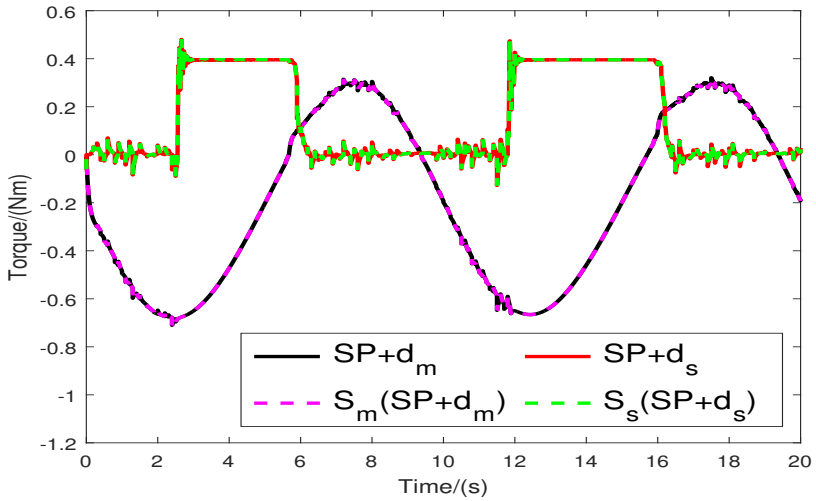

Figure 2.15: Unsaturated and saturated SP+d terms on master: $SP+d_m$, $S_m(SP+d_m)$ and on slave: $SP+d_s$ and $S_s(SP+d_s)$.

two different controllers. Figure. 2.14 and Figure. 2.15 display the saturation details of proportional control and saturated proportional plus damping control torques, which are similar to Figure. 2.4 and Figure. 2.5. Estimated and real joint velocities of the master robot are compared in Figure. 2.16. It shows that the estimated velocity is almost the same as the real version, which implies that the designed observer achieves velocity estimation convergence.

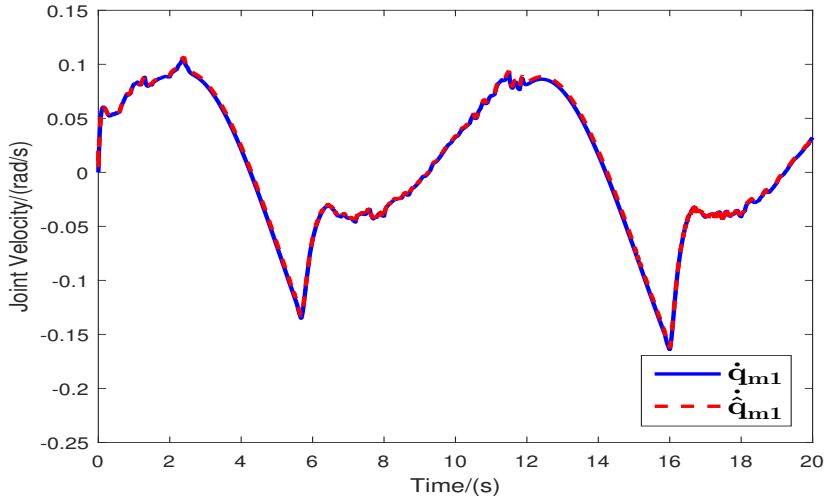

Figure 2.16: Actual velocity $\dot{q}_{m1}$, estimated velocity $\hat{\dot{q}}_{m1}$ of the first joint of the master robot.

2.5 Conclusions

This chapter has explored the two representative open problems: bounded actuation and output feedback control, in two channel teleoperation. An inner and an outer saturations have been introduced for bounding the proportional control and bounded proportional plus damping control, respectively, and a projection-based adaptive gravity compensation law has also been integrated in the bounded state feedback control. Lyapunov-Krasovskii energy analysis has shown that properly selecting control gains guarantees stable bilateral teleoepration in the presence of model uncertainties, time-varying delays and bounded actuations. For output feedback control, an augmented I&I observer has been proposed and integrated in the conventional P+d control, which achieves not only stable position synchronization of time-delayed bilateral teleoperation but also globally exponential velocity estimation convergence. For the more challenging case, bounded output feedback control, this chapter has illustrated that the developed bounding strategy in Section 2.2 and the augmented I&I observer in Section 2.3 can be combined together to solve the problem with more conservative controller design criteria.

Two channel teleoperation with only position exchanges between the master and slave sites can achieve position synchronization in free motion with simple P+d control. However, simulation results in this chapter have depicted that it cannot tightly constrain the master and slave robots, i.e., the position error between the two robots

increases in hard contact, especially in slave-environment contact. Beside, torque spikes occur upon slave-environment contact could not be reflected to the master side through two channel teleoperation. These two problems will be explored in the next chapter through four channel teleoperation control.

Chapter 3

Four Channel Teleoperation

To constrain the master and slave sites tightly and reflect interaction forces to the master side, this chapter explores the control of four channel teleoperation with both position and force exchanges in communication channels. A hybrid damping and stiffness adjustment strategy has been firstly developed for ISS teleoperation, which shows that the augmented force channels can reduce position errors and reflect interaction forces during hard contact. Then, a nonsingular version has been proposed to deal with the singularity problem in the hybrid strategy, thus unexpected torque spikes due to singular control can be avoided. Further, this chapter also proposes a reduced-order strategy to achieve guaranteed position synchronization for arbitrarily large position errors and to main tight master-slave coupling.

3.1 Hybrid Damping and Stiffness Adjustment

Two channel teleoperation can achieve position coordination in free motion but large position error and lack of interaction reflection during hard contact would damage telepresence. To overcome the two problems, external interaction forces are necessarily incorporated in the closed-loop without threatening system stability.

The hybrid damping and stiffness adjustment teleoperation strategy incorporates nonlinear position- and velocity-dependent terms into conventional P+d with gravity compensation control [29], to which it also adds direct transmission of hand and environment torques:

$$\begin{aligned} \boldsymbol{\tau}_m &= -\dot{\mathbf{q}}_m^{\star}(\mathbf{q}_m - \mathbf{q}_{sd})^{\mathsf{T}}\mathbf{B}_m(\mathbf{q}_m - \mathbf{q}_{sd}) - \mathbf{K}_m\dot{\mathbf{q}}_m - \mathbf{P}(\mathbf{q}_m - \mathbf{q}_{sd}) + \mathbf{g}_m + \boldsymbol{\tau}_{ed} \\ \boldsymbol{\tau}_s &= -\dot{\mathbf{q}}_s^{\star}(\mathbf{q}_s - \mathbf{q}_{md})^{\mathsf{T}}\mathbf{B}_s(\mathbf{q}_s - \mathbf{q}_{md}) - \mathbf{K}_s\dot{\mathbf{q}}_s - \mathbf{P}(\mathbf{q}_s - \mathbf{q}_{md}) + \mathbf{g}_s + \boldsymbol{\tau}_{hd} \end{aligned}. \quad (3.1)$$

In Equation (3.1), $\mathbf{q}_{md} = \mathbf{q}_m(t - d_m(t))$ and $\mathbf{q}_{sd} = \mathbf{q}_s(t - d_s(t))$; $\mathbf{B}_i$, $\mathbf{K}_i$ and $\mathbf{P}$ are positive diagonal gain matrices, $i = m, s$; and $\dot{\mathbf{q}}_i^\star = \left[\dot{q}_{i1}^\star, \cdots, \dot{q}_{in}^\star\right]^\mathsf{T}$ is a vector with the property

$$\dot{q}_{ik}^\star = \begin{cases} \frac{1}{l\dot{q}_{ik}} & \dot{q}_{ik} \neq 0 \\ 0 & \dot{q}_{ik} = 0 \end{cases} \quad \Longrightarrow \quad \dot{\mathbf{q}}_i^\mathsf{T}\dot{\mathbf{q}}_i^\star = \begin{cases} 1 & \dot{\mathbf{q}}_i \neq 0 \\ 0 & \dot{\mathbf{q}}_i = 0 \end{cases}$$

where $k = 1, \cdots, n$ and l is the number of joints with non-zero velocity.

In Equation (3.1), besides the disturbances introduced in the proportional control terms $\mathbf{P}(\mathbf{q}_m - \mathbf{q}_{md})$ and $\mathbf{P}(\mathbf{q}_s - \mathbf{q}_{sd})$ by the time-varying delays, the transmitted hand and environment torques $\boldsymbol{\tau}_{hd}$ an $\boldsymbol{\tau}_{ed}$ are not guaranteed passive. The delay-induced disturbances and non-passive external forces may lead to energy accumulation in the closed-loop teleoperation system, threatening its stability and safety. Damping injection can be used to dissipate, or restrict in an acceptable range, the harmful energy. As Equation (3.1) shows, this section proposes a damping injection scheme based on a nonlinear control term dependent on the velocity at the local site and the position error between the two sites. The nonlinear term has the two-sided effect of adjusting the injected damping and/or the stiffness of the master-slave coupling. The hybrid nonlinear term behaves as auxiliary damping because it always opposes velocity. At the same time, it strengthens the proportional term when the velocity is opposite to proportional control torque and weakens it when the velocity is in the same direction as the proportional control torque. This behaviour is physically reasonable because added damping slows down the robots and relaxed coupling between them increases the stability robustness of closed-loop teleoperation.

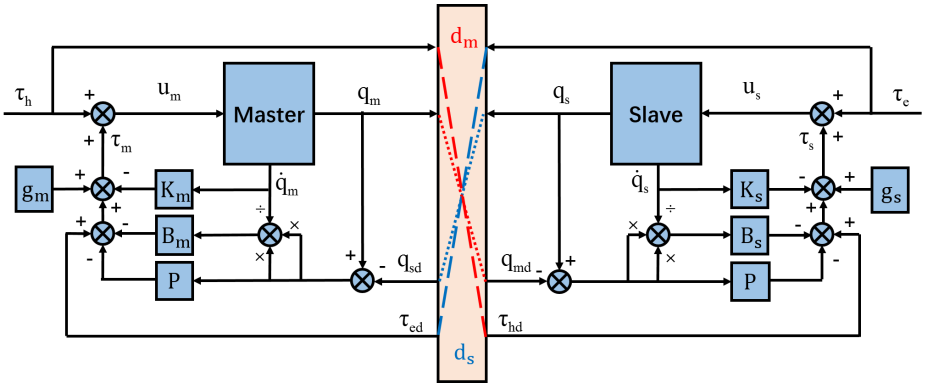

Figure 3.1: Teleoperation system under the hybrid damping and stiffness adjustment control in Equation (3.1).

Figure. 3.1 shows the frame of the closed-loop four channel teleoperation system with the hybrid damping and stiffness adjustment strategy. Sending the external forces $\boldsymbol{\tau}_h$ and $\boldsymbol{\tau}_e$ to, and directly applying them on, the slave and master robots, respectively, is not the best method to exploit them. In general, the external forces include desired components that assist the controller to coordinate the two robots both in free motion and in contact, and undesirable components that damage the coupling between the robots and can even lead to finite time escaping velocities. Distinguishing the desirable from the harmful components and rejecting the latter without knowing their bounds is not trivial. In P+d control, fixed local damping injection is effective because the disturbances in the proportional term are related to the robot velocity at the other side. Considering the harmful components of the external forces as bounded disturbances is not helpful because it is impossible to determine a fixed damping sufficient to reject them without knowing their bounds. The proposed hybrid damping and stiffness adjustment offers an alternative approach for increasing the robustness of the system to the bounded but unknown external disturbances. Because the nonlinear hybrid terms switch at zero velocity, the control torques are not smooth but chattering and noisy. A modification of the hybrid strategy that aims to avoid this chattering and lessen the noise in the control torques is introduced in the nest section.

The stability of the system Equation (2.1) under the control of Equation (3.1) is investigated using the following Lyapunov-Krasovskii functional:

$$V = V_1 + V_2 + V_3 \tag{3.2}$$

with:

$$\begin{aligned}
V_1 =& \frac{1}{2}\dot{\mathbf{q}}_m^{\mathsf{T}}\mathbf{M}_m\dot{\mathbf{q}}_m + \frac{1}{2}\dot{\mathbf{q}}_s^{\mathsf{T}}\mathbf{M}_s\dot{\mathbf{q}}_s \\
V_2 =& \frac{1}{2}(\mathbf{q}_m - \mathbf{q}_s)^{\mathsf{T}}\mathbf{P}(\mathbf{q}_m - \mathbf{q}_s) \\
V_3 =& \int_{-\bar{d}_m}^{0}\int_{t+\theta}^{t} e^{-\gamma(t-\xi)}\dot{\mathbf{q}}_m^{\mathsf{T}}(\xi)\mathbf{Q}_m\dot{\mathbf{q}}_m(\xi)d\xi d\theta + \int_{-\bar{d}_s}^{0}\int_{t+\theta}^{t} e^{-\gamma(t-\xi)}\dot{\mathbf{q}}_s^{\mathsf{T}}(\xi)\mathbf{Q}_s\dot{\mathbf{q}}_s(\xi)d\xi d\theta.
\end{aligned}$$

Here, V_3 is a measure of the energy introduced by the time delays in the forward and backward communication channels. The exponential decay coefficient $e^{-\gamma(t-\xi)}$ facilitates the construction of a function $\beta \in \mathcal{KL}$ needed in the ISS proof and maintains $V_3 \geq 0$ with positive definite diagonal matrices $\mathbf{Q}_i$, $i = m, s$.

Using property P2, the derivative of V_1 is computed as:

$$\begin{aligned}
\dot{V}_1 =& -\dot{\mathbf{q}}_m^\mathsf{T}\mathbf{K}_m\dot{\mathbf{q}}_m - \dot{\mathbf{q}}_m^\mathsf{T}\mathbf{P}(\mathbf{q}_m-\mathbf{q}_{sd}) - (\mathbf{q}_m-\mathbf{q}_{sd})^\mathsf{T}\mathbf{B}_m(\mathbf{q}_m-\mathbf{q}_{sd}) + \dot{\mathbf{q}}_m^\mathsf{T}(\boldsymbol{\tau}_h+\boldsymbol{\tau}_{ed}) \\
& -\dot{\mathbf{q}}_s^\mathsf{T}\mathbf{K}_s\dot{\mathbf{q}}_s - \dot{\mathbf{q}}_s^\mathsf{T}\mathbf{P}(\mathbf{q}_s-\mathbf{q}_{md}) - (\mathbf{q}_s-\mathbf{q}_{md})^\mathsf{T}\mathbf{B}_s(\mathbf{q}_s-\mathbf{q}_{md}) + \dot{\mathbf{q}}_s^\mathsf{T}(\boldsymbol{\tau}_e+\boldsymbol{\tau}_{hd}) \\
\leq& -\dot{\mathbf{q}}_m^\mathsf{T}\mathbf{K}_m\dot{\mathbf{q}}_m - \dot{\mathbf{q}}_m^\mathsf{T}\mathbf{P}(\mathbf{q}_m-\mathbf{q}_s) - \dot{\mathbf{q}}_m^\mathsf{T}\mathbf{P}\int_{t-d_s}^{t}\dot{\mathbf{q}}_s(\xi)d\xi \\
& -(\mathbf{q}_m-\mathbf{q}_s)^\mathsf{T}\mathbf{B}_m(\mathbf{q}_m-\mathbf{q}_s) + \dot{\mathbf{q}}_m^\mathsf{T}(\boldsymbol{\tau}_h+\boldsymbol{\tau}_{ed}) - 2(\mathbf{q}_m-\mathbf{q}_s)^\mathsf{T}\mathbf{B}_m\int_{t-d_s}^{t}\dot{\mathbf{q}}_s(\xi)d\xi \\
& -\dot{\mathbf{q}}_s^\mathsf{T}\mathbf{K}_s\dot{\mathbf{q}}_s - \dot{\mathbf{q}}_s^\mathsf{T}\mathbf{P}(\mathbf{q}_s-\mathbf{q}_m) - \dot{\mathbf{q}}_s^\mathsf{T}\mathbf{P}\int_{t-d_m}^{t}\dot{\mathbf{q}}_m(\xi)d\xi \\
& -(\mathbf{q}_m-\mathbf{q}_s)^\mathsf{T}\mathbf{B}_s(\mathbf{q}_m-\mathbf{q}_s) + \dot{\mathbf{q}}_s^\mathsf{T}(\boldsymbol{\tau}_e+\boldsymbol{\tau}_{hd}) - 2(\mathbf{q}_s-\mathbf{q}_m)^\mathsf{T}\mathbf{B}_s\int_{t-d_m}^{t}\dot{\mathbf{q}}_m(\xi)d\xi.
\end{aligned} \tag{3.3}$$

The terms coupling velocities and external torques can be upper-bounded by:

$$\begin{aligned}
\dot{\mathbf{q}}_m^\mathsf{T}(\boldsymbol{\tau}_h+\boldsymbol{\tau}_{ed}) \leq& \frac{1}{2}\dot{\mathbf{q}}_m^\mathsf{T}\boldsymbol{\Upsilon}_m\dot{\mathbf{q}}_m + \frac{1}{2}(\boldsymbol{\tau}_h+\boldsymbol{\tau}_{ed})^\mathsf{T}\boldsymbol{\Upsilon}_m^{-1}(\boldsymbol{\tau}_h+\boldsymbol{\tau}_{ed}), \\
\dot{\mathbf{q}}_s^\mathsf{T}(\boldsymbol{\tau}_e+\boldsymbol{\tau}_{hd}) \leq& \frac{1}{2}\dot{\mathbf{q}}_s^\mathsf{T}\boldsymbol{\Upsilon}_s\dot{\mathbf{q}}_s + \frac{1}{2}(\boldsymbol{\tau}_e+\boldsymbol{\tau}_{hd})^\mathsf{T}\boldsymbol{\Upsilon}_s^{-1}(\boldsymbol{\tau}_e+\boldsymbol{\tau}_{hd}),
\end{aligned} \tag{3.4}$$

where $\boldsymbol{\Upsilon}_m$ and $\boldsymbol{\Upsilon}_s$ are positive definite diagonal matrices.

Further, the time derivative of V_2 is given by

$$\dot{V}_2 = (\mathbf{q}_m-\mathbf{q}_s)^\mathsf{T}\mathbf{P}\dot{\mathbf{q}}_m - (\mathbf{q}_m-\mathbf{q}_s)^\mathsf{T}\mathbf{P}\dot{\mathbf{q}}_s, \tag{3.5}$$

and, after some algebraic manipulation, V_3 becomes

$$V_3 = e^{-\gamma t}\int_{-\overline{d}_m}^{0}\int_{t+\theta}^{t} e^{\gamma\xi}\dot{\mathbf{q}}_m^\mathsf{T}(\xi)\mathbf{Q}_m\dot{\mathbf{q}}_m(\xi)d\xi d\theta + e^{-\gamma t}\int_{-\overline{d}_s}^{0}\int_{t+\theta}^{t} e^{\gamma\xi}\dot{\mathbf{q}}_s^\mathsf{T}(\xi)\mathbf{Q}_s\dot{\mathbf{q}}_s(\xi)d\xi d\theta,$$

with derivative

$$\begin{aligned}
\dot{V}_3 =& -\gamma V_3 + \overline{d}_m\dot{\mathbf{q}}_m^\mathsf{T}\mathbf{Q}_m\dot{\mathbf{q}}_m - \int_{t-\overline{d}_m}^{t} e^{-\gamma(t-\xi)}\dot{\mathbf{q}}_m^\mathsf{T}(\xi)\mathbf{Q}_m\dot{\mathbf{q}}_m(\xi)d\xi \\
& + \overline{d}_s\dot{\mathbf{q}}_s^\mathsf{T}\mathbf{Q}_s\dot{\mathbf{q}}_s - \int_{t-\overline{d}_s}^{t} e^{-\gamma(t-\xi)}\dot{\mathbf{q}}_s^\mathsf{T}(\xi)\mathbf{Q}_s\dot{\mathbf{q}}_s(\xi)d\xi \\
\leq& -\gamma V_3 + \overline{d}_m\dot{\mathbf{q}}_m^\mathsf{T}\mathbf{Q}_m\dot{\mathbf{q}}_m - e^{-\gamma\overline{d}_m}\int_{t-d_m}^{t}\dot{\mathbf{q}}_m^\mathsf{T}(\xi)\mathbf{Q}_m\dot{\mathbf{q}}_m(\xi)d\xi \\
& + \overline{d}_s\dot{\mathbf{q}}_s^\mathsf{T}\mathbf{Q}_s\dot{\mathbf{q}}_s - e^{-\gamma\overline{d}_s}\int_{t-d_s}^{t}\dot{\mathbf{q}}_s^\mathsf{T}(\xi)\mathbf{Q}_s\dot{\mathbf{q}}_s(\xi)d\xi.
\end{aligned} \tag{3.6}$$

From the lemma L.2, it follows that

$$\begin{aligned}
&-\left[\dot{\mathbf{q}}_m^\mathsf{T}\mathbf{P}+2(\mathbf{q}_m-\mathbf{q}_s)^\mathsf{T}\mathbf{B}_m\right]\int_{t-d_s}^{t}\dot{\mathbf{q}}_s(\xi)d\xi-e^{-\gamma\bar{d}_s}\int_{t-d_s}^{t}\dot{\mathbf{q}}_s^\mathsf{T}(\xi)\mathbf{Q}_s\dot{\mathbf{q}}_s(\xi)d\xi\\
=&-\dot{\mathbf{q}}_m^\mathsf{T}\mathbf{P}\int_{t-d_s}^{t}\dot{\mathbf{q}}_s(\xi)d\xi-\eta_s e^{-\gamma\bar{d}_s}\int_{t-d_s}^{t}\dot{\mathbf{q}}_s^\mathsf{T}(\xi)\mathbf{Q}_s\dot{\mathbf{q}}_s(\xi)d\xi\\
&-2(\mathbf{q}_m-\mathbf{q}_s)^\mathsf{T}\mathbf{B}_m\int_{t-d_s}^{t}\dot{\mathbf{q}}_s(\xi)d\xi-(1-\eta_s)e^{-\gamma\bar{d}_s}\int_{t-d_s}^{t}\dot{\mathbf{q}}_s^\mathsf{T}(\xi)\mathbf{Q}_s\dot{\mathbf{q}}_s(\xi)d\xi\\
\leq&\frac{\bar{d}_s e^{\gamma\bar{d}_s}}{4\eta_s}\dot{\mathbf{q}}_m^\mathsf{T}\mathbf{P}\mathbf{Q}_s^{-1}\mathbf{P}^\mathsf{T}\dot{\mathbf{q}}_m+\frac{\bar{d}_s e^{\gamma\bar{d}_s}}{1-\eta_s}(\mathbf{q}_m-\mathbf{q}_s)^\mathsf{T}\mathbf{B}_m\mathbf{Q}_s^{-1}\mathbf{B}_m^\mathsf{T}(\mathbf{q}_m-\mathbf{q}_s)
\end{aligned}\tag{3.7}$$

with $0<\eta_s<1$ a scalar constant, and similarly

$$\begin{aligned}
&-\left[\dot{\mathbf{q}}_s^\mathsf{T}\mathbf{P}+2(\mathbf{q}_s-\mathbf{q}_m)^\mathsf{T}\mathbf{B}_s\right]\int_{t-d_m}^{t}\dot{\mathbf{q}}_m(\xi)d\xi-e^{-\gamma\bar{d}_m}\int_{t-d_m}^{t}\dot{\mathbf{q}}_m^\mathsf{T}(\xi)\mathbf{Q}_m\dot{\mathbf{q}}_m(\xi)d\xi\\
\leq&\frac{\bar{d}_m e^{\gamma\bar{d}_m}}{4\eta_m}\dot{\mathbf{q}}_s^\mathsf{T}\mathbf{P}\mathbf{Q}_m^{-1}\mathbf{P}^\mathsf{T}\dot{\mathbf{q}}_s+\frac{\bar{d}_m e^{\gamma\bar{d}_m}}{1-\eta_m}(\mathbf{q}_m-\mathbf{q}_s)^\mathsf{T}\mathbf{B}_s\mathbf{Q}_m^{-1}\mathbf{B}_s^\mathsf{T}(\mathbf{q}_m-\mathbf{q}_s)
\end{aligned}\tag{3.8}$$

with $0<\eta_m<1$ another scalar constant.

Based on the property P1, the sum of V_1 and V_2 is upper-bounded by:

$$V_1+V_2\leq\frac{1}{2}\lambda_{m2}\dot{\mathbf{q}}_m^\mathsf{T}\dot{\mathbf{q}}_m+\frac{1}{2}\lambda_{s2}\dot{\mathbf{q}}_s^\mathsf{T}\dot{\mathbf{q}}_s+\frac{1}{2}(\mathbf{q}_m-\mathbf{q}_s)^\mathsf{T}\mathbf{P}(\mathbf{q}_m-\mathbf{q}_s).\tag{3.9}$$

Defining the state of the closed-loop teleoperation system to be $\boldsymbol{\theta}=[\dot{\mathbf{q}}_m^\mathsf{T}\quad\dot{\mathbf{q}}_s^\mathsf{T}\quad(\mathbf{q}_m-\mathbf{q}_s)^\mathsf{T}]^\mathsf{T}$, the derivative of the proposed Lyapunov-Krasovskii functional can then be computed by adding Equations (3.3), (3.5) and (3.6) and using the inequalities (3.4), (3.7), (3.8) and (3.9):

$$\dot{V}\leq-\gamma V-\boldsymbol{\theta}^\mathsf{T}\boldsymbol{\Psi}\boldsymbol{\theta}+\chi(\boldsymbol{\tau}_h,\boldsymbol{\tau}_e),\tag{3.10}$$

where the diagonal elements of the symmetric matrix $\boldsymbol{\Psi}=\mathrm{diag}\{\boldsymbol{\Psi}_{11},\boldsymbol{\Psi}_{22},\boldsymbol{\Psi}_{33}\}$ are

$$\begin{aligned}
\boldsymbol{\Psi}_{11}=&\mathbf{K}_m-\frac{\boldsymbol{\Upsilon}_m}{2}-\bar{d}_m\mathbf{Q}_m-\frac{1}{2}\gamma\lambda_{m2}\mathbf{I}-\frac{\bar{d}_s e^{\gamma\bar{d}_s}}{4\eta_s}\mathbf{P}\mathbf{Q}_s^{-1}\mathbf{P}^\mathsf{T}\\
\boldsymbol{\Psi}_{22}=&\mathbf{K}_s-\frac{\boldsymbol{\Upsilon}_s}{2}-\bar{d}_s\mathbf{Q}_s-\frac{1}{2}\gamma\lambda_{s2}\mathbf{I}-\frac{\bar{d}_m e^{\gamma\bar{d}_m}}{4\eta_m}\mathbf{P}\mathbf{Q}_m^{-1}\mathbf{P}^\mathsf{T}\\
\boldsymbol{\Psi}_{33}=&\mathbf{B}_m-\frac{\bar{d}_s e^{\gamma\bar{d}_s}}{1-\eta_s}\mathbf{B}_m\mathbf{Q}_s^{-1}\mathbf{B}_m^\mathsf{T}+\mathbf{B}_s-\frac{\bar{d}_m e^{\gamma\bar{d}_m}}{1-\eta_m}\mathbf{B}_s\mathbf{Q}_m^{-1}\mathbf{B}_s^\mathsf{T}-\frac{1}{2}\gamma\mathbf{P}
\end{aligned}\tag{3.11}$$

and the function $\chi(\boldsymbol{\tau}_h, \boldsymbol{\tau}_e)$ is

$$\chi(\boldsymbol{\tau}_h, \boldsymbol{\tau}_e) = \frac{1}{2}(\boldsymbol{\tau}_h + \boldsymbol{\tau}_{ed})^{\mathsf{T}} \boldsymbol{\Upsilon}_m^{-1} (\boldsymbol{\tau}_h + \boldsymbol{\tau}_{ed}) + \frac{1}{2}(\boldsymbol{\tau}_e + \boldsymbol{\tau}_{hd})^{\mathsf{T}} \boldsymbol{\Upsilon}_s^{-1} (\boldsymbol{\tau}_e + \boldsymbol{\tau}_{hd}).$$

Based on the above analysis, the following theorem serves as the design criterion for the controller proposed in Equation (3.1) for teleoperation systems with asymmetric time-varying delays.

Theorem 4. *Consider the teleoperation system in Equation (2.1) with the controller in Equation (3.1). If there exist positive definite matrix control gains* $\mathbf{K}_i$, $\mathbf{P}$, $\mathbf{B}_i$ *and* $\boldsymbol{\Upsilon}_i$ *and positive scalars* η_i, γ *with* $i = m, s$ *such that the diagonal elements of matrix* $\boldsymbol{\Psi}$ *in Equation (3.11) are nonpositive, then*

1 *The closed-loop system is exponentially input-to-state stable with velocities* $\dot{\mathbf{q}}_m$, $\dot{\mathbf{q}}_s$ *and position tracking error* $\mathbf{q}_m - \mathbf{q}_s$ *as the state variables and the human and environment torques,* $\boldsymbol{\tau}_h$ *and* $\boldsymbol{\tau}_e$ *respectively, as the inputs, i.e.* $\{\dot{\mathbf{q}}_m, \dot{\mathbf{q}}_s, (\mathbf{q}_m - \mathbf{q}_s)\} \in \mathcal{L}_\infty$ *if* $\{\boldsymbol{\tau}_h, \boldsymbol{\tau}_e\} \in \mathcal{L}_\infty$.

2 *When the operator applies no force on the master and the slave is not in contact with the remote environment, i.e.* $\boldsymbol{\tau}_h = \boldsymbol{\tau}_e = \mathbf{0}$, *the master and slave velocities asymptotically converge to zero and position tracking is achieved, i.e.* $\{\dot{\mathbf{q}}_m, \dot{\mathbf{q}}_s, (\mathbf{q}_m - \mathbf{q}_s)\} \to \mathbf{0}$ *as* $t \to \infty$.

3 *In steady state with the slave in contact with the remote environment, i.e.* $\dot{\mathbf{q}}_m = \dot{\mathbf{q}}_s = \mathbf{0}$ *and* $\boldsymbol{\tau}_h + \boldsymbol{\tau}_e = \mathbf{0}$, *the position error between the master and slave robots vanishes, i.e.* $\mathbf{q}_m - \mathbf{q}_s = \mathbf{0}$.

Remark. Similar to [34], the bounding of the derivative of the proposed Lyapunov-Krasovskii functional in Equation (3.2) has not required any assumption on the operator or remote environment. In other words, the proposed controller can maintain the closed-loop teleoperation system ISS even when the user and the environment are active.

Proof. Together, the condition that $\boldsymbol{\Psi}$ be negative semi-definite and Equation (3.10) lead to:

$$\dot{V} \leq -\gamma V + \chi(\boldsymbol{\tau}_h, \boldsymbol{\tau}_e)$$

for any state $\boldsymbol{\theta}$. Further, because $\boldsymbol{\Upsilon}_m$ and $\boldsymbol{\Upsilon}_s$ are gains selected through design, there always exist constant positive scalars υ_i such that $\boldsymbol{\Upsilon}_i^{-1} \leq \upsilon_i \mathbf{I}$, $i = m, s$. Then, the function $\chi(\boldsymbol{\tau}_h, \boldsymbol{\tau}_e)$ is bounded by

$$\begin{aligned}\chi(\boldsymbol{\tau}_h, \boldsymbol{\tau}_e) \leq & \frac{1}{2}\upsilon_m(\boldsymbol{\tau}_h + \boldsymbol{\tau}_{ed})^{\mathsf{T}}(\boldsymbol{\tau}_h + \boldsymbol{\tau}_{ed}) + \frac{1}{2}\upsilon_s(\boldsymbol{\tau}_e + \boldsymbol{\tau}_{hd})^{\mathsf{T}}(\boldsymbol{\tau}_e + \boldsymbol{\tau}_{hd}) \\ \leq & (\upsilon_m + \upsilon_s)(\sup_{0\leq\xi\leq t} ||\boldsymbol{\tau}_h(\xi)||^2 + \sup_{0\leq\xi\leq t} ||\boldsymbol{\tau}_e(\xi)||^2) \\ = & \alpha(\sup_{0\leq\xi\leq t} ||\boldsymbol{\tau}_h(\xi)||, \sup_{0\leq\xi\leq t} ||\boldsymbol{\tau}_e(\xi)||)\end{aligned}$$

and

$$\dot{V} \leq -\gamma V + \alpha(\sup_{0\leq\xi\leq t} ||\boldsymbol{\tau}_h(\xi)||, \sup_{0\leq\xi\leq t} ||\boldsymbol{\tau}_e(\xi)||). \tag{3.12}$$

Time integration of Equation (3.12) yields

$$V \leq e^{-\gamma t}V_{t_0} + \frac{1}{\gamma}\alpha(\sup_{0\leq\xi\leq t} ||\boldsymbol{\tau}_h(\xi)||, \sup_{0\leq\xi\leq t} ||\boldsymbol{\tau}_e(\xi)||),$$

where V_{t_0} is the value of V at time $t_0 = 0$. From its definition, V is lower bounded by

$$V \geq \frac{1}{2}\lambda_{m1}||\dot{\mathbf{q}}_m||^2 + \frac{1}{2}\lambda_{s1}||\dot{\mathbf{q}}_s||^2 + \frac{1}{2}\underline{p}||\mathbf{q}_m - \mathbf{q}_s||^2, \tag{3.13}$$

where $\underline{p}$ is the smallest eigenvalue of $\mathbf{P}$. Therefore, it follows that

$$\begin{aligned}||\dot{\mathbf{q}}_i||^2 &\leq \frac{2}{\lambda_{i1}}\left\{e^{-\gamma t}V_{t_0} + \frac{1}{\gamma}\alpha(\sup_{0\leq\xi\leq t} ||\boldsymbol{\tau}_h(\xi)||, \sup_{0\leq\xi\leq t} ||\boldsymbol{\tau}_e(\xi)||)\right\}, \quad i = m, s, \\ ||\mathbf{q}_m - \mathbf{q}_s||^2 &\leq \frac{2}{\underline{p}}\left\{e^{-\gamma t}V_{t_0} + \frac{1}{\gamma}\alpha(\sup_{0\leq\xi\leq t} ||\boldsymbol{\tau}_h(\xi)||, \sup_{0\leq\xi\leq t} ||\boldsymbol{\tau}_e(\xi)||)\right\},\end{aligned}$$

which shows that four channel teleoperation with the proposed hybrid damping and stiffness adjustment is ISS with input $\begin{pmatrix}\boldsymbol{\tau}_h^{\mathsf{T}} & \boldsymbol{\tau}_e^{\mathsf{T}}\end{pmatrix}^{\mathsf{T}}$ and state $\begin{pmatrix}\dot{\mathbf{q}}_m^{\mathsf{T}} & \dot{\mathbf{q}}_s^{\mathsf{T}} & (\mathbf{q}_m - \mathbf{q}_s)^{\mathsf{T}}\end{pmatrix}^{\mathsf{T}}$.

To prove the second part of Theorem 4, assume that hand and environment torques are exerted on the system until some time instant $0 \leq t_1 < \infty$ and become zero afterwards. In this case, the time derivative of the proposed Lyapunov-Krasovskii

functional is

$$\dot{V} \leq \begin{cases} -\gamma V + \alpha(\sup\limits_{0\leq\xi\leq t} ||\boldsymbol{\tau}_h(\xi)||, \sup\limits_{0\leq\xi\leq t} ||\boldsymbol{\tau}_e(\xi)||) & 0 \leq t < t_1 \\ -\gamma V & t_1 \leq t \end{cases}, \tag{3.14}$$

which, after integration, yields $V \leq e^{-\gamma(t-t_1)}V_{t_1}$, $\forall t > t_1$, where V_{t_1} is the value of the functional at time instant t_1:

$$V_{t_1} = e^{-\gamma t_1}V_{t_0} + \frac{1}{\gamma}\alpha(\sup_{0\leq\xi\leq t_1} ||\boldsymbol{\tau}_h(\xi)||, \sup_{0\leq\xi\leq t_1} ||\boldsymbol{\tau}_e(\xi)||).$$

From the first part of Theorem 1, V_{t_1} is bounded. Hence, V exponentially decreases to 0 as $t \to \infty$. Since V is also lower bounded as in Equation (3.13), it follows that $\{\dot{\mathbf{q}}_m, \dot{\mathbf{q}}_s, (\mathbf{q}_m - \mathbf{q}_s)\} \to \mathbf{0}$ as $t \to \infty$.

For the proof of the last part of Theorem 4, assume zero master and slave velocities, $\dot{\mathbf{q}}_m = \dot{\mathbf{q}}_s = \mathbf{0}$. Then, the nonlinear control torques $\dot{\mathbf{q}}_m^{-1}(\mathbf{q}_m - \mathbf{q}_{sd})^\mathsf{T}\mathbf{B}_m(\mathbf{q}_m - \mathbf{q}_{sd})$ and $\dot{\mathbf{q}}_s^{-1}(\mathbf{q}_s - \mathbf{q}_{md})^\mathsf{T}\mathbf{B}_s(\mathbf{q}_s - \mathbf{q}_{md})$ and the master and slave accelerations are also zero. The closed-loop system dynamics simplify to

$$\boldsymbol{\tau}_h + \boldsymbol{\tau}_{ed} - \mathbf{P}(\mathbf{q}_m - \mathbf{q}_{sd}) = \mathbf{0}$$
$$\boldsymbol{\tau}_e + \boldsymbol{\tau}_{hd} - \mathbf{P}(\mathbf{q}_s - \mathbf{q}_{md}) = \mathbf{0}.$$

From $\boldsymbol{\tau}_h + \boldsymbol{\tau}_e = \mathbf{0}$, it follows that $\boldsymbol{\tau}_h + \boldsymbol{\tau}_{ed} = \boldsymbol{\tau}_e + \boldsymbol{\tau}_{hd} = \mathbf{0}$ and, further, that $\mathbf{q}_m - \mathbf{q}_{sd} = \mathbf{q}_s - \mathbf{q}_{md} = \mathbf{q}_m - \mathbf{q}_s = \mathbf{0}$. That is, the position error tends to zero in steady state when the hand and environment torques are balanced. □

The first two inferences in the theorem are similar to Theorem 1. They guarantee that the master and slave velocities do not escape in finite time, and that the two robots are coupled through the proportional control term. The third inference is similar to a classical result in robot force control [81]: in static contact with the environment, i.e., when both the master and slave have zero velocity and the slave end effector is in contact with the remote object, the hand and environment torques are also constant and, as a result, the external forces balance each other and the position error is eliminated.

As in single robot control, the P+d strategy behaves as a virtual spring damper in teleoperation without time delays: the spring connects the master and slave robots, and the two local dampers connect each robot to the ground. In the absence of

perturbations, the virtual spring tends to drive the robots to each other. The potential energy stored in the spring is converted into kinetic energy of the two robots, which the local dampers dissipate. As a result, the energy of the teleoperation system in closed loop with P+d control asymptotically tends to zero and the two robots converge to the same position. In the presence of perturbing forces, the motion of the two robots is driven by the virtual spring, the local dampers and the external perturbations themselves. If the perturbations inject only limited energy, or if the local dampers can maintain the total energy of the closed loop teleoperation system bounded, then the P+d control guarantees bounded velocities of, and position error between, the master and slave robots. For teleoperation systems with time-varying delays, the P+d controller still builds local dampers on both the master and slave sides, but the proportional control component behaves as a distorted spring. The delays introduce disturbances in the master and slave proportional control terms $\mathbf{P}(\mathbf{q}_m - \mathbf{q}_{sd})$ and $\mathbf{P}(\mathbf{q}_s - \mathbf{q}_{md})$, disturbances that threaten stability by injecting energy in the closed loop system. However, because the disturbances depend only on the velocity of the other side, they can be dissipated through sufficient local damping injection and the effective proportional control term can work as a spring connecting the two robots.

If the hand and environment torques are not assumed passive, they behave as perturbations for the master and slave robots. In this paper, the external torques and their transmissions to the other side $\boldsymbol{\tau}_h$, $\boldsymbol{\tau}_{hd}$, $\boldsymbol{\tau}_e$ and $\boldsymbol{\tau}_{ed}$ are called perturbations instead of disturbances to distinguish their effects from those of the distortions in the proportional terms $\mathbf{P}(\mathbf{q}_m - \mathbf{q}_{md})$ and $\mathbf{P}(\mathbf{q}_s - \mathbf{q}_{sd})$. In the classical definition of stability, a system is totally stable [82] if it is stable for every input-output pairs, and it is asymptotically totally stable if the state asymptotically converges to the equilibrium for every input. According to this definition, a teleoperation system is totally stable if the master and slave velocities and positions are bounded. However, it seems unreasonable to design a controller to guarantee bounded positions of the master and slave robots over infinite time without assuming passive terminations. If the user keeps moving the master along some direction, with bounded force and without violating the physical constraints of the system, then the positions both of the master and of the slave should increase to infinity as the time grows to infinity. However, teleoperation systems work as human-environment interaction systems that operate over finite time intervals. Therefore, this paper posits that it is practical to consider finite-time stability for teleoperation systems under perturbing forces [83]. If the master and slave velocities are bounded, then over the finite time interval when

the system is in use, the master and slave positions are also bounded.

The effectiveness of the proposed hybrid damping and stiffness adjustment strategy is verified through simulations on a pair of 2-DOF planar manipulators with only revolute joints, as in Section 2.2. Their link masses and lengths are $m_{mk} = 1$ kg, $m_{sk} = 2$ kg, $l_{ik} = 0.5$ m, $i = m, s$ and $k = 1, 2$. The positive asymmetric time-varying delays d_m and d_s are upper bounded by $\overline{d}_m = 0.2$ s and $\overline{d}_s = 0.1$ s. The master and slave robots start to move from $\begin{pmatrix} \mathbf{q}_{m0} & \dot{\mathbf{q}}_{m0} \end{pmatrix}^{\mathsf{T}} = \begin{pmatrix} \mathbf{q}_{s0} & \dot{\mathbf{q}}_{s0} \end{pmatrix}^{\mathsf{T}} = \begin{pmatrix} \mathbf{0} & \mathbf{0} \end{pmatrix}^{\mathsf{T}}$, under the sinusoidal user-applied force $F_{hy} = 0.5 + \sin(0.1\pi)$ N. The environment is located at $y_e = 0.5$ m. Because the user and environment forces are along the y-axis, it can be assumed that $-\frac{\pi}{2} \leq q_{i2} \leq \frac{\pi}{2}$, $i = m, s$, and it follows that $\lambda_{m2} = 1.46$ and $\lambda_{s2} = 2.92$. After selecting $\eta_m = \eta_s = 0.5$, $\boldsymbol{\Upsilon}_m = \boldsymbol{\Upsilon}_s = \mathbf{I}$ and $\gamma = 0.01$, $\boldsymbol{\Psi}$ can be made negative definite by choosing $\mathbf{K}_m = \mathbf{K}_s = 11\mathbf{I}$, $\mathbf{P} = 10\mathbf{I}$ and $\mathbf{B}_m = \mathbf{B}_s = 0.1\mathbf{I}$.

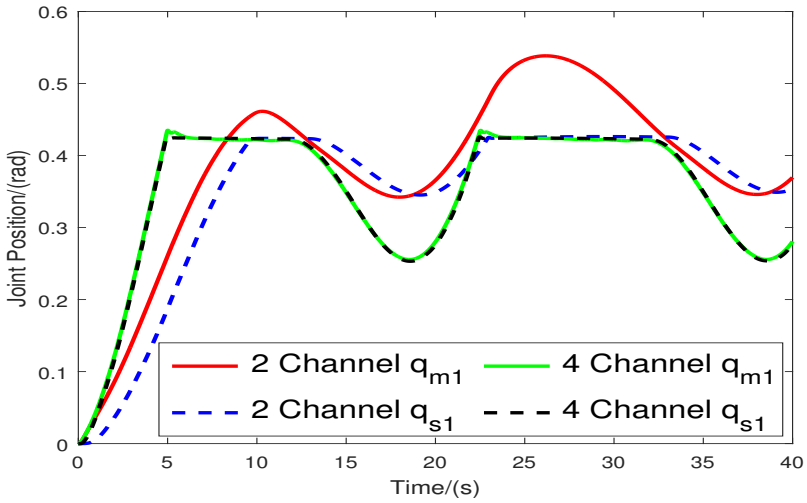

Figure 3.2: Position tracking comparison between two channel (P+d) and four channel (hybrid damping and stiffness adjustment) teleoperation: q_{m1} and q_{s1}.

Case 1. Passive Environment

In the first simulation, the user interacts with a passive environment, a virtual wall with stiffness $k_e = 1000$ N/m and damping $d_e = 40$ Ns/m, as widely used in haptic interface design [84]. The proposed four channel controller with hybrid damping and stiffness adjustment is contrasted to the classical P+d controller in Figures. 3.2-3.4. Because the second joints perform similarly, Figures. 3.2-3.4 present only the positions and torques of the first joints of the master and slave robots. Figure. 3.2 shows that four channel control with hybrid damping and stiffness adjustment can

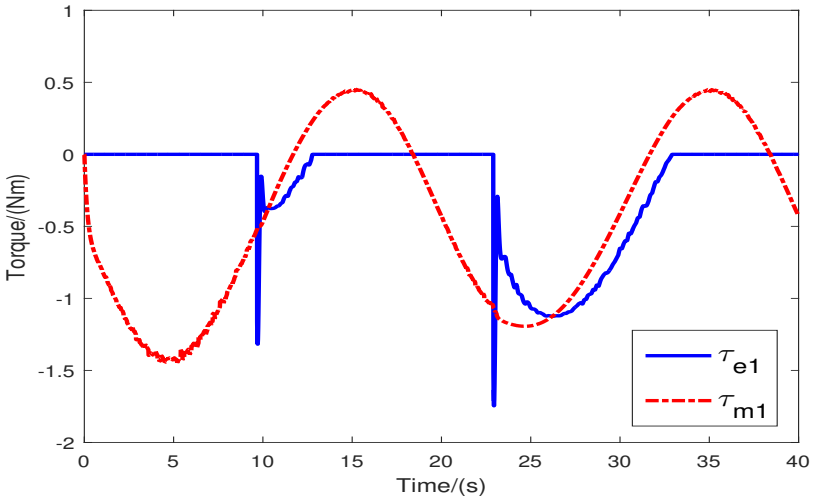

Figure 3.3: Two channel teleoperation with P+d control: τ_{e1} and τ_{m1}.

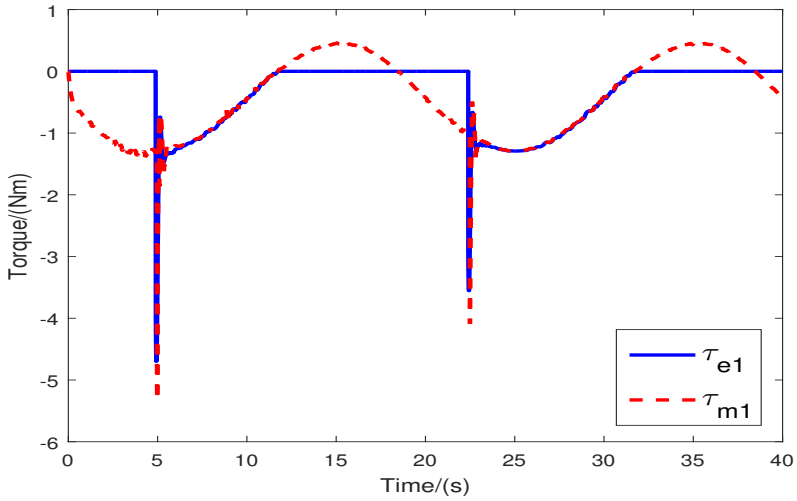

Figure 3.4: Four channel teleoperation with hybrid damping and stiffness adjustment: τ_{e1} and τ_{m1}.

coordinate the master and slave positions effectively both during free motion and during contact, whereas two channel P+d control does not coordinate the master and slave robots as tightly and incurs larger position error, especially during contact. Figures. 3.3-3.4 illustrate that only the four channel controller with hybrid damping and stiffness adjustment reflects to the master the large torques generated by the environment upon contact. Large forces upon contact lead to large accelerations and high fidelity force feedback [85] and, therefore, are expected to improve the operator's

perception of contact in remote rigid environments.

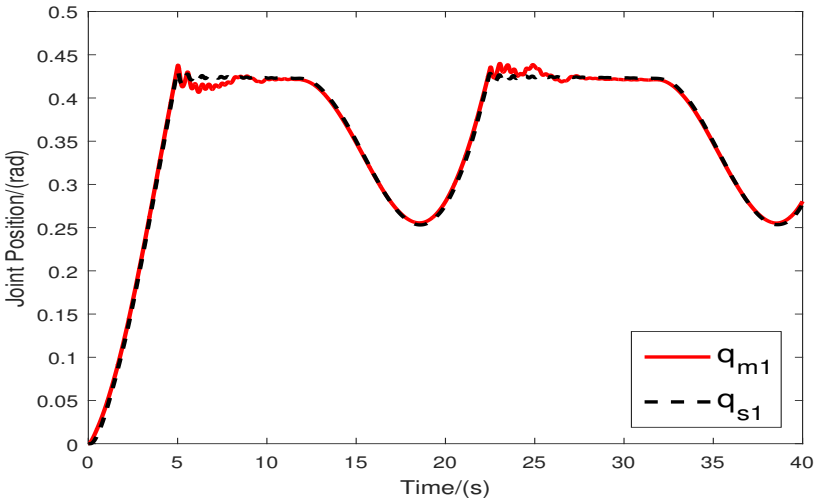

Figure 3.5: Position tracking in joint space: q_{m1} and q_{s1}.

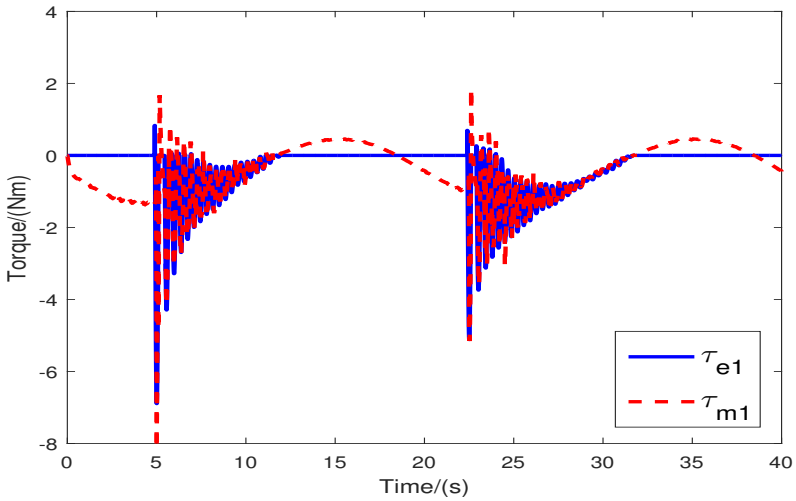

Figure 3.6: Force tracking in joint space: τ_{e1} and τ_{m1}.

Case 2. Active Environment

To verify that the hybrid damping and stiffness adjustment strategy proposed in this paper guarantees bounded velocities of, and position error between, the master and slave robots even for non-passive operator or environment, the second simulation examines the teleoperation within an active environment. The virtual wall at the slave side has stiffness $k_e = 1000$ N/m and damping $d_e = -10$ Ns/m. The simulation

results in Figure. 3.5 show that the active environment induces master vibrations upon contact, but the vibrations remain bounded during the interaction with the active environment. Figure. 3.6 illustrates that maintaining the interaction with an active environment ISS requires large control torques, as the controller aims to reflect the environment torques to the master. Such large torques may impose a heavy burden on the actuators and may damage them.

3.2 Nonsingular Spring-Damper Adjustment

When a joint velocity nears zero in the presence of non-zero position error in (3.1), the nonlinear term opposing the joint velocity overwhelms the other terms along the joint space direction and stops the motion of the joint. When the joint velocity becomes zero, the nonlinear term becomes zero along the kth joint space direction and the other control terms drive the kth joint again. The controller in Equation (3.1) then leads to spikes in the control torque and chatters in the joint velocity.

To overcome the limitation of the controller in Equation (3.1), this section proposes the following singularity-free nonlinear controller:

$$\begin{aligned}\boldsymbol{\tau}_m =& -\mathbf{S}_m(\dot{\mathbf{q}}_m)(\mathbf{q}_m-\mathbf{q}_{sd})^{\mathsf{T}}\mathbf{B}_m(\mathbf{q}_m-\mathbf{q}_{sd})-\mathbf{K}_m\dot{\mathbf{q}}_m-\mathbf{P}(\mathbf{q}_m-\mathbf{q}_{sd})+\mathbf{g}_m+\boldsymbol{\tau}_{ed}\\ \boldsymbol{\tau}_s =& -\mathbf{S}_s(\dot{\mathbf{q}}_s)(\mathbf{q}_s-\mathbf{q}_{md})^{\mathsf{T}}\mathbf{B}_s(\mathbf{q}_s-\mathbf{q}_{md})-\mathbf{K}_s\dot{\mathbf{q}}_s-\mathbf{P}(\mathbf{q}_s-\mathbf{q}_{md})+\mathbf{g}_s+\boldsymbol{\tau}_{hd}\end{aligned} \tag{3.15}$$

where:

$$\mathbf{S}_i(\dot{\mathbf{q}}_i)=\left[\frac{\mathrm{sat}(\dot{q}_{i1})\mathrm{sgn}(\dot{q}_{i1})}{n\dot{q}_{i1}},\cdots,\frac{\mathrm{sat}(\dot{q}_{in})\mathrm{sgn}(\dot{q}_{in})}{n\dot{q}_{in}}\right]^{\mathsf{T}},$$

$$\mathrm{sat}(\dot{q}_{ik})=\begin{cases}\dot{q}_{ik} & |\dot{q}_{ik}|\le\overline{\dot{q}}_i\\ \overline{\dot{q}}_i\mathrm{sgn}(\dot{q}_{ik}) & |\dot{q}_{ik}|>\overline{\dot{q}}_i\end{cases}$$

and $\mathrm{sgn}(\cdot)$ is the signum function, $i=m,s$ and $k=1,\cdots,n$. The new controller in Equation (3.15) replaces the singular terms $\dot{\mathbf{q}}_m^{\star}$ and $\dot{\mathbf{q}}_s^{\star}$ in Equation (3.1) with the nonsingular terms $\mathbf{S}_m(\dot{\mathbf{q}}_m)$ and $\mathbf{S}_s(\dot{\mathbf{q}}_s)$. When a joint velocity $\dot{q}_{ik}$ nears zero in the presence of non-zero position error, $\frac{\mathrm{sat}(\dot{q}_{ik})\mathrm{sgn}(\dot{q}_{ik})}{n\dot{q}_{ik}}=\frac{\mathrm{sgn}(\dot{q}_{ik})}{n}$ and the singularity is eliminated.

A teleoperation system with the nonsingular springer-damper adjustment control is shown in Figure. 3.7. Stability of the system is analyzed using the following

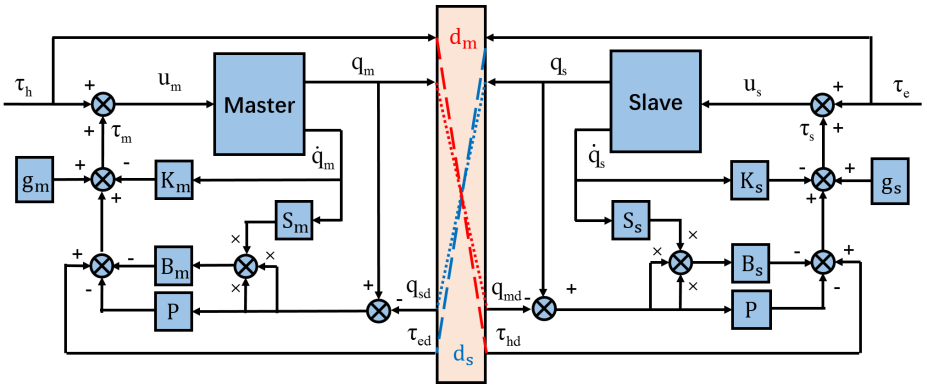

Figure 3.7: Teleoperation system under the nonsingular spring-damper adjustment control in Equation (3.15).

Lyapunov-like functional:

$$V = V_1 + V_2 + V_3, \tag{3.16}$$

where:

$$\begin{aligned}
V_1 =& \frac{1}{2}\dot{\mathbf{q}}_m^{\mathsf{T}}\mathbf{M}_m\dot{\mathbf{q}}_m + \frac{1}{2}\dot{\mathbf{q}}_s^{\mathsf{T}}\mathbf{M}_s\dot{\mathbf{q}}_s \\
V_2 =& \frac{1}{2}(\mathbf{q}_m - \mathbf{q}_s)^{\mathsf{T}}\mathbf{P}(\mathbf{q}_m - \mathbf{q}_s) \\
V_3 =& \int_{-\bar{d}_m}^{0}\int_{t+\theta}^{t} e^{-\int_{\xi}^{t}\sigma du}\dot{\mathbf{q}}_m^{\mathsf{T}}\mathbf{Q}_m\dot{\mathbf{q}}_m d\xi d\theta + \int_{-\bar{d}_s}^{0}\int_{t+\theta}^{t} e^{-\int_{\xi}^{t}\sigma du}\dot{\mathbf{q}}_s^{\mathsf{T}}\mathbf{Q}_s\dot{\mathbf{q}}_s d\xi d\theta
\end{aligned}$$

with $\sigma = \max(\sigma_m, \sigma_s)$ and $\sigma_i = \frac{1}{n}\sum_{k=1}^{n}\mathrm{sat}(\dot{q}_{ik})\mathrm{sgn}(\dot{q}_{ik})$, $i = m, s$. Different from the stability analysis in Section 3.1, the integrands in V_3 are bounded by non-constant exponentials in this section.

Similar to Section 3.1, using property P.2, the derivative of V_1 satisfies:

$$\begin{aligned}
\dot{V}_1 \leq& \dot{\mathbf{q}}_m^{\mathsf{T}}(\boldsymbol{\tau}_h + \boldsymbol{\tau}_{ed}) - \dot{\mathbf{q}}_m^{\mathsf{T}}\mathbf{K}_m\dot{\mathbf{q}}_m - \dot{\mathbf{q}}_m^{\mathsf{T}}\mathbf{P}\int_{t-d_s}^{t}\dot{\mathbf{q}}_s d\xi - \dot{\mathbf{q}}_m^{\mathsf{T}}\mathbf{P}(\mathbf{q}_m - \mathbf{q}_s) \\
& - \sigma_m(\mathbf{q}_m - \mathbf{q}_s)^{\mathsf{T}}\mathbf{B}_m(\mathbf{q}_m - \mathbf{q}_s) - 2\sigma_m(\mathbf{q}_m - \mathbf{q}_s)^{\mathsf{T}}\mathbf{B}_m\int_{t-d_s}^{t}\dot{\mathbf{q}}_s d\xi \\
& + \dot{\mathbf{q}}_s^{\mathsf{T}}(\boldsymbol{\tau}_e + \boldsymbol{\tau}_{hd}) - \dot{\mathbf{q}}_s^{\mathsf{T}}\mathbf{K}_s\dot{\mathbf{q}}_s - \dot{\mathbf{q}}_s^{\mathsf{T}}\mathbf{P}\int_{t-d_m}^{t}\dot{\mathbf{q}}_m d\xi - \dot{\mathbf{q}}_s^{\mathsf{T}}\mathbf{P}(\mathbf{q}_s - \mathbf{q}_m) \\
& - \sigma_s(\mathbf{q}_s - \mathbf{q}_m)^{\mathsf{T}}\mathbf{B}_s(\mathbf{q}_s - \mathbf{q}_m) - 2\sigma_s(\mathbf{q}_s - \mathbf{q}_m)^{\mathsf{T}}\mathbf{B}_s\int_{t-d_m}^{t}\dot{\mathbf{q}}_m d\xi,
\end{aligned} \tag{3.17}$$

and the derivatives of V_2 and V_3 are

$$\dot{V}_2 = \dot{\mathbf{q}}_m^\mathsf{T}\mathbf{P}(\mathbf{q}_m - \mathbf{q}_s) + \dot{\mathbf{q}}_s^\mathsf{T}\mathbf{P}(\mathbf{q}_s - \mathbf{q}_m), \tag{3.18}$$

$$\begin{aligned}\dot{V}_3 \leq & -\sigma V_3 + \overline{d}_m\dot{\mathbf{q}}_m^\mathsf{T}\mathbf{Q}_m\dot{\mathbf{q}}_m - e^{-\overline{d}_m\overline{\sigma}}\int_{t-d_m}^{t}\dot{\mathbf{q}}_m^\mathsf{T}\mathbf{Q}_m\dot{\mathbf{q}}_m d\xi \\ & + \overline{d}_s\dot{\mathbf{q}}_s^\mathsf{T}\mathbf{Q}_s\dot{\mathbf{q}}_s - e^{-\overline{d}_s\overline{\sigma}}\int_{t-d_s}^{t}\dot{\mathbf{q}}_s^\mathsf{T}\mathbf{Q}_s\dot{\mathbf{q}}_s d\xi,\end{aligned} \tag{3.19}$$

where $\overline{\sigma} = \max\{\overline{\dot{q}}_m, \overline{\dot{q}}_s\}$. According to the lemma L.2, we have

$$\begin{aligned}& -\dot{\mathbf{q}}_m^\mathsf{T}\mathbf{P}\int_{t-d_s}^{t}\dot{\mathbf{q}}_s d\xi - e^{-\overline{d}_s\overline{\sigma}}\int_{t-d_s}^{t}\dot{\mathbf{q}}_s^\mathsf{T}\mathbf{Q}_s\dot{\mathbf{q}}_s d\xi - 2\sigma_m(\mathbf{q}_m - \mathbf{q}_s)^\mathsf{T}\mathbf{B}_m\int_{t-d_s}^{t}\dot{\mathbf{q}}_s d\xi \\ \leq & \frac{\overline{d}_s\sigma_m^2 e^{\overline{d}_s\overline{\sigma}}}{1-\eta_s}(\mathbf{q}_m - \mathbf{q}_s)^\mathsf{T}\mathbf{B}_m\mathbf{Q}_s^{-1}\mathbf{B}_m^\mathsf{T}(\mathbf{q}_m - \mathbf{q}_s) + \frac{\overline{d}_s e^{\overline{d}_s\overline{\sigma}}}{4\eta_s}\dot{\mathbf{q}}_m^\mathsf{T}\mathbf{P}\mathbf{Q}_s^{-1}\mathbf{P}^\mathsf{T}\dot{\mathbf{q}}_m\end{aligned} \tag{3.20}$$

$$\begin{aligned}& -\dot{\mathbf{q}}_s^\mathsf{T}\mathbf{P}\int_{t-d_m}^{t}\dot{\mathbf{q}}_m d\xi - e^{-\overline{d}_m\overline{\sigma}}\int_{t-d_m}^{t}\dot{\mathbf{q}}_m^\mathsf{T}\mathbf{Q}_m\dot{\mathbf{q}}_m d\xi - 2\sigma_s(\mathbf{q}_s - \mathbf{q}_m)^\mathsf{T}\mathbf{B}_s\int_{t-d_m}^{t}\dot{\mathbf{q}}_m d\xi \\ \leq & \frac{\overline{d}_m\sigma_s^2 e^{\overline{d}_m\overline{\sigma}}}{1-\eta_m}(\mathbf{q}_s - \mathbf{q}_m)^\mathsf{T}\mathbf{B}_s\mathbf{Q}_m^{-1}\mathbf{B}_s^\mathsf{T}(\mathbf{q}_s - \mathbf{q}_m) + \frac{\overline{d}_m e^{\overline{d}_m\overline{\sigma}}}{4\eta_m}\dot{\mathbf{q}}_s^\mathsf{T}\mathbf{P}\mathbf{Q}_m^{-1}\mathbf{P}^\mathsf{T}\dot{\mathbf{q}}_s\end{aligned} \tag{3.21}$$

with $0 < \eta_i < 1$, $i = m, s$, two scalar constants.

From the property L.1 and the definition of V_1 and V_2, we conclude that

$$V_1 + V_2 \leq \frac{1}{2}\lambda_{m2}\dot{\mathbf{q}}_m^\mathsf{T}\dot{\mathbf{q}}_m + \frac{1}{2}\lambda_{s2}\dot{\mathbf{q}}_s^\mathsf{T}\dot{\mathbf{q}}_s + \frac{1}{2}(\mathbf{q}_m - \mathbf{q}_s)^\mathsf{T}\mathbf{P}(\mathbf{q}_m - \mathbf{q}_s), \tag{3.22}$$

then, adding Equations (3.17)-(3.19) together and using Equations (3.20)-(3.22), the time derivative of V can be bounded by:

$$\begin{aligned}\dot{V} \leq & -\dot{\mathbf{q}}_m^\mathsf{T}\mathbf{K}_m\dot{\mathbf{q}}_m + \overline{d}_m\dot{\mathbf{q}}_m^\mathsf{T}\mathbf{Q}_m\dot{\mathbf{q}}_m + \frac{\overline{d}_s e^{\overline{d}_s\overline{\sigma}}}{4\eta_s}\dot{\mathbf{q}}_m^\mathsf{T}\mathbf{P}\mathbf{Q}_s^{-1}\mathbf{P}^\mathsf{T}\dot{\mathbf{q}}_m + \frac{1}{2}\sigma\lambda_{m2}\dot{\mathbf{q}}_m^\mathsf{T}\dot{\mathbf{q}}_m \\ & - \sigma_m(\mathbf{q}_m - \mathbf{q}_s)^\mathsf{T}\mathbf{B}_m(\mathbf{q}_m - \mathbf{q}_s) + \frac{\overline{d}_s\sigma_m^2 e^{\overline{d}_s\overline{\sigma}}}{1-\eta_s}(\mathbf{q}_m - \mathbf{q}_s)^\mathsf{T}\mathbf{B}_m\mathbf{Q}_s^{-1}\mathbf{B}_m^\mathsf{T}(\mathbf{q}_m - \mathbf{q}_s) \\ & - \dot{\mathbf{q}}_s^\mathsf{T}\mathbf{K}_s\dot{\mathbf{q}}_s + \overline{d}_s\dot{\mathbf{q}}_s^\mathsf{T}\mathbf{Q}_s\dot{\mathbf{q}}_s + \frac{\overline{d}_m e^{\overline{d}_m\overline{\sigma}}}{4\eta_m}\dot{\mathbf{q}}_s^\mathsf{T}\mathbf{P}\mathbf{Q}_m^{-1}\mathbf{P}^\mathsf{T}\dot{\mathbf{q}}_s + \frac{1}{2}\sigma\lambda_{s2}\dot{\mathbf{q}}_s^\mathsf{T}\dot{\mathbf{q}}_s \\ & - \sigma_s(\mathbf{q}_s - \mathbf{q}_m)^\mathsf{T}\mathbf{B}_s(\mathbf{q}_s - \mathbf{q}_m) + \frac{\overline{d}_m\sigma_s^2 e^{\overline{d}_m\overline{\sigma}}}{1-\eta_m}(\mathbf{q}_s - \mathbf{q}_m)^\mathsf{T}\mathbf{B}_s\mathbf{Q}_m^{-1}\mathbf{B}_s^\mathsf{T}(\mathbf{q}_s - \mathbf{q}_m)\end{aligned}$$

$$+\frac{1}{2}\sigma(\mathbf{q}_m-\mathbf{q}_s)^{\mathsf{T}}\mathbf{P}(\mathbf{q}_m-\mathbf{q}_s)-\sigma V+\dot{\mathbf{q}}_m^{\mathsf{T}}(\boldsymbol{\tau}_h+\boldsymbol{\tau}_{ed})+\dot{\mathbf{q}}_s^{\mathsf{T}}(\boldsymbol{\tau}_e+\boldsymbol{\tau}_{hd}). \tag{3.23}$$

Consider

$$\dot{\mathbf{q}}_m^{\mathsf{T}}(\boldsymbol{\tau}_h+\boldsymbol{\tau}_{ed})=\sum_{k=1}^{n}\dot{q}_{mk}(\tau_{hk}+\tau_{edk}),\quad \dot{\mathbf{q}}_s^{\mathsf{T}}(\boldsymbol{\tau}_e+\boldsymbol{\tau}_{hd})=\sum_{k=1}^{n}\dot{q}_{sk}(\tau_{ek}+\tau_{hdk}),$$

if $|\dot{q}_{mk}|\leq\overline{\dot{q}}_m$, $\forall k=1,\cdots,n$, then

$$\dot{\mathbf{q}}_m^{\mathsf{T}}(\boldsymbol{\tau}_h+\boldsymbol{\tau}_{ed})\leq\sum_{k=1}^{n}|\dot{q}_{mk}(\tau_{hk}+\tau_{edk})|\leq n\sigma_m(\overline{\tau}_h+\overline{\tau}_e)\leq n\sigma(\overline{\tau}_h+\overline{\tau}_e),$$

else if $|\dot{q}_{mk}|>\overline{\dot{q}}_m$, $\exists k=1,\cdots,n$, then $\sigma\geq\sigma_m\geq\frac{1}{n}\overline{\dot{q}}_m$ and

$$\begin{aligned}\dot{\mathbf{q}}_m^{\mathsf{T}}(\boldsymbol{\tau}_h+\boldsymbol{\tau}_{ed})\leq&\frac{1}{2\sigma}\dot{\mathbf{q}}_m^{\mathsf{T}}\boldsymbol{\Upsilon}_m\dot{\mathbf{q}}_m+\frac{1}{2}\sigma(\boldsymbol{\tau}_h+\boldsymbol{\tau}_{ed})^{\mathsf{T}}\boldsymbol{\Upsilon}_m^{-1}(\boldsymbol{\tau}_h+\boldsymbol{\tau}_{ed})\\ \leq&\frac{n}{2\overline{\dot{q}}_m}\dot{\mathbf{q}}_m^{\mathsf{T}}\boldsymbol{\Upsilon}_m\dot{\mathbf{q}}_m+\frac{1}{2}\sigma(\boldsymbol{\tau}_h+\boldsymbol{\tau}_{ed})^{\mathsf{T}}\boldsymbol{\Upsilon}_m^{-1}(\boldsymbol{\tau}_h+\boldsymbol{\tau}_{ed}),\end{aligned}$$

so we conclude

$$\dot{\mathbf{q}}_m^{\mathsf{T}}(\boldsymbol{\tau}_h+\boldsymbol{\tau}_{ed})\leq\frac{n}{2\overline{\dot{q}}_m}\dot{\mathbf{q}}_m^{\mathsf{T}}\boldsymbol{\Upsilon}_m\dot{\mathbf{q}}_m+\sigma\left(\frac{1}{2}(\boldsymbol{\tau}_h+\boldsymbol{\tau}_{ed})^{\mathsf{T}}\boldsymbol{\Upsilon}_m^{-1}(\boldsymbol{\tau}_h+\boldsymbol{\tau}_{ed})+n(\overline{\tau}_h+\overline{\tau}_e)\right). \tag{3.24}$$

Similarly, if $|\dot{q}_{sk}|\leq\overline{\dot{q}}_s$, $\forall k=1,\cdots,n$, then

$$\dot{\mathbf{q}}_s^{\mathsf{T}}(\boldsymbol{\tau}_e+\boldsymbol{\tau}_{hd})\leq\sum_{k=1}^{n}|\dot{q}_{sk}(\tau_{ek}+\tau_{hdk})|\leq n\sigma_s(\overline{\tau}_h+\overline{\tau}_e)\leq n\sigma(\overline{\tau}_h+\overline{\tau}_e),$$

else if $|\dot{q}_{sk}|>\overline{\dot{q}}_s$, $\exists k=1,\cdots,n$, then $\sigma\geq\sigma_s\geq\frac{1}{n}\overline{\dot{q}}_s$ and

$$\begin{aligned}\dot{\mathbf{q}}_s^{\mathsf{T}}(\boldsymbol{\tau}_e+\boldsymbol{\tau}_{hd})\leq&\frac{1}{2\sigma}\dot{\mathbf{q}}_s^{\mathsf{T}}\boldsymbol{\Upsilon}_s\dot{\mathbf{q}}_s+\frac{1}{2}\sigma(\boldsymbol{\tau}_e+\boldsymbol{\tau}_{hd})^{\mathsf{T}}\boldsymbol{\Upsilon}_s^{-1}(\boldsymbol{\tau}_e+\boldsymbol{\tau}_{hd})\\ \leq&\frac{n}{2\overline{\dot{q}}_s}\dot{\mathbf{q}}_s^{\mathsf{T}}\boldsymbol{\Upsilon}_s\dot{\mathbf{q}}_s+\frac{1}{2}\sigma(\boldsymbol{\tau}_e+\boldsymbol{\tau}_{hd})^{\mathsf{T}}\boldsymbol{\Upsilon}_s^{-1}(\boldsymbol{\tau}_e+\boldsymbol{\tau}_{hd}),\end{aligned}$$

so we conclude

$$\dot{\mathbf{q}}_s^{\mathsf{T}}(\boldsymbol{\tau}_e+\boldsymbol{\tau}_{hd})\leq\frac{n}{2\overline{\dot{q}}_s}\dot{\mathbf{q}}_s^{\mathsf{T}}\boldsymbol{\Upsilon}_s\dot{\mathbf{q}}_s+\sigma\left(\frac{1}{2}(\boldsymbol{\tau}_e+\boldsymbol{\tau}_{hd})^{\mathsf{T}}\boldsymbol{\Upsilon}_s^{-1}(\boldsymbol{\tau}_e+\boldsymbol{\tau}_{hd})+n(\overline{\tau}_h+\overline{\tau}_e)\right). \tag{3.25}$$

Defining $\boldsymbol{\Theta} = \left[\dot{\mathbf{q}}_m^\mathsf{T}, \dot{\mathbf{q}}_s^\mathsf{T}, (\mathbf{q}_m - \mathbf{q}_s)^\mathsf{T}\right]^\mathsf{T}$ and substituting Equations (3.24)-(3.25) in Equation (3.23), then the derivative of V can be bounded by

$$\dot{V} \leq -\sigma V - \boldsymbol{\Theta}^\mathsf{T}\boldsymbol{\Psi}\boldsymbol{\Theta} + \sigma\chi(\boldsymbol{\tau}_h, \boldsymbol{\tau}_e), \tag{3.26}$$

where $\boldsymbol{\Psi} = \text{diag}\{\boldsymbol{\Psi}_{11}, \boldsymbol{\Psi}_{22}, \boldsymbol{\Psi}_{33}\}$ with

$$\begin{aligned}
\boldsymbol{\Psi}_{11} =& \mathbf{K}_m - \overline{d}_m\mathbf{Q}_m - \frac{\overline{d}_s e^{\overline{d}_s\overline{\sigma}}}{4\eta_s}\mathbf{P}\mathbf{Q}_s^{-1}\mathbf{P}^\mathsf{T} - \frac{1}{2}\sigma\lambda_{m2}\mathbf{I} - \frac{n}{2\dot{\overline{q}}_m}\boldsymbol{\Upsilon}_m \\
\boldsymbol{\Psi}_{22} =& \mathbf{K}_s - \overline{d}_s\mathbf{Q}_s - \frac{\overline{d}_m e^{\overline{d}_m\overline{\sigma}}}{4\eta_m}\mathbf{P}\mathbf{Q}_m^{-1}\mathbf{P}^\mathsf{T} - \frac{1}{2}\sigma\lambda_{s2}\mathbf{I} - \frac{n}{2\dot{\overline{q}}_s}\boldsymbol{\Upsilon}_s \\
\boldsymbol{\Psi}_{33} =& \sigma_m\mathbf{B}_m - \frac{\overline{d}_s\sigma_m^2 e^{\overline{d}_s\overline{\sigma}}}{1-\eta_s}\mathbf{B}_m\mathbf{Q}_s^{-1}\mathbf{B}_m^\mathsf{T} + \sigma_s\mathbf{B}_s - \frac{\overline{d}_m\sigma_s^2 e^{\overline{d}_m\overline{\sigma}}}{1-\eta_m}\mathbf{B}_s\mathbf{Q}_m^{-1}\mathbf{B}_s^\mathsf{T} - \frac{\sigma}{2}\mathbf{P}
\end{aligned} \tag{3.27}$$

and the function $\chi(\boldsymbol{\tau}_h, \boldsymbol{\tau}_e)$ is

$$\chi(\boldsymbol{\tau}_h, \boldsymbol{\tau}_e) = \frac{1}{2}(\boldsymbol{\tau}_h + \boldsymbol{\tau}_{ed})^\mathsf{T}\boldsymbol{\Upsilon}_m^{-1}(\boldsymbol{\tau}_h + \boldsymbol{\tau}_{ed}) + \frac{1}{2}(\boldsymbol{\tau}_e + \boldsymbol{\tau}_{hd})^\mathsf{T}\boldsymbol{\Upsilon}_s^{-1}(\boldsymbol{\tau}_e + \boldsymbol{\tau}_{hd}) + 2n(\overline{\tau}_h + \overline{\tau}_e).$$

In $\boldsymbol{\Psi}_{33}$, $\sigma_m + \sigma_s$ upper bounds $\sigma = \max(\sigma_m, \sigma_s)$. As they represent the master and slave velocity magnitudes, σ_m and σ_s are time-dependent. Then, for $\boldsymbol{\Psi}$ to be positive semi-definite (i) the gains appearing in $\boldsymbol{\Psi}_{11}$ and $\boldsymbol{\Psi}_{22}$ should be selected to make them positive semidefinite, and (ii) $\boldsymbol{\Psi}_{33}$ should be positive semidefinite for any σ_m and σ_s. Since $\boldsymbol{\Psi}_{33}$ is quadratic in σ_m and σ_s, and zero when $\sigma_m = \sigma_s = 0$, proper choice of $\mathbf{B}_m$ and $\mathbf{B}_s$ renders $\mathbf{B}_m - \frac{1}{2}\mathbf{P}$ and $\mathbf{B}_s - \frac{1}{2}\mathbf{P}$ positive definite and the other solution $(\hat{\sigma}_m, \hat{\sigma}_s)$ for the quadratic positive. Then, selecting $\text{sat}(\dot{q}_{ij})$ such that $0 < \overline{\sigma} \leq \min(\hat{\sigma}_m, \hat{\sigma}_s)$ makes $\boldsymbol{\Psi}_{33}$ positive semi-definite.

Theorem 5. *Consider the teleoperation system in Equation (2.1) with the controller in Equation (3.15). If the control gains ($\mathbf{B}_i$, $\mathbf{K}_i$ and $\mathbf{P}$), the parameters ($\mathbf{Q}_i$, η_i, $\boldsymbol{\Upsilon}_i$) and the nonlinear functions $\mathbf{S}_i(\dot{\mathbf{q}}_i)$, $i = m, s$ are selected such that the diagonal matrix $\boldsymbol{\Psi}$ is positive semi-definite, then the system possesses three the same properties as in Theorem 4.*

Proof. Assuming that $\boldsymbol{\Psi}$ is positive semi-definite, i.e. $-\boldsymbol{\Theta}\boldsymbol{\Psi}\boldsymbol{\Theta} \leq 0$, $\forall\boldsymbol{\Theta}$ then Equation (3.26) can be rewritten as $\dot{V} \leq -\sigma V + \sigma\chi(\boldsymbol{\tau}_h, \boldsymbol{\tau}_e)$. Further, $\boldsymbol{\Upsilon}_i$ are positive

definite diagonal matrices,

$$\chi(\boldsymbol{\tau}_h, \boldsymbol{\tau}_e) \leq \alpha \left(\sup_{0\leq\xi\leq t} ||\boldsymbol{\tau}_h||, \sup_{0\leq\xi\leq t} ||\boldsymbol{\tau}_e|| \right),$$

where $\alpha(\cdot)$ is a $\mathcal{K}_\infty$ function. Then the solution of $\dot{V}$ becomes

$$V \leq V_{t_0} e^{-\int_0^t \sigma d\xi} + \alpha \left(\sup_{0\leq\xi\leq t} ||\boldsymbol{\tau}_h||, \sup_{0\leq\xi\leq t} ||\boldsymbol{\tau}_e|| \right),$$

where V_{t_0} is the value of V at time $t = 0$.

From the definition of V and the property P.1, one further has

$$V \geq \frac{1}{2}\lambda_{m1}||\dot{\mathbf{q}}_m||^2 + \frac{1}{2}\lambda_{s1}||\dot{\mathbf{q}}_s||^2 + \frac{1}{2}\underline{p}||\mathbf{q}_m - \mathbf{q}_s||^2,$$

where $\underline{p}$ is the minimum eigenvalue of $\mathbf{P}$. Using the property that all three terms are non-negative, we get

$$\begin{aligned} ||\dot{\mathbf{q}}_i||^2 &\leq \frac{2}{\lambda_{i1}} \left[V_{t_0} e^{-\int_0^t \sigma d\xi} + \alpha \left(\sup_{0\leq\xi\leq t} ||\boldsymbol{\tau}_h||, \sup_{0\leq\xi\leq t} ||\boldsymbol{\tau}_e|| \right) \right], \\ ||\mathbf{q}_m - \mathbf{q}_s||^2 &\leq \frac{2}{\underline{p}} \left[V_{t_0} e^{-\int_0^t \sigma d\xi} + \alpha \left(\sup_{0\leq\xi\leq t} ||\boldsymbol{\tau}_h||, \sup_{0\leq\xi\leq t} ||\boldsymbol{\tau}_e|| \right) \right], \end{aligned} \tag{3.28}$$

$i = m, s$, and σ is non-negative, so $V_{t_0} e^{-\int_0^t \sigma d\xi} \leq V_{t_0}$. Besides, under the condition that assumption A.3 holds, $\boldsymbol{\tau}_h$ and $\boldsymbol{\tau}_e$ are bounded, the second term in the above three inequalities are bounded, i.e., $\alpha \left(\sup_{0\leq\xi\leq t} ||\boldsymbol{\tau}_h||, \sup_{0\leq\xi\leq t} ||\boldsymbol{\tau}_e|| \right) < \infty$. Therefore, velocities of the master and slave robots and the position error between the master and slave robots all are bounded, i.e. $\{\dot{\mathbf{q}}_m, \dot{\mathbf{q}}_s, \mathbf{q}_m - \mathbf{q}_s\} \in \mathcal{L}_\infty$, the proof for the first part of the theorem is completed.

To prove the second part, let us first look at the first two inequalities in (3.28). Under the condition that the hand and environment torques disappear from the time instant $t = t_1$, they can be rewritten as

$$||\dot{\mathbf{q}}_i||^2 \leq \frac{1}{\lambda_{i1}} V_{t_1} e^{-\int_{t_1}^t \sigma d\xi} \leq \frac{1}{\lambda_{i1}} V_{t_1} e^{-\int_{t_1}^t \sigma_i d\xi},$$

$i = m, s$, where

$$V_{t_1} = V_0 e^{-\int_0^{t_1} \sigma d\xi} + r(\sup_{0\le\xi\le t_1} ||\boldsymbol{\tau}_h||, \sup_{0\le\xi\le t_1} ||\boldsymbol{\tau}_e||, \overline{\tau}_h, \overline{\tau}_e).$$

Obviously, V_{t_1} is bounded from the above analysis and the function $e^{-\int_{t_1}^{t} \sigma_i d\xi}$ is decreasing with time t as long as $\dot{\mathbf{q}}_m \neq \mathbf{0}$ or $\dot{\mathbf{q}}_s \neq \mathbf{0}$. If the functions $e^{-\int_{t_1}^{t} \sigma_m d\xi}$ and $e^{-\int_{t_1}^{t} \sigma_s d\xi}$ do not tend to zero as $t \to \infty$, we must have $\int_{t_1}^{t} \sigma_i d\xi < \infty$, $i = m, s$. The derivative of σ_i is $\frac{d}{dt}(\sigma_i) = \frac{1}{n}\sum_{k=1}^{n} \left(\text{sat}(|\dot{q}_{ik}|)' |\dot{q}_{ik}|' \ddot{q}_{ik}\right)$. Return to (2.1), given the proof for the first part of the theorem, $\dot{\mathbf{q}}_m$, $\dot{\mathbf{q}}_s$ and $\mathbf{q}_m - \mathbf{q}_s$ all are bounded, it is obvious that the right side of (2.1) is bounded, with the property P.1, we conclude that $\ddot{\mathbf{q}}_m$ and $\ddot{\mathbf{q}}_s$ both are also bounded. From the fact that $\ddot{\mathbf{q}}_m$ and $\ddot{\mathbf{q}}_s$ are bounded and

$$sat(|\dot{q}_{ik}|)' = \begin{cases} 1 & |\dot{q}_{ik}| \le \overline{\dot{q}}_i^- \\ 0 & |\dot{q}_{ik}| \ge \overline{\dot{q}}_i^+ \end{cases}, \quad |\dot{q}_{ik}|' = \begin{cases} 1 & \dot{q}_{ik} \ge 0^+ \\ -1 & \dot{q}_{ik} \le 0^- \end{cases},$$

so $\frac{d}{dt}(\sigma_i)$ is bounded. Using the Barbalat's Lemma, we have $\sigma_i \to 0$, $i = m, s$, which equals that $\{\dot{\mathbf{q}}_m, \dot{\mathbf{q}}_s\} \to \mathbf{0}$. To discuss the convergence of position error $\mathbf{q}_m - \mathbf{q}_s$, it is clear from (2.1) that the convergence is guaranteed if we can prove that $\{\ddot{\mathbf{q}}_m, \ddot{\mathbf{q}}_s\} \to \mathbf{0}$ as $\{\dot{\mathbf{q}}_m, \dot{\mathbf{q}}_s\} \to \mathbf{0}$. Because we have concluded that $\{\dot{\mathbf{q}}_m, \dot{\mathbf{q}}_s\} \to \mathbf{0}$, we assume that from the time instant $t = t_2$ both $\dot{\mathbf{q}}_m$ and $\dot{\mathbf{q}}_s$ converge to the linear section of $\text{sat}(\dot{q}_{ik})$, i.e. $\mathbf{S}_i(\dot{\mathbf{q}}_i) = \frac{1}{n}\text{sgn}(\dot{\mathbf{q}}_i)$, then the closed-loop system (2.1) can be rewritten as

$$\mathbf{A}_i\mathbf{M}_i\ddot{\mathbf{q}}_i = -\mathbf{A}_i\mathbf{C}_i\dot{\mathbf{q}}_i - \mathbf{A}_i\mathbf{K}_i\dot{\mathbf{q}}_i - \mathbf{A}_i\mathbf{P}(\mathbf{q}_i - \mathbf{q}_{jd}) - \frac{1}{n}\mathbf{A}_i\text{sgn}(\dot{\mathbf{q}}_i)(\mathbf{q}_i - \mathbf{q}_{jd})^{\mathsf{T}}\mathbf{B}_i(\mathbf{q}_i - \mathbf{q}_{jd})$$

where $\mathbf{A}_i = \text{diag}\{|\dot{q}_{i1}|, |\dot{q}_{i2}|, \cdots, |\dot{q}_{in}|\}$ with $i, j = \{m, s\}$ and $i \neq j$. With $\mathbf{A}_i\text{sgn}(\dot{\mathbf{q}}_i) = \dot{\mathbf{q}}_i$, the derivative of the closed-loop system is

$$\begin{aligned}
&(\dot{\mathbf{A}}_i\mathbf{M}_i + \mathbf{A}_i\dot{\mathbf{M}}_i)\ddot{\mathbf{q}}_i + \mathbf{A}_i\mathbf{M}_i\dddot{\mathbf{q}}_i \\
=& -(\dot{\mathbf{A}}_i\mathbf{C}_i + \mathbf{A}_i\dot{\mathbf{C}}_i)\dot{\mathbf{q}}_i - \mathbf{A}_i\mathbf{C}_i\ddot{\mathbf{q}}_i - \mathbf{K}_i(\dot{\mathbf{A}}_i\dot{\mathbf{q}}_i + \mathbf{A}_i\ddot{\mathbf{q}}_i) - \frac{1}{n}\ddot{\mathbf{q}}_m(\mathbf{q}_i - \mathbf{q}_{jd})^{\mathsf{T}}\mathbf{B}_i(\mathbf{q}_i - \mathbf{q}_{jd}) \\
&- \mathbf{P}\left[\dot{\mathbf{A}}_i(\mathbf{q}_i - \mathbf{q}_{jd}) + \mathbf{A}_i\left(\dot{\mathbf{q}}_i - \frac{d}{dt}\dot{\mathbf{q}}_{jd}(1 - \dot{d}_j)\right)\right] - \frac{\dot{\mathbf{q}}_i}{n}\frac{d}{dt}[(\mathbf{q}_i - \mathbf{q}_{jd})^{\mathsf{T}}\mathbf{B}_i(\mathbf{q}_i - \mathbf{q}_{jd})]
\end{aligned}$$

Since all other terms are bounded and the derivative of time delays $\dot{d}_i$ are bounded, it is obvious that $\dddot{\mathbf{q}}_i$ are bounded. Combined with the conclusion that $\dot{\mathbf{q}}_m$ and $\dot{\mathbf{q}}_s$ tend

to zero, one can conclude that $\{\ddot{\mathbf{q}}_m, \ddot{\mathbf{q}}_s\} \to 0$ according to the Barbalat's Theorem. Therefore, the position error converges to zero when $\boldsymbol{\tau}_h = \boldsymbol{\tau}_e = 0$, the second part is proved completely.

The proof of the third conclusion is the same as in the proof for Theorem 4, so it is omitted here. Then the whole theorem is proved completely. □

For simplicity, we use the system model as in Section 2.3 with the same robot parameters and communication delays. After choosing $\overline{\sigma} = \overline{\dot{q}}_i = 0.1$, $\boldsymbol{\Upsilon}_i = 0.001\mathbf{I}$, $\eta_i = 0.5$, $\mathbf{Q}_i = 10\mathbf{I}$, $\boldsymbol{\Psi}$ can be made negative semi-definite by selecting $\mathbf{K}_m = \mathbf{K}_s = 12\mathbf{I}$, $\mathbf{P}_m = \mathbf{P}_s = 10\mathbf{I}$ and $\mathbf{B}_m = \mathbf{B}_s = 3\mathbf{I}$. The master and slave robots start from $(\mathbf{q}_m^\mathsf{T}\ \dot{\mathbf{q}}_m^\mathsf{T})^\mathsf{T} = (\mathbf{q}_s^\mathsf{T}\ \dot{\mathbf{q}}_s^\mathsf{T})^\mathsf{T} = (\mathbf{0}^\mathsf{T}\ \mathbf{0}^\mathsf{T})^\mathsf{T}$, under the sinusoidal user-applied force $F_{hy} = 0.7\sin(0.1\pi t) + 0.3$ N. The environment with stiffness $k_e = 1000$ N/m is located at $y_e = 0.5$ m.

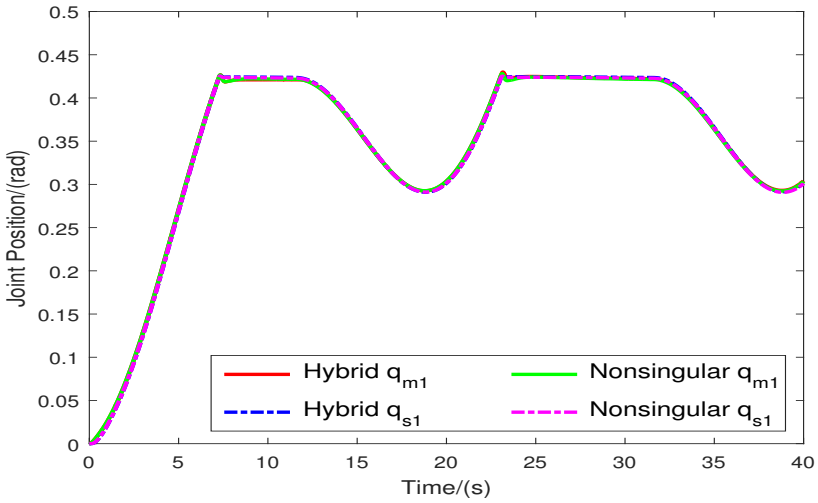

Figure 3.8: Position tracking in joint space: q_{m1} and q_{s1}.

The performance of the proposed nonsingular controller is compared with that of the hybrid controller in Section 3.1 in Figures. 3.8-3.10. From Figure. 3.8, both controllers have similar joint space position tracking performance, thus we conclude that the position tracking performance of the new controller is not worse than the previous singular controller. Nevertheless, the master and slave torques are quite different for the two controllers. Compared with Figure. 3.9(a), the control torque applied on the slave robot in Figure. 3.9(b) is smoother when the slave robot is interacting with the remote stiff wall. While the force feedback τ_{m1} is smoother than the slave torque in Figure. 3.10(a), it is clear that the control torques applied on the

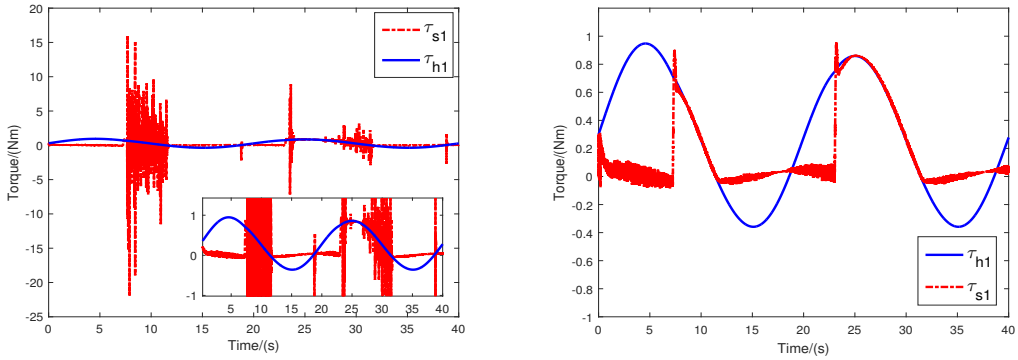

(a) Hybrid damping and stiffness adjustment. (b) Nonsingular damping and stiffness adjustment.

Figure 3.9: Hand and the slave control torque comparison between the hybrid and the nonsingular controllers: τ_{h1} and τ_{s1}.

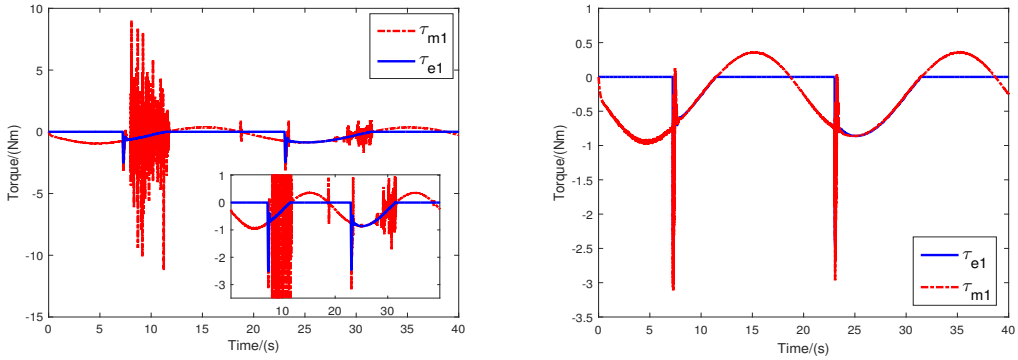

(a) Hybrid damping and stiffness adjustment. (b) Nonsingular damping and stiffness adjustment.

Figure 3.10: Environment and the master control torque comparison between the hybrid and the nonsingular controllers: τ_{e1} and τ_{m1}.

master robot are noisy both in free motion or in contact. On the contrary, the new nonsingular controller provides force feedback τ_{m1} in Figure. 3.10(b) that is noise-free and almost the same as the environment torques, τ_{e1}, when the slave robot is in contact with the remote wall.

3.3 Reduced-Order Coupling Control

In Section 3.2, a nonsingular controller is introduced to achieve smooth force feedback. However, when the position error is unexpectedly large such that the velocity- and position error-dependent control term overwhelms the proportional control term and

the master and slave robots cannot be synchronized, which is named sticking. In practical situations, before telemanipulation tasks, the master and slave robots should be initialized to start from the same position. Therefore, potential sticking should be avoided in controller design. This section introduces a new non-sticking controller. It also provides stability analysis of the closed-loop teleoperation system with the non-sticking controller and the controller parameters selection method.

For stable and sticking-free teleoperation with time delays, this section proposes the following controller:

$$\begin{aligned} \boldsymbol{\tau}_m &= -\Big[\mathbf{P} + \mathbf{S}(\dot{\mathbf{q}}_m, \mathbf{q}_m - \mathbf{q}_{sd})\Big](\mathbf{q}_m - \mathbf{q}_{sd}) - \mathbf{K}_m\dot{\mathbf{q}}_m + \boldsymbol{\tau}_{ed} + \mathbf{g}_m \\ \boldsymbol{\tau}_s &= -\Big[\mathbf{P} + \mathbf{S}(\dot{\mathbf{q}}_s, \mathbf{q}_s - \mathbf{q}_{md})\Big](\mathbf{q}_s - \mathbf{q}_{md}) - \mathbf{K}_s\dot{\mathbf{q}}_s + \boldsymbol{\tau}_{hd} + \mathbf{g}_s \end{aligned}, \tag{3.29}$$

where: $\mathbf{S}(\dot{\mathbf{q}}_i, \mathbf{q}_i - \mathbf{q}_{jd}) = \gamma \text{sgn}(\dot{\mathbf{q}}_i)\text{sgn}(\mathbf{q}_i - \mathbf{q}_{jd})^\mathsf{T}$ and $\text{sgn}(\mathbf{u}) = \Big[\text{sgn}(u_1), \cdots, \text{sgn}(u_n)\Big]^\mathsf{T}$ and $\text{sgn}(\cdot)$ represents the signum function; γ is a positive constant scalar; $\mathbf{P}$, $\mathbf{K}_i$ are positive diagonal gain matrices, $i, j = \{m, s\}$ and $i \neq j$.

In Equation (3.29), the nonlinear term, $\mathbf{S}_i(\dot{\mathbf{q}}_i, \mathbf{q}_i - \mathbf{q}_{jd})$, together with the diagonal gain matrix, $\mathbf{P}$, forms a new gain matrix, $\mathbf{P} + \mathbf{S}_i(\dot{\mathbf{q}}_i, \mathbf{q}_i - \mathbf{q}_{jd})$. One can find that the product of the new matrix and the position error generates a position synchronization term, $-p_k(q_{ik} - q_{jdk}) - \gamma \text{sgn}(\dot{q}_{ik})\|\mathbf{q}_i - \mathbf{q}_{jd}\|_1$, for each joint. For the joint with the largest position error, if $p_k > n\gamma$, then the conventional proportional part$(-p_k(q_{ik} - q_{jdk}))$ weighs more than the other part$(-\gamma \text{sgn}(\dot{q}_{ik})\|\mathbf{q}_i - \mathbf{q}_{jd}\|)$, and thus the controller tends to limit the position error along this joint space direction. Therefore, position tracking can be achieved even the initial position error is large. This is the main advantage of the controller in Equation (3.29) over the nonsingular controller in the previous section.

Figure. 3.11 displays the teleopration system under the control of the reduced-order damping and stiffness adjustment strategy. To analyze the stability of the system, we use the following Lyapunov-like energy function:

$$V = V_1 + V_2 + V_3 \tag{3.30}$$

with

$$V_1 = \frac{1}{2}\dot{\mathbf{q}}_m^\mathsf{T}\mathbf{M}_m\dot{\mathbf{q}}_m + \frac{1}{2}\dot{\mathbf{q}}_s^\mathsf{T}\mathbf{M}_s\dot{\mathbf{q}}_s$$

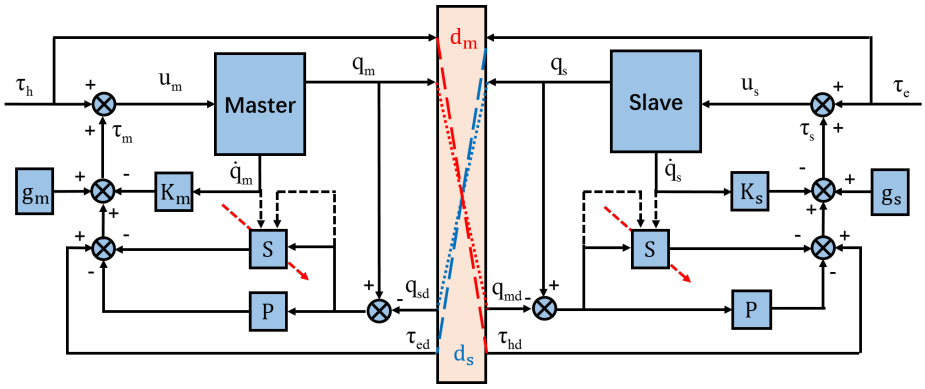

Figure 3.11: Teleoperation system under the reduced-order coupling control in Equation (3.29).

$$V_2 = \frac{1}{2}(\mathbf{q}_m - \mathbf{q}_s)^\mathsf{T}\mathbf{P}(\mathbf{q}_m - \mathbf{q}_s)$$
$$V_3 = \int_{-\bar{d}_m}^{0}\int_{t+\theta}^{t} e^{-\int_\xi^t \sigma du}\dot{\mathbf{q}}_m^\mathsf{T}(\xi)\mathbf{Q}_m\dot{\mathbf{q}}_m(\xi)d\xi d\theta + \int_{-\bar{d}_s}^{0}\int_{t+\theta}^{t} e^{-\int_\xi^t \sigma du}\dot{\mathbf{q}}_s^\mathsf{T}(\xi)\mathbf{Q}_s\dot{\mathbf{q}}_s(\xi)d\xi d\theta,$$

where: $\sigma = \min(\overline{\sigma}, \sigma_m + \sigma_s)$ with

$$\sigma_m = \frac{\max(|\dot{q}_{mk}|)\max(|q_{mk} - q_{sk}|)\epsilon}{\frac{1}{2}(\mathbf{q}_m - \mathbf{q}_s)^\mathsf{T}\mathbf{P}(\mathbf{q}_m - \mathbf{q}_s)}, \quad \sigma_s = \frac{\max(|\dot{q}_{sk}|)\max(|q_{mk} - q_{sk}|)\epsilon}{\frac{1}{2}(\mathbf{q}_m - \mathbf{q}_s)^\mathsf{T}\mathbf{P}(\mathbf{q}_m - \mathbf{q}_s)}$$

and: $\min(a, b)$ is the minimum of a and b; $\max(u_k)$ is the maximum of u_k for all possible k; $\overline{\sigma}$ and ϵ are two positive constants.

With the property L.2, the time derivative of V_1 is

$$\begin{aligned}\dot{V}_1 =& -\dot{\mathbf{q}}_m^\mathsf{T}\mathbf{K}_m\dot{\mathbf{q}}_m + \dot{\mathbf{q}}_m^\mathsf{T}(\boldsymbol{\tau}_h + \boldsymbol{\tau}_{ed}) - \dot{\mathbf{q}}_m^\mathsf{T}\mathbf{P}(\mathbf{q}_m - \mathbf{q}_s) - \dot{\mathbf{q}}_m^\mathsf{T}\mathbf{P}\int_{t-d_s}^{t}\dot{\mathbf{q}}_s(\xi)d\xi \\ & -\dot{\mathbf{q}}_s^\mathsf{T}\mathbf{K}\dot{\mathbf{q}}_s + \dot{\mathbf{q}}_s^\mathsf{T}(\boldsymbol{\tau}_e + \boldsymbol{\tau}_{hd}) - \dot{\mathbf{q}}_s^\mathsf{T}\mathbf{P}(\mathbf{q}_s - \mathbf{q}_m) - \dot{\mathbf{q}}_s^\mathsf{T}\mathbf{P}\int_{t-d_m}^{t}\dot{\mathbf{q}}_m(\xi)d\xi \\ & -\dot{\mathbf{q}}_m^\mathsf{T}\mathbf{S}(\dot{\mathbf{q}}_m, \mathbf{q}_m - \mathbf{q}_{sd})(\mathbf{q}_m - \mathbf{q}_{sd}) - \dot{\mathbf{q}}_s^\mathsf{T}\mathbf{S}(\dot{\mathbf{q}}_s, \mathbf{q}_s - \mathbf{q}_{md})(\mathbf{q}_s - \mathbf{q}_{md}).\end{aligned} \tag{3.31}$$

The derivatives of V_2 and V_3 are

$$\dot{V}_2 = \dot{\mathbf{q}}_m^\mathsf{T}\mathbf{P}(\mathbf{q}_m - \mathbf{q}_s) + \dot{\mathbf{q}}_s^\mathsf{T}\mathbf{P}(\mathbf{q}_s - \mathbf{q}_m), \tag{3.32}$$

$$\begin{aligned}\dot{V}_3 \leq & \overline{d}_m \dot{\mathbf{q}}_m^{\mathsf{T}} \mathbf{Q}_m \dot{\mathbf{q}}_m - e^{-\sigma \overline{d}_m} \int_{t-d_m}^{t} \dot{\mathbf{q}}_m^{\mathsf{T}}(\xi) \mathbf{Q}_m \dot{\mathbf{q}}_m(\xi) d\xi \\ & + \overline{d}_s \dot{\mathbf{q}}_s^{\mathsf{T}} \mathbf{Q}_s \dot{\mathbf{q}}_s - e^{-\sigma \overline{d}_s} \int_{t-d_s}^{t} \dot{\mathbf{q}}_s^{\mathsf{T}}(\xi) \mathbf{Q}_s \dot{\mathbf{q}}_s(\xi) d\xi - \sigma V_3.\end{aligned} \tag{3.33}$$

Further, from the definition of $\mathbf{S}(\dot{\mathbf{q}}_i, \mathbf{q}_i - \mathbf{q}_{jd})$, we have

$$\begin{aligned}& - \dot{\mathbf{q}}_m^{\mathsf{T}} \mathbf{S}(\dot{\mathbf{q}}_m, \mathbf{q}_m - \mathbf{q}_{sd})(\mathbf{q}_m - \mathbf{q}_{sd}) \\ = & - \gamma \dot{\mathbf{q}}_m^{\mathsf{T}} sgn(\dot{\mathbf{q}}_m) sgn(\mathbf{q}_m - \mathbf{q}_{sd})^{\mathsf{T}} (\mathbf{q}_m - \mathbf{q}_{sd}) = -\gamma \left(\sum_{k=1}^{n} |\dot{q}_{mk}| \right) \left(\sum_{k=1}^{n} |q_{mk} - q_{sdk}| \right) \\ \leq & - \gamma \left(\sum_{k=1}^{n} |\dot{q}_{mk}| \right) \left(\sum_{k=1}^{n} |q_{mk} - q_{sk}| \right) + \gamma \sum_{k=1}^{n} \left(|\dot{\mathbf{q}}_{mk}|^{\mathsf{T}} \int_{t-d_s}^{t} |\dot{\mathbf{q}}_s(\xi)| d\xi \right)\end{aligned} \tag{3.34}$$

and similarly

$$\begin{aligned}& - \dot{\mathbf{q}}_s^{\mathsf{T}} \mathbf{S}(\dot{\mathbf{q}}_s, \mathbf{q}_s - \mathbf{q}_{md})(\mathbf{q}_s - \mathbf{q}_{md}) \\ \leq & - \gamma \left(\sum_{k=1}^{n} |\dot{q}_{sk}| \right) \left(\sum_{k=1}^{n} |q_{sk} - q_{mk}| \right) + \gamma \sum_{k=1}^{n} \left(|\dot{\mathbf{q}}_{sk}|^{\mathsf{T}} \int_{t-d_m}^{t} |\dot{\mathbf{q}}_m(\xi)| d\xi \right)\end{aligned} \tag{3.35}$$

where $\dot{\mathbf{q}}_{ik} = \left[\dot{q}_{ik}, \dot{q}_{ik}, \cdots, \dot{q}_{ik} \right]^{\mathsf{T}}$, $i = m, s$. Using the lemma L.2,

$$\begin{aligned}& \left(-\dot{\mathbf{q}}_m^{\mathsf{T}} \mathbf{P} + \gamma \sum_{k=1}^{n} |\dot{\mathbf{q}}_{mk}|^{\mathsf{T}} \right) \int_{t-d_s}^{t} \dot{\mathbf{q}}_s(\xi) d\xi - e^{-\sigma \overline{d}_s} \int_{t-d_s}^{t} \dot{\mathbf{q}}_s^{\mathsf{T}}(\xi) \mathbf{Q}_s \dot{\mathbf{q}}_s(\xi) d\xi \\ = & - \dot{\mathbf{q}}_m^{\mathsf{T}} \mathbf{P} \int_{t-d_s}^{t} \dot{\mathbf{q}}_s(\xi) d\xi - \eta_s e^{-\sigma \overline{d}_s} \int_{t-d_s}^{t} \dot{\mathbf{q}}_s^{\mathsf{T}}(\xi) \mathbf{Q}_s \dot{\mathbf{q}}_s(\xi) d\xi \\ & + \gamma \sum_{k=1}^{n} \left(|\dot{\mathbf{q}}_{mk}|^{\mathsf{T}} \int_{t-d_s}^{t} |\dot{\mathbf{q}}_s(\xi)| d\xi \right) - (1 - \eta_s) e^{-\sigma \overline{d}_s} \int_{t-d_s}^{t} \dot{\mathbf{q}}_s^{\mathsf{T}}(\xi) \mathbf{Q}_s \dot{\mathbf{q}}_s(\xi) d\xi \\ \leq & \frac{\overline{d}_s \gamma^2 e^{\sigma \overline{d}_s}}{4(1 - \eta_s)} \left(\sum_{i=1}^{n} \sum_{j=1}^{n} |\dot{\mathbf{q}}_{mi}|^{\mathsf{T}} \mathbf{Q}_s^{-1} |\dot{\mathbf{q}}_{mj}| \right) + \frac{\overline{d}_s e^{\sigma \overline{d}_s}}{4\eta_s} \dot{\mathbf{q}}_m^{\mathsf{T}} \mathbf{P} \mathbf{Q}_s^{-1} \mathbf{P}^{\mathsf{T}} \dot{\mathbf{q}}_m \\ \leq & \frac{n \overline{d}_s \gamma^2 e^{\sigma \overline{d}_s}}{4(1 - \eta_s)} \mathrm{trace}(\mathbf{Q}_s^{-1}) \dot{\mathbf{q}}_m^{\mathsf{T}} \dot{\mathbf{q}}_m + \frac{\overline{d}_s e^{\sigma \overline{d}_s}}{4\eta_s} \dot{\mathbf{q}}_m^{\mathsf{T}} \mathbf{P} \mathbf{Q}_s^{-1} \mathbf{P}^{\mathsf{T}} \dot{\mathbf{q}}_m\end{aligned} \tag{3.36}$$

where trace$(\mathbf{Q}_s^{-1})$ is the trace of $\mathbf{Q}_s^{-1}$ and $0 < \eta_s < 1$. Similarly,

$$\begin{aligned}&\left(-\dot{\mathbf{q}}_s^{\mathsf{T}}\mathbf{P} + \gamma \sum_{k=1}^{n} |\dot{\mathbf{q}}_{sk}|^{\mathsf{T}}\right) \int_{t-d_m}^{t} \dot{\mathbf{q}}_m(\xi)d\xi - e^{-\sigma \overline{d}_m} \int_{t-d_m}^{t} \dot{\mathbf{q}}_m^{\mathsf{T}}(\xi)\mathbf{Q}_m\dot{\mathbf{q}}_m(\xi)d\xi \\ \leq &\frac{n\overline{d}_m\gamma^2 e^{\sigma\overline{d}_m}}{4(1-\eta_m)}\text{trace}(\mathbf{Q}_m^{-1})\dot{\mathbf{q}}_s^{\mathsf{T}}\dot{\mathbf{q}}_s + \frac{\overline{d}_m e^{\sigma\overline{d}_m}}{4\eta_m}\dot{\mathbf{q}}_s^{\mathsf{T}}\mathbf{P}\mathbf{Q}_m^{-1}\mathbf{P}^{\mathsf{T}}\dot{\mathbf{q}}_s\end{aligned} \tag{3.37}$$

where trace$(\mathbf{Q}_m^{-1})$ is the trace of $\mathbf{Q}_m^{-1}$ and $0 < \eta_m < 1$, and

$$\sigma V_1 \leq \frac{1}{2}\sigma\lambda_{m2}\dot{\mathbf{q}}_m^{\mathsf{T}}\dot{\mathbf{q}}_m + \frac{1}{2}\sigma\lambda_{s2}\dot{\mathbf{q}}_s^{\mathsf{T}}\dot{\mathbf{q}}_s, \tag{3.38}$$

$$\begin{aligned}\sigma V_2 \leq &\frac{1}{2}(\sigma_m + \sigma_s)(\mathbf{q}_m - \mathbf{q}_s)^T\mathbf{P}(\mathbf{q}_m - \mathbf{q}_s) \\ \leq &\max(|\dot{q}_{mk}|)\max(|q_{mk} - q_{sk}|)\epsilon + \max(|\dot{q}_{sk}|)\max(|q_{mk} - q_{sk}|)\epsilon.\end{aligned} \tag{3.39}$$

Because σ is a state-dependent function, it is varying and switching between $\overline{\sigma}$ and $\sigma_m + \sigma_s$ with time. We discuss the two cases independently as following.

Case 1. $\sigma = \sigma_m + \sigma_s$

$$\begin{aligned}&\dot{\mathbf{q}}_m^{\mathsf{T}}(\boldsymbol{\tau}_h + \boldsymbol{\tau}_{ed}) \leq \frac{1}{2\sigma}\dot{\mathbf{q}}_m^{\mathsf{T}}\boldsymbol{\Upsilon}_m\dot{\mathbf{q}}_m + \frac{\sigma}{2}(\boldsymbol{\tau}_h + \boldsymbol{\tau}_{ed})^{\mathsf{T}}\boldsymbol{\Upsilon}_m^{-1}(\boldsymbol{\tau}_h + \boldsymbol{\tau}_{ed}) \\ \leq &\frac{\upsilon_m\overline{p}}{4\epsilon}\frac{\left(\sum_{k=1}^{n}\dot{q}_{mk}^2\right)\left(\sum_{k=1}^{n}|q_{mk} - q_{sk}|^2\right)}{\max(|\dot{q}_{mk}|)\max(|q_{mk} - q_{sk}|)} + \frac{\sigma}{2}(\boldsymbol{\tau}_h + \boldsymbol{\tau}_{ed})^{\mathsf{T}}\boldsymbol{\Upsilon}_m^{-1}(\boldsymbol{\tau}_h + \boldsymbol{\tau}_{ed}) \\ \leq &\frac{\upsilon_m\overline{p}}{4\epsilon}\left(\sum_{k=1}^{n}|\dot{q}_{mk}|\right)\left(\sum_{k=1}^{n}|q_{mk} - q_{sk}|\right) + \frac{\sigma}{2}(\boldsymbol{\tau}_h + \boldsymbol{\tau}_{ed})^{\mathsf{T}}\boldsymbol{\Upsilon}_m^{-1}(\boldsymbol{\tau}_h + \boldsymbol{\tau}_{ed}) \\ = &\frac{\upsilon_m\overline{p}}{4\epsilon}\sum_{i=1}^{n}\sum_{j=1}^{n}|\dot{q}_{mi}||q_{mj} - q_{sj}| + \frac{\sigma}{2}(\boldsymbol{\tau}_h + \boldsymbol{\tau}_{ed})^{\mathsf{T}}\boldsymbol{\Upsilon}_m^{-1}(\boldsymbol{\tau}_h + \boldsymbol{\tau}_{ed}),\end{aligned} \tag{3.40}$$

where $\boldsymbol{\Upsilon}_m$ is a positive diagonal matrix and υ_m is its maximum eigenvalue; $\overline{p}$ is the maximum eigenvalue of $\mathbf{P}$. Similarly,

$$\dot{\mathbf{q}}_s^{\mathsf{T}}(\boldsymbol{\tau}_e + \boldsymbol{\tau}_{hd}) \leq \frac{\upsilon_s\overline{p}}{4\epsilon}\sum_{i=1}^{n}\sum_{j=1}^{n}|\dot{q}_{si}||q_{mj} - q_{sj}| + \frac{\sigma}{2}(\boldsymbol{\tau}_e + \boldsymbol{\tau}_{hd})^{\mathsf{T}}\boldsymbol{\Upsilon}_s^{-1}(\boldsymbol{\tau}_e + \boldsymbol{\tau}_{hd}), \tag{3.41}$$

where $\boldsymbol{\Upsilon}_s$ is a positive diagonal matrix and υ_s is its maximum eigenvalue.

Adding Equations (3.31)-(3.33) together and using Equations (3.34)-(3.41), the

derivative of V can then be bounded by

$$\begin{aligned}\dot{V} \leq & -\sigma V + \sigma\chi(\boldsymbol{\tau}_h, \boldsymbol{\tau}_e) - \dot{\mathbf{q}}_m^{\mathsf{T}}\boldsymbol{\Psi}_{m1}\dot{\mathbf{q}}_m - \dot{\mathbf{q}}_s^{\mathsf{T}}\boldsymbol{\Psi}_{s1}\dot{\mathbf{q}}_s \\ & - \psi_{m1}\sum_{i=1}^{n}\sum_{j=1}^{n}|\dot{q}_{mi}||q_{mj}-q_{sj}| - \psi_{s1}\sum_{i=1}^{n}\sum_{j=1}^{n}|\dot{q}_{si}||q_{mj}-q_{sj}|\end{aligned}$$

where $\chi(\boldsymbol{\tau}_h, \boldsymbol{\tau}_e) = \frac{1}{2}(\boldsymbol{\tau}_h + \boldsymbol{\tau}_{ed})^{\mathsf{T}}\boldsymbol{\Upsilon}_m^{-1}(\boldsymbol{\tau}_h + \boldsymbol{\tau}_{ed}) + \frac{1}{2}(\boldsymbol{\tau}_e + \boldsymbol{\tau}_{hd})^{\mathsf{T}}\boldsymbol{\Upsilon}_s^{-1}(\boldsymbol{\tau}_e + \boldsymbol{\tau}_{hd})$ and

$$\begin{aligned}\boldsymbol{\Psi}_{m1} =& \mathbf{K}_m - \overline{d}_m\mathbf{Q}_m - \frac{1}{2}\sigma\lambda_{m2}\mathbf{I} - \frac{n\overline{d}_s\gamma^2 e^{\sigma\overline{d}_s}\mathrm{trace}(\mathbf{Q}_s^{-1})}{4(1-\eta_s)}\mathbf{I} - \frac{\overline{d}_s e^{\sigma\overline{d}_s}}{4\eta_s}\mathbf{P}\mathbf{Q}_s^{-1}\mathbf{P}^{\mathsf{T}}, \\ \boldsymbol{\Psi}_{s1} =& \mathbf{K}_s - \overline{d}_s\mathbf{Q}_s - \frac{1}{2}\sigma\lambda_{s2}\mathbf{I} - \frac{n\overline{d}_m\gamma^2 e^{\sigma\overline{d}_m}trace(\mathbf{Q}_m^{-1})}{4(1-\eta_m)}\mathbf{I} - \frac{\overline{d}_m e^{\sigma\overline{d}_m}}{4\eta_m}\mathbf{P}\mathbf{Q}_m^{-1}\mathbf{P}^{\mathsf{T}}, \\ \psi_{m1} =& \gamma - \epsilon - \frac{\upsilon_m\overline{p}}{4\epsilon}, \quad \psi_{s1} = \gamma - \epsilon - \frac{\upsilon_s\overline{p}}{4\epsilon}.\end{aligned}$$

Therefore, if we choose proper parameters such that $\boldsymbol{\Psi}_{i1} \succeq \mathbf{0}$ and $\psi_{i1} \geq 0$, $i = m, s$, then the derivative of V can be simplified to

$$\dot{V} \leq -\sigma V + \sigma\chi(\boldsymbol{\tau}_h, \boldsymbol{\tau}_e).$$

Case 2. $\sigma = \overline{\sigma}$

$$\begin{aligned}\dot{\mathbf{q}}_m^{\mathsf{T}}(\boldsymbol{\tau}_h + \boldsymbol{\tau}_{ed}) \leq & \frac{1}{2\sigma}\dot{\mathbf{q}}_m^{\mathsf{T}}\boldsymbol{\Upsilon}_m\dot{\mathbf{q}}_m + \frac{\sigma}{2}(\boldsymbol{\tau}_h + \boldsymbol{\tau}_{ed})^{\mathsf{T}}\boldsymbol{\Upsilon}_m^{-1}(\boldsymbol{\tau}_h + \boldsymbol{\tau}_{ed}), \\ \dot{\mathbf{q}}_s^{\mathsf{T}}(\boldsymbol{\tau}_e + \boldsymbol{\tau}_{hd}) \leq & \frac{1}{2\sigma}\dot{\mathbf{q}}_s^{\mathsf{T}}\boldsymbol{\Upsilon}_s\dot{\mathbf{q}}_s + \frac{\sigma}{2}(\boldsymbol{\tau}_e + \boldsymbol{\tau}_{hd})^{\mathsf{T}}\boldsymbol{\Upsilon}_s^{-1}(\boldsymbol{\tau}_e + \boldsymbol{\tau}_{hd})\end{aligned} \tag{3.42}$$

where $\boldsymbol{\Upsilon}_i$, $i = m, s$, are the same positive diagonal matrices as in case 1.

Adding Equations (3.31)-(3.33) together and using Equation (3.42), then the derivative of V becomes

$$\begin{aligned}\dot{V} \leq & -\sigma V + \sigma\chi(\boldsymbol{\tau}_h, \boldsymbol{\tau}_e) - \dot{\mathbf{q}}_m^{\mathsf{T}}\boldsymbol{\Psi}_{m2}\dot{\mathbf{q}}_m - \dot{\mathbf{q}}_s^{\mathsf{T}}\boldsymbol{\Psi}_{s2}\dot{\mathbf{q}}_s \\ & - \psi_{m2}\sum_{i=1}^{n}\sum_{j=1}^{n}|\dot{q}_{mi}||q_{mj}-q_{sj}| - \psi_{s2}\sum_{i=1}^{n}\sum_{j=1}^{n}|\dot{q}_{si}||q_{mj}-q_{sj}|\end{aligned}$$

where $\chi(\tau_h, \tau_e) = \frac{1}{2}(\boldsymbol{\tau}_h + \boldsymbol{\tau}_{ed})^{\mathsf{T}}\boldsymbol{\Upsilon}_m^{-1}(\boldsymbol{\tau}_h + \boldsymbol{\tau}_{ed}) + \frac{1}{2}(\boldsymbol{\tau}_e + \boldsymbol{\tau}_{hd})^{\mathsf{T}}\boldsymbol{\Upsilon}_s^{-1}(\boldsymbol{\tau}_e + \boldsymbol{\tau}_{hd})$ and

$$\boldsymbol{\Psi}_{m2} = \mathbf{K}_m - \overline{d}_m\mathbf{Q}_m - \frac{1}{2\sigma}\boldsymbol{\Upsilon}_m - \frac{\overline{d}_s e^{\sigma\overline{d}_s}}{4\eta_s}\mathbf{P}\mathbf{Q}_s^{-1}\mathbf{P}^{\mathsf{T}} - \frac{n\overline{d}_s\gamma^2 e^{\sigma\overline{d}_s}\mathrm{trace}(\mathbf{Q}_s^{-1})}{4(1-\eta_s)}\mathbf{I} - \frac{1}{2}\sigma\lambda_{m2}\mathbf{I},$$

$$\boldsymbol{\Psi}_{s2} = \mathbf{K}_s - \overline{d}_s \mathbf{Q}_s - \frac{1}{2\sigma}\boldsymbol{\Upsilon}_s - \frac{\overline{d}_m e^{\sigma \overline{d}_m}}{4\eta_m}\mathbf{P}\mathbf{Q}_m^{-1}\mathbf{P}^{\mathsf{T}} - \frac{n\overline{d}_m \gamma^2 e^{\sigma \overline{d}_m}\mathrm{trace}(\mathbf{Q}_m^{-1})}{4(1-\eta_m)}\mathbf{I} - \frac{1}{2}\sigma\lambda_{s2}\mathbf{I},$$

$$\psi_{m2} = \psi_{s2} = \gamma - \epsilon.$$

Therefore, if we can choose proper parameter such that $\boldsymbol{\Psi}_{i2} \succeq \mathbf{0}$ and $\psi_{i2} \geq 0$, $i = m, s$, then the derivative of V can be simplified to

$$\dot{V} \leq -\sigma V + \sigma\chi(\boldsymbol{\tau}_h, \boldsymbol{\tau}_e).$$

Although σ is a state-dependent function that switches between $\overline{\sigma}$ and $\sigma_m + \sigma_s$ with time, from the analysis of the above two cases, if we can select parameters properly such that

$$\begin{aligned} \boldsymbol{\Psi}_i &= \min\{\boldsymbol{\Psi}_{i1}, \boldsymbol{\Psi}_{i2}\} = \boldsymbol{\Psi}_{i2} \succeq \mathbf{0} \\ \psi_i &= \min\{\psi_{i1}, \psi_{i2}\} = \psi_{i1} \geq 0 \end{aligned} \tag{3.43}$$

with $i = m, s$, then the Lyapunov-like function satisfies

$$\dot{V} \leq -\sigma V + \sigma\chi(\boldsymbol{\tau}_h, \boldsymbol{\tau}_e)$$

for each case of σ.

Theorem 6. *Consider the teleoperation system in Equation (2.1) with the controller in Equation (3.29). If the control gains($\mathbf{K}_i$, $\mathbf{P}$ and γ), the parameters($\mathbf{Q}_i$, η_i, $\boldsymbol{\Upsilon}_i$, $\overline{\sigma}$, ϵ) are selected properly such that Equation (3.43) is satisfied, then the system possesses three the same properties as in Theorem 1 and avoids sticking and noisy control torques.*

Proof. The proof is similar to the proof of Theorem 4 and Theorem 5, for saving space, it is omitted here. □

The parameter selection is carried out as follows:(1) select $\mathbf{P}$; (2) choose γ, ϵ and $\boldsymbol{\Upsilon}_i$ small enough to satisfy the second condition in Equation (3.43) and $\gamma < np_k$; (3) select $\mathbf{Q}_i$, $\overline{\sigma}$ and η_i such that the damping $\mathbf{K}_i$ can be selected small enough to guarantee the first condition in Equation (3.43). The parameter selection procedure is more straightforward than solving the matrix in the parameter design procedure in Section 3.2, which is second contribution of this section.

Simulation results are presented to verify the effectiveness of the reduced-order coupling control in Equation (3.29). The simulated robots with communication delays

are driven by the sinusoidal user force and interact with a stiff environment, of which parameters are the same as in Section 3.2. After choosing $\mathbf{P} = 5\mathbf{I}$ and $\boldsymbol{\Upsilon}_m = \boldsymbol{\Upsilon}_s = 0.0001\mathbf{I}$, $\epsilon = 0.1$, $\gamma = 0.05$, $\eta_m = \eta_s = 0.5$ and $\mathbf{Q}_m = \mathbf{Q}_s = 10\mathbf{I}$, ψ_m and ψ_s can be made nonpositive by choosing $\overline{\sigma} = 0.1$, and $\boldsymbol{\Psi}_m$ and $\boldsymbol{\Psi}_s$ can be made negative semi-definite by choosing $\mathbf{K}_m = 5\mathbf{I}$ and $\mathbf{K}_s = 10\mathbf{I}$.

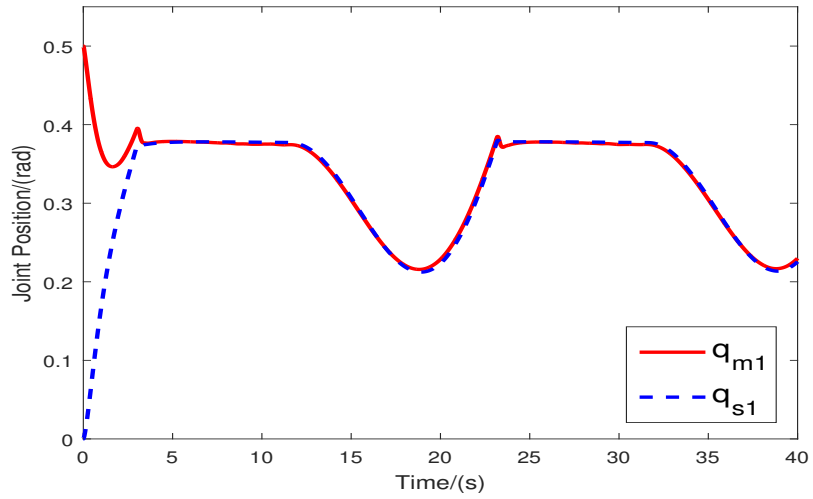

Figure 3.12: Position tracking in joint space: q_{m1} and q_{s1}.

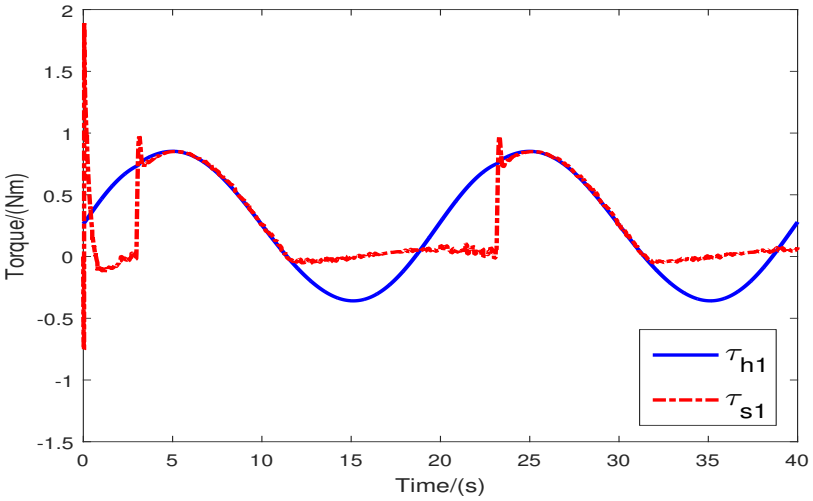

Figure 3.13: Hand and slave control torques: q_{m1} and q_{s1}.

Figure. 3.12 shows that the master is tightly constrained to the slave when the slave is in contact with the remote wall and that position tracking is achieved both in

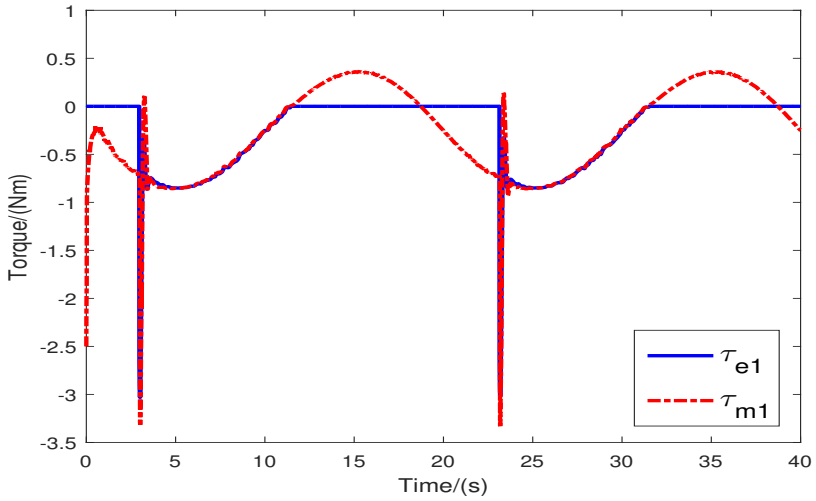

Figure 3.14: Environment and master control torques: q_{m1} and q_{s1}.

free motion and in hard contact. Figure. 3.13 illustrates the controller torques applied on the slave robot, τ_{s1}, track the hand torques, τ_{h1}, in contact, but they are a little bit noisy in free motion, which is caused by time-varying delays and is harmful for the actuators. Figure. 3.14 shows the force feedback performance of the system along the first joint space direction. Upon slave contact with the remote environment, torque spikes in τ_{m1} indicate to the user the beginning of interaction on the remote side.

3.4 Conclusions

This chapter has introduced a hybrid damping and stiffness adjustment strategy to guarantee ISS bilateral teleoperation when hand and environment forces are incorporated in the closed control loop. It has shown that four channel teleoperation can maintain a tight coupling between the master and slave sites, and hence a tight user-environment coupling. However, since the nonlinear hybrid adjusting terms in controller become singular at zero velocities, chattering problem may damage the system performance and even destroy actuators. The nonsingular version employs a saturation function to avoid the singularity problem, and, thus, torque spikes due to controller singularity are eliminated. Because the nonlinear velocity and position error coupling terms is quadratic in position error, sticking problem occurs when the position error becomes unexpected large. The reduced-order strategy has been developed to solve the sticking problem, i.e., to guarantee position coordination for

arbitrarily large position errors, and maintain the main advantages of four channel teleoperation.

Simulation results have shown the effectiveness of the proposed strategies for four channel teleoperation. However, all these results are still needed to be experimentally tested. ISS teleoperation is not the best choice from the perspective of control, so deeper research efforts are expected to exploit the transmitted forces, distinguish the harmful components from the wanted part and reject the disturbing transmissions. Four channel teleoperation requires precise force measurements, which is hard to be achieved because force sensors exposed to environments are easily to be disturbed and destroyed.

Chapter 4

Conclusions and Future work

Time-varying delays in communication channels damage bilateral teleoperation system performance, and, more importantly, threaten the safety of the system. To improve performance and guarantee stability of time-delayed bilateral teleoperation systems, this thesis has explored several damping injection-based controllers of two channel and four channel bilateral teleoperation systems to provide a systematic control strategy.

Within the scheme of two channel teleoperation with only position exchanges, a bounded state feedback with adaptive gravity compensation controller has firstly been proposed to tackle the teleoperation control in the presence of time-varying delays, model uncertainties and bounded actuations. By incorporating an inner and an outer saturation functions to bound the proportional control and saturated proportional plus damping control, respectively, the designed controller can reserve sufficient damping injection and adaptive gravity compensation capabilities for stabilizing the system. Then, an augmented I&I velocity observer has been designed and incorporated in the conventional P+d control to obtain stable teleoperation with time-varying delays with no velocity measurement and to achieve globally exponential velocity estimation convergence. The main advantage of the augmented I&I observer over other related observer designs is that it dramatically simplifies observer design procedure and satisfies the specific requirement of teleoperation systems on global velocity estimation. For the more challenging bounded output feedback control, this thesis has also proved that the former developed techniques, bounded state feedback control and globally convergent I&I velocity observer, can be combined together to globally stabilize bilateral teleoperation system in the presence of time-varying delays without using velocity measurements through more conservative gains selections.

In terms of four channel teleoperation, a hybrid damping and stiffness strategy has been introduced which employs the user and environment force transmissions and applies them on the slave and master robots directly to keep tight master-slave coupling. The nonlinear velocity and position error coupling terms are adopted to vary the stiffness of proportional control and/or to adjust the injected damping, which guarantee ISS teleoperation with no assumption on external terminators passivity. Further, the nonsingular version avoids unexpected control torque spikes due to singularity at zero velocity of the hybrid damping and stiffness adjustment strategy and achieves stable teleoperation by introducing a saturation function in the singular nonlinear control term. However, the nonlinear velocity and position error coupling terms in the two strategies are quadratic in position errors, so sticking problems occur when the position errors become unexpected large. To this end, a reduced-order controller has been proposed to ensure effective position synchronization for arbitrarily large position errors and maintain the tight constraints between the master and slave sites.

The above research results discussed in this thesis provide several theoretical methodologies for achieving stable bilateral teleoperation with time-varying delays and some other constraints, which has been verified through Lyapunov-Krasovskii energy analysis and numerical simulations. Nevertheless, they are not necessarily the best options from the perspective of performance.

In the bounded state feedback with adaptive gravity compensation control, only the worst cases are considered in each saturation scenarios. For example, in the situation that only the outer saturation function on one side is breached, the derived stability criterion employs the minimum possible velocity of that saturated side. Another example is that the gravity compensations have not been incorporated in the outer saturation functions and the bounds of outer saturation functions are limited to stay within the linear actuator output section when maximum gravities occur. Therefore, the actuator capabilities have not been fully exploited and the designed controller is conservative. For the output feedback control, the designed I&I observer guarantees globally exponential velocity estimation convergence under the assumption that the model of the system is exactly known and the exerting user and environment forces can be precisely measured, which is obviously impractical for teleoperation realization.

In four channel teleoperation control, the three proposed damping and stiffness adjustment strategies employs the user and environment force transmissions and applies them on the slave and master robots directly. It is known that the communication

delays are time-varying and might randomly jumping within a certain range, so the transmitted forces are disturbed by the communication delays and become noisy as it can seen in simulations. It is worth mentioning that the reduced-order strategy overcomes the sticking problem of the other two strategies by using the sign of velocities and position errors. Therefore, the reduced-order velocity and position error coupling terms would switch signs around zero velocities and/or zero position errors, which varies the master-slave coupling stiffness and thus deteriorates human-environment interaction experience. Another problem in four channel teleoperation is measuring force. Most commercial robots are not equipped with force sensors, of which the reason is that external force sensors can be easily disturbed and destroyed.

As discussed above, several open problems are still remained to be addressed. Future directions to continue this research can be given in the following different areas:

1. Less conservative state feedback control for fully exploiting actuator capabilities and improving position synchronization performance.

2. Adaptive output feedback control of two channel teleoperation in the presence of model uncertainties without using velocity measurements.

3. Filtering noisy force transmissions or decreasing the sensitivity of the system to transmission noises without destabilizing four channel teleoperation.

Besides, it is interesting that the developed techniques for stable bilateral teleoperation with time-varying delays in this thesis can be easily extended to consensus control of multi-agent systems in the presence of time-varying communication delays if the network topology is undirected and connected. Therefore, future study can also explore more general applications in multi-agent systems with different types of network topologies and physical constraints.

Bibliography

[1] D. A. Lawrence, "Stability and transparency in bilateral teleoperation," *IEEE Transactions on Robotics and Automation*, vol. 9, no. 5, pp. 624–637, Oct 1993.

[2] Y. Yokokohji and T. Yoshikawa, "Bilateral control of master-slave manipulators for ideal kinesthetic coupling-formulation and experiment," *IEEE Transactions on Robotics and Automation*, vol. 10, no. 5, pp. 605–620, Oct 1994.

[3] J. Park and O. Khatib, "A haptic teleoperation approach based on contact force control," *The International Journal of Robotics Research*, vol. 25, no. 5-6, pp. 575–591, 2006.

[4] R. J. Anderson and M. W. Spong, "Bilateral control of teleoperators with time delay," *IEEE Transactions on Automatic Control*, vol. 34, no. 5, pp. 494–501, May 1989.

[5] N. Chopra, M. W. Spong, R. Ortega, and N. E. Barabanov, "On tracking performance in bilateral teleoperation," *IEEE Transactions on Robotics*, vol. 22, no. 4, pp. 861–866, Aug 2006.

[6] H. Li, K. Tadano, and K. Kawashima, "Experimental validation of stability and performance for position-error-based tele-surgery," in *2015 IEEE International Conference on Advanced Intelligent Mechatronics (AIM)*, July 2015, pp. 848–853.

[7] C. A. L. Martınez, "A model-based robust control approach for bilateral teleoperation systems," 2015.

[8] K. Cleary and C. Nguyen, "State of the art in surgical robotics: Clinical applications and technology challenges," *Computer Aided Surgery*, vol. 6, no. 6, pp. 312–328, 2001.

[9] M. Cenk Çavusoglu, W. Williams, F. Tendick, and S. Shankar Sastry, "Robotics for telesurgery: second generation Berkeley/UCSF laparoscopic telesurgical workstation and looking towards the future applications," *Industrial Robot: An International Journal*, vol. 30, no. 1, pp. 22–29, 2003.

[10] G. Moustris, S. Hiridis, K. Deliparaschos, and K. Konstantinidis, "Evolution of autonomous and semi-autonomous robotic surgical systems: a review of the literature," *The International Journal of Medical Robotics and Computer Assisted Surgery*, vol. 7, no. 4, pp. 375–392, 2011.

[11] J. K. Koehn and K. J. Kuchenbecker, "Surgeons and non-surgeons prefer haptic feedback of instrument vibrations during robotic surgery," *Surgical Endoscopy*, vol. 29, no. 10, pp. 2970–2983, 2015.

[12] A. M. Okamura, L. N. Verner, C. Reiley, and M. Mahvash, "Haptics for robot-assisted minimally invasive surgery," in *Robotics Research*. Springer, 2010, pp. 361–372.

[13] C. R. Wottawa, J. R. Cohen, R. E. Fan, J. W. Bisley, M. O. Culjat, W. S. Grundfest, and E. P. Dutson, "The role of tactile feedback in grip force during laparoscopic training tasks," *Surgical Endoscopy*, vol. 27, no. 4, pp. 1111–1118, 2013.

[14] B. Weber and S. Schneider, "The effects of force feedback on surgical task performance: a meta-analytical integration," in *International Conference on Human Haptic Sensing and Touch Enabled Computer Applications*. Springer, 2014, pp. 150–157.

[15] G. A. Christiansson, "An experimental study of haptic feedback in a teleoperated assembly task," *Journal of Computing and Information Science in Engineering*, vol. 8, no. 4, p. 041003, 2008.

[16] P. F. Hokayem and M. W. Spong, "Bilateral teleoperation: An historical survey," *Automatica*, vol. 42, no. 12, pp. 2035 – 2057, 2006.

[17] J.-H. Ryu, D.-S. Kwon, and B. Hannaford, "Stable teleoperation with time-domain passivity control," *IEEE Transactions on Robotics and Automation*, vol. 20, no. 2, pp. 365–373, April 2004.

[18] C. Seo, J.-P. Kim, J. Kim, H.-S. Ahn, and J. Ryu, "Robustly stable bilateral teleoperation under time-varying delays and data losses: an energy-bounding approach," *Journal of Mechanical Science and Technology*, vol. 25, no. 8, pp. 2089–2100, 2011.

[19] M. Franken, S. Stramigioli, S. Misra, C. Secchi, and A. Macchelli, "Bilateral telemanipulation with time delays: A two-layer approach combining passivity and transparency," *IEEE Transactions on Robotics*, vol. 27, no. 4, pp. 741–756, Aug 2011.

[20] L. Mártori, "Time domain passivity based teleoperation applying bounded output controllers," in *2013 IEEE 14th International Symposium on Computational Intelligence and Informatics*. IEEE, 2013, pp. 89–94.

[21] Y. Ye, Y. J. Pan, and T. Hilliard, "Bilateral teleoperation with time-varying delay: A communication channel passification approach," *IEEE/ASME Transactions on Mechatronics*, vol. 18, no. 4, pp. 1431–1434, Aug 2013.

[22] V. Chawda and M. K. OMalley, "Position synchronization in bilateral teleoperation under time-varying communication delays," *IEEE/ASME Transactions on Mechatronics*, vol. 20, no. 1, pp. 245–253, Feb 2015.

[23] D. Sun, F. Naghdy, and H. Du, "Wave-variable-based passivity control of four-channel nonlinear bilateral teleoperation system under time delays," *IEEE/ASME Transactions on Mechatronics*, vol. 21, no. 1, pp. 238–253, Feb 2016.

[24] D. Lee and M. W. Spong, "Passive bilateral teleoperation with constant time delay," *IEEE Transactions on Robotics*, vol. 22, no. 2, pp. 269–281, April 2006.

[25] E. Nuño, R. Ortega, N. Barabanov, and L. Basañez, "A globally stable pd controller for bilateral teleoperators," *IEEE Transactions on Robotics*, vol. 24, no. 3, pp. 753–758, 2008.

[26] E. Nuño, R. Ortega, L. Basañez, and N. Barabanov, "A new proportional controller for nonlinear bilateral teleoperators," *IFAC Proceedings Volumes*, vol. 41, no. 2, pp. 15 660–15 665, 2008.

[27] E. Nuño, L. Basañez, and M. Prada, "Asymptotic stability of teleoperators with variable time-delays," in *2009 IEEE International Conference on Robotics and Automation*. IEEE, 2009, pp. 4332–4337.

[28] E. Nuño, L. Basañez, and R. Ortega, *Control of Teleoperators with Time-Delay: A Lyapunov Approach*. Berlin, Heidelberg: Springer Berlin Heidelberg, 2009, pp. 371–381.

[29] E. Nuño, L. Basañez, R. Ortega, and M. W. Spong, "Position tracking for non-linear teleoperators with variable time delay," *The International Journal of Robotics Research*, vol. 28, no. 7, pp. 895–910, 2009.

[30] E. Nuño, D. Valle, I. Sarras, and L. Basañez, "Bilateral teleoperation of flexible-joint manipulators with dynamic gravity compensation and variable time-delays," in *2013 IEEE/RSJ International Conference on Intelligent Robots and Systems*, Nov 2013, pp. 5439–5444.

[31] E. Slawiñski and V. Mut, "Pd-like controllers for delayed bilateral teleoperation of manipulators robots," *International Journal of Robust and Nonlinear Control*, vol. 25, no. 12, pp. 1801–1815, 2015.

[32] C. Hua and X. P. Liu, "Delay-dependent stability criteria of teleoperation systems with asymmetric time-varying delays," *IEEE Transactions on Robotics*, vol. 26, no. 5, pp. 925–932, Oct 2010.

[33] C. Hua and Y. Yang, "Bilateral teleoperation design with/without gravity measurement," *IEEE Transactions on Instrumentation and Measurement*, vol. 61, no. 12, pp. 3136–3146, Dec 2012.

[34] C. Hua and X. P. Liu, "A new coordinated slave torque feedback control algorithm for network-based teleoperation systems," *IEEE/ASME Transactions on Mechatronics*, vol. 18, no. 2, pp. 764–774, April 2013.

[35] V. Santibáñez and R. Kelly, "Global regulation for robot manipulators under SP-SD feedback," in *Proceedings of IEEE International Conference on Robotics and Automation*, vol. 1, Apr 1996, pp. 927–932 vol.1.

[36] R. Kelly, V. Santibáñez, and H. Berghuis, "Point-to-point robot control under actuator constraints," *Control Engineering Practice*, vol. 5, no. 11, pp. 1555 – 1562, 1997.

[37] V. Santibáñez, R. Kelly, and F. Reyes, "A new set-point controller with bounded torques for robot manipulators," *IEEE Transactions on Industrial Electronics*, vol. 45, no. 1, pp. 126–133, Feb 1998.

[38] A. Loría, R. Kelly, R. Ortega, and V. Santibáñez, "On global output feedback regulation of Euler-Lagrange systems with bounded inputs," *IEEE Transactions on Automatic Control*, vol. 42, no. 8, pp. 1138–1143, Aug 1997.

[39] R. Colbaugh, E. Barany, and K. Glass, "Global regulation of uncertain manipulators using bounded controls," in *Proceedings of International Conference on Robotics and Automation*, vol. 2, Apr 1997, pp. 1148–1155 vol.2.

[40] A. Laib, "Adaptive output regulation of robot manipulators under actuator constraints," *IEEE Transactions on Robotics and Automation*, vol. 16, no. 1, pp. 29–35, Feb 2000.

[41] D. J. López-Araujo, A. Zavala-Río, V. Santibáñez, and F. Reyes, "A generalized scheme for the global adaptive regulation of robot manipulators with bounded inputs," *Robotica*, vol. 31, no. 7, pp. 1103–1117, 10 2013.

[42] W. E. Dixon, "Adaptive regulation of amplitude limited robot manipulators with uncertain kinematics and dynamics," *IEEE Transactions on Automatic Control*, vol. 52, no. 3, pp. 488–493, March 2007.

[43] H. Yazarel, C. C. Cheah, and H. C. Liaw, "Adaptive SP-D control of a robotic manipulator in the presence of modeling error in a gravity regressor matrix: theory and experiment," *IEEE Transactions on Robotics and Automation*, vol. 18, no. 3, pp. 373–379, Jun 2002.

[44] A. Zavala-Río and V. Santibáñez, "Simple extensions of the PD-with-gravity-compensation control law for robot manipulators with bounded inputs," *IEEE Transactions on Control Systems Technology*, vol. 14, no. 5, pp. 958–965, Sept 2006.

[45] ——, "A natural saturating extension of the PD-with-desired-gravity-compensation control law for robot manipulators with bounded inputs," *IEEE Transactions on Robotics*, vol. 23, no. 2, pp. 386–391, April 2007.

[46] J. Alvarez-Ramirez, R. Kelly, and I. Cervantes, "Semiglobal stability of saturated linear PID control for robot manipulators," *Automatica*, vol. 39, no. 6, pp. 989 – 995, 2003.

[47] J. Alvarez-Ramirez, V. Santibáñez, and R. Campa, "Stability of robot manipulators under saturated PID compensation," *IEEE Transactions on Control Systems Technology*, vol. 16, no. 6, pp. 1333–1341, Nov 2008.

[48] R. Gorez, "Globally stable PID-like control of mechanical systems," *Systems & Control Letters*, vol. 38, no. 1, pp. 61 – 72, 1999.

[49] Y. Su, P. C. Müller, and C. Zheng, "A global asymptotic stable output feedback PID regulator for robot manipulators," in *Proceedings of 2007 IEEE International Conference on Robotics and Automation*, April 2007, pp. 4484–4489.

[50] ——, "Global asymptotic saturated PID control for robot manipulators," *IEEE Transactions on Control Systems Technology*, vol. 18, no. 6, pp. 1280–1288, Nov 2010.

[51] D. Sun, S. Hu, X. Shao, and C. Liu, "Global stability of a saturated nonlinear PID controller for robot manipulators," *IEEE Transactions on Control Systems Technology*, vol. 17, no. 4, pp. 892–899, July 2009.

[52] F. Morabito, A. R. Teel, and L. Zaccarian, "Results on anti-windup design for Euler-Lagrange systems," in *Proceedings 2002 IEEE International Conference on Robotics and Automation*, vol. 4, 2002, pp. 3442–3447 vol.4.

[53] ——, "Nonlinear antiwindup applied to Euler-Lagrange systems," *IEEE Transactions on Robotics and Automation*, vol. 20, no. 3, pp. 526–537, June 2004.

[54] A. Loría and H. Nijmeijer, "Bounded output feedback tracking control of fully actuated Euler-Lagrange systems," *Systems & Control Letters*, vol. 33, no. 3, pp. 151 – 161, 1998.

[55] W. E. Dixon, M. S. de Queiroz, F. Zhang, and D. M. Dawson, "Tracking control of robot manipulators with bounded torque inputs," *Robotica*, vol. 17, no. 02, pp. 121–129, 1999.

[56] E. Aguiñaga-Ruiz, A. Zavala-Río, V. Santibáñez, and F. Reyes, "Global trajectory tracking through static feedback for robot manipulators with input saturations," in *2008 47th IEEE Conference on Decision and Control*, Dec 2008, pp. 3516–3522.

[57] ——, "Global trajectory tracking through static feedback for robot manipulators with bounded inputs," *IEEE Transactions on Control Systems Technology*, vol. 17, no. 4, pp. 934–944, July 2009.

[58] D. J. López-Araujo, A. Zavala-Río, V. Santibáñez, and F. Reyes, "A generalized global adaptive tracking control scheme for robot manipulators with bounded inputs," *International Journal of Adaptive Control and Signal Processing*, vol. 29, no. 2, pp. 180–200, 2015.

[59] N. Fischer, Z. Kan, and W. E. Dixon, "Saturated RISE feedback control for Euler-Lagrange systems," in *2012 American Control Conference (ACC)*, June 2012, pp. 244–249.

[60] N. Fischer, Z. Kan, R. Kamalapurkar, and W. E. Dixon, "Saturated RISE feedback control for a class of second-order nonlinear systems," *IEEE Transactions on Automatic Control*, vol. 59, no. 4, pp. 1094–1099, April 2014.

[61] F. Hashemzadeh, I. Hassanzadeh, and M. Tavakoli, "Teleoperation in the presence of varying time delays and sandwich linearity in actuators," *Automatica*, vol. 49, no. 9, pp. 2813 – 2821, 2013.

[62] C. Hua, Y. Yang, and P. X. Liu, "Output-feedback adaptive control of networked teleoperation system with time-varying delay and bounded inputs," *IEEE/ASME Transactions on Mechatronics*, vol. 20, no. 5, pp. 2009–2020, Oct 2015.

[63] D.-H. Zhai and Y. Xia, "Robust saturation-based control of bilateral teleoperation without velocity measurements," *International Journal of Robust and Nonlinear Control*, vol. 25, no. 15, pp. 2582–2607, 2015.

[64] C. Hua, X. Yang, J. Yan, and X. P. Guan, "On exploring the domain of attraction for bilateral teleoperator subject to interval delay and saturated P+d control scheme," *IEEE Transactions on Automatic Control*, vol. PP, no. 99, pp. 1–1, 2016.

[65] D. H. Zhai and Y. Xia, "Adaptive control for teleoperation system with varying time-delays and input saturation constraints," *IEEE Transactions on Industrial Electronics*, vol. PP, no. 99, pp. 1–1, 2016.

[66] S.-J. Lee and H.-S. Ahn, "Controller designs for bilateral teleoperation with input saturation," *Control Engineering Practice*, vol. 33, pp. 35 – 47, 2014.

[67] J. Yan, Y. Wan, C. Chen, C. Hua, and X. Guan, "Formation control of teleoperating cyber-physical system subject to time delay and actuator saturation constraints," in *2016 IEEE 55th Conference on Decision and Control (CDC)*, Dec 2016, pp. 4358–4363.

[68] E. Nuño, L. Basañez, C. López-Franco, and N. Arana-Daniel, "Stability of nonlinear teleoperators using PD controllers without velocity measurements," *Journal of the Franklin Institute*, vol. 351, no. 1, pp. 241 – 258, 2014.

[69] C. Hua and X. P. Liu, "Teleoperation over the internet with/without velocity signal," *IEEE Transactions on Instrumentation and Measurement*, vol. 60, no. 1, pp. 4–13, Jan 2011.

[70] A. Astolfi, R. Ortega, and A. Venkatraman, "A globally exponentially convergent immersion and invariance speed observer for n degrees of freedom mechanical systems," in *Proceedings of 2009 IEEE Conference on Decision and Control*, Dec 2009, pp. 6508–6513.

[71] ——, "A globally exponentially convergent immersion and invariance speed observer for mechanical systems with non-holonomic constraints," *Automatica*, vol. 46, no. 1, pp. 182 – 189, 2010.

[72] J. G. Romero, I. Sarras, and R. Ortega, "A globally exponentially stable tracking controller for mechanical systems using position feedback," in *2013 American Control Conference*, June 2013, pp. 4969–4974.

[73] J. G. Romero, R. Ortega, and I. Sarras, "A globally exponentially stable tracking controller for mechanical systems using position feedback," *IEEE Transactions on Automatic Control*, vol. 60, no. 3, pp. 818–823, March 2015.

[74] Ø. N. Stamnes, O. M. Aamo, and G.-O. Kaasa, "A constructive speed observer design for general Euler–Lagrange systems," *Automatica*, vol. 47, no. 10, pp. 2233–2238, 2011.

[75] ——, "Global output feedback tracking control of Euler–Lagrange systems," *IFAC Proceedings Volumes*, vol. 44, no. 1, pp. 215–220, 2011.

[76] J. Artigas Esclusa, "Time domain passivity control for delayed teleoperation," 2014.

[77] J. Rebelo and A. Schiele, "Time domain passivity controller for 4-channel time-delay bilateral teleoperation," *IEEE Transactions on Haptics*, vol. 8, no. 1, pp. 79–89, Jan 2015.

[78] H. Li and K. Kawashima, "Bilateral teleoperation with delayed force feedback using time domain passivity controller," *Robotics and Computer-Integrated Manufacturing*, vol. 37, pp. 188 – 196, 2016.

[79] I. Sarras, E. Nuño, L. Basañez, and M. Kinnaert, "Position tracking in delayed bilateral teleoperators without velocity measurements," *International Journal of Robust and Nonlinear Control*, vol. 26, no. 7, pp. 1437–1455, 2016, rnc.3358.

[80] M. Krstic, P. V. Kokotovic, and I. Kanellakopoulos, *Nonlinear and Adaptive Control Design*, 1st ed. New York, NY, USA: John Wiley & Sons, Inc., 1995.

[81] B. Siciliano and L. Villani, *Robot force control*. Springer Science & Business Media, 2012, vol. 540.

[82] C. T. Chen, *Linear System Theory and Design*, 2nd ed. New York, NY, USA: Oxford University Press, Inc., 1995.

[83] L. Weiss and E. Infante, "Finite time stability under perturbing forces and on product spaces," *IEEE Transactions on Automatic Control*, vol. 12, no. 1, pp. 54–59, February 1967.

[84] B. Hannaford and J.-H. Ryu, "Time-domain passivity control of haptic interfaces," *IEEE Transactions on Robotics and Automation*, vol. 18, no. 1, pp. 1–10, Feb 2002.

[85] K. J. Kuchenbecker, J. Fiene, and G. Niemeyer, "Improving contact realism through event-based haptic feedback," *IEEE Transactions on Visualization and Computer Graphics*, vol. 12, no. 2, pp. 219–230, March 2006.